

A Model for Stress-Driven
Diffusion in Polymers

Thesis by
Robert William Cox

In Partial Fulfillment of the Requirements
for the Degree of
Doctor of Philosophy

California Institute of Technology
Pasadena, California

1988

(Submitted December 11, 1987)

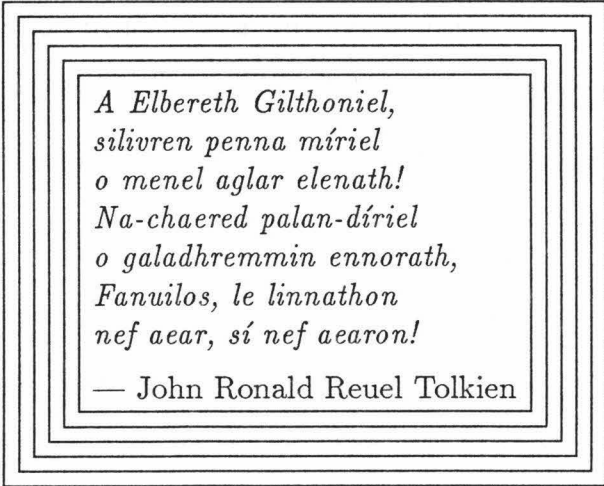
Acknowledgments

I am very grateful to Professor Donald S. Cohen for his support during my years at Caltech. Besides his invaluable guidance on this thesis project, he has consistently encouraged me in many ways when the going was slow. I also thank Michael J. Ward for his careful and time consuming perusal of this work, which resulted in significant improvements in several areas.

To my parents, brothers, and sisters, I owe a great deal for their love and support over the (seeming) æons of undergraduate and graduate studies at Caltech. I even include my in-laws in this acknowledgment of familial succor!

I thank the Institute for financial support in the form of Graduate Teaching Assistantships, Graduate Research Assistantships, and a Graduate Fellowship.

Ultimately, this thesis must be dedicated to the person without whom it quite literally would have been impossible: my wife, **Sharon Rose Streight Cox**.



*A Elbereth Gilthoniel,
silivren penna míriel
o menel aglar elenath!
Na-chaered palan-díriel
o galadhremmin ennorath,
Fanuilos, le linnathon
nef aear, sí nef aearon!*

— John Ronald Reuel Tolkien

Abstract

Penetration of solvents into polymers is sometimes characterized by steep concentration gradients that move into the polymer and last for long times. The behavior of these *fronts* cannot be explained by standard diffusion equations, even with concentration dependent diffusion coefficients. The addition of stress terms to the diffusive flux can produce such progressive fronts. Model equations are proposed that include solvent flux due to stress gradients in addition to the Fickian flux. The stress in turn obeys an concentration dependent evolution equation.

The model equations are analyzed in the limit of small diffusivity for the problem of penetration into a semi-infinite medium. Provided that the coefficient functions obey certain monotonicity conditions, the solvent concentration profile is shown to have a steep front that progresses into the the medium. A formula governing the progression of the front is developed. After the front decays away, the long time behavior of the solution is shown to be a similarity solution. Two techniques for approximating the solvent concentration and the front position are presented. The first approximation method is a series expansion; formulas are given for the initial speed and deceleration of the front. The second approximation method uses a portion of the long time similarity solution to represent the short time solution behind the front.

The addition of a convective term to the solvent flux is shown to raise the possibility of a traveling wave solution. The existence of the traveling wave solution is shown for certain types of coefficient functions. The way the initial front speed evolves onto the traveling wave speed is sketched out.

Contents

| | |
|---|-----------|
| Acknowledgments | ii |
| Abstract | iii |
| List of Figures | vi |
| 1 Prolegomenon | 1 |
| 2 Setting Up the Problem | 6 |
| 3 Short Time Behavior | 11 |
| 3.1 Numerical Solutions | 11 |
| 3.2 Solution Away from the Front | 12 |
| 3.3 Solution Near the Front | 28 |
| 3.4 When $k(C)$ Is <i>NOT</i> Increasing | 39 |
| 3.5 Very Short Times | 40 |
| 4 Long Time Behavior | 46 |
| 4.1 Asymptotic Similarity Solution | 46 |
| 4.2 Similarity Equation Has a Solution | 49 |
| 4.3 When $h(C)$ Is <i>NOT</i> Increasing | 53 |
| 4.4 Similarity and Short Time Outer Solutions | 58 |

| | | |
|----------|--|-----------|
| 5 | Convective Term and Traveling Waves | 69 |
| 5.1 | Traveling Wave Solution | 70 |
| 5.2 | Early Times | 76 |
| 5.3 | When a Depends on σ | 80 |
| A | Number Crunching | 83 |
| | Bibliography | 90 |

List of Figures

| | | |
|-----|---|----|
| 3.1 | C and σ vs. x for $f(C) = C$ | 13 |
| 3.2 | C and σ vs. x for $f(C) \equiv 1$ | 14 |
| 3.3 | $\dot{\mathcal{X}}$ vs. t for $f(C) = C$ | 24 |
| 3.4 | $\dot{\mathcal{X}}$ vs. t for $f(C) = C(2 - C)$ | 26 |
| 3.5 | $\dot{\mathcal{X}}$ vs. t for $f(C) = C$ and $f(C) = C(2 - C)$ | 27 |
| 3.6 | R vs. t for $f(C) = C$ and $f(C) = C(2 - C)$ | 29 |
| 3.7 | C vs. x for $f(C) = g(C) = \sqrt{C^{5/2} + .27 C \sin(2\pi C)}$ | 41 |
| 3.8 | C vs. x at very short times, for $f(C) = C$ | 45 |
| 4.1 | C vs. x for $f(C) = C$ | 47 |
| 4.2 | Equilibrium Discontinuous Solutions | 57 |
| 4.3 | Discontinuous Solution with a Front | 59 |
| 4.4 | Errors in \mathcal{X} , $\int C dx$ from Similarity Approximation | 63 |
| 5.1 | Layout of (C_T, σ_T) Phase Plane | 72 |
| 5.2 | Local Behavior in (C_T, σ_T) Phase Plane | 74 |
| 5.3 | C vs. x for $f(C) = a(C) = C$ | 79 |
| 5.4 | C vs. x for $f(C) = C$, $a(C, \sigma) = 1.1C\sigma^2$ | 82 |

Chapter 1

Prolegomenon

TRANSPORT OF A SOLVENT in a polymer is sometimes characterized by a sharp diffusion front which moves with near-constant speed. As a result, the amount of solvent taken up is nearly proportional to time. In the polymer science literature, this behavior is called **Case II diffusion** — the term Case I diffusion (or Fickian diffusion) is reserved for systems that are adequately modeled by a standard diffusion equation. In Case I diffusion, the amount of solvent taken up by the medium is proportional to (time)^{1/2}. Some nice experimental results illustrating the Case II phenomenon are given by Thomas and Windle [11].

One proposed explanation for Case II diffusion is that the Fickian flux of solvent must be supplemented by a flux due to pressure gradients. In this model, the polymer is deformed by the intrusion of the solvent, and so stress builds up in the polymer. This stress in turn reacts back on the penetrant, tending to squeeze it from regions of high stress to regions of low stress.

Let K and Σ denote the solvent concentration and polymer stress; let ξ and τ be the space and time coordinates. Define the chemical potential of the solvent by $\mu = \frac{\partial U}{\partial K}$, where U is the internal energy of the system at a given point (ξ, τ) . Then near-equilibrium transport theory (see [7, Chapter III] or [10], for example) says that the flux J of solvent is given by $J = -D^*K \frac{\partial \mu}{\partial \xi}$, where D^* is the transport coefficient for solvent molecules in the polymer medium and ξ is the spatial coordinate. For ideal thermodynamic behavior, and ignoring stress effects, $\mu(K) \propto \log K$, and the

Fickian flux results: $J \propto -\frac{\partial K}{\partial \xi}$. Non-ideal thermodynamic behavior is certainly possible, but as long as $\mu = \mu(K)$, all that results is having the diffusion coefficient depend on K : that is to say, nonlinear diffusion, but still just Case I.

Pressure on the solvent from the material stress will increase the system's internal energy and so its chemical potential. This is the basis for the theory of Case II diffusion of Thomas and Windle [12]: $\mu = \mu_0(K) + \alpha\Sigma$, where α is some constant. Then the flux is given by $J = -D(K)\frac{\partial K}{\partial \xi} - F(K)\frac{\partial \Sigma}{\partial \xi}$, where $F(K) = \alpha D^* \cdot K$. In what follows, I will allow $F(K)$ to depend almost arbitrarily on K .

A much more elaborate and thermodynamically based justification of stress-aided diffusion is given by Stanley [10]. Another author that has used the idea of stress as a driving force for Case II diffusion is Durning [5].

The addition of Σ as a dependent variable means that an equation for its evolution is needed. A general model for this is

$$\frac{\partial \Sigma}{\partial \tau} + B(K)\Sigma = B(K)G(K, \frac{\partial K}{\partial \tau});$$

here, $B(K)$ and $G(K, \frac{\partial K}{\partial \tau})$ depend on the properties of the solvent and the polymer. This general model is an amalgamation of the Maxwell viscoelastic model and the Kelvin-Voigt elastic model (see [3, Chapter 1], for example). In [5], Durning takes G to be a linear function of $\frac{\partial K}{\partial \tau}$ only. With this choice, he fails to get true Case II behavior. In this thesis, I will take the opposite extreme and assume that G depends *only* on K and not on $\frac{\partial K}{\partial \tau}$. This model means that the medium must be such as to support stresses at equilibrium. The functions $B(K)$ and $G(K)$ will be allowed to be almost arbitrary.

Thus, the model equations that this thesis revolves around are

$$\frac{\partial K}{\partial \tau} = \frac{\partial}{\partial \xi} \left[D(K) \frac{\partial K}{\partial \xi} + F(K) \frac{\partial \Sigma}{\partial \xi} \right] \quad (1.1)$$

$$\frac{\partial \Sigma}{\partial \tau} = B(K)[G(K) - \Sigma], \quad (1.2)$$

where ξ = spatial coordinate,
 τ = time coordinate,
 K = solvent concentration,
 Σ = material stress,
 D = diffusion coefficient,
 $1/B$ = stress relaxation time, and
 F, G = non-negative functions of K .

In a more abstract sense, it is not necessary to interpret Σ literally as “material stress.” It is just a mechanism for allowing past values of K to influence the diffusion process. Since Eq.(1.2) is really just an ordinary differential equation for Σ at each point ξ , it quite easily can be solved in terms of K . Assuming the initial condition $\Sigma(\xi, 0) = 0$, then

$$\Sigma(\xi, \tau) = \int_0^\tau e^{-\int_\theta^\tau B(K(\xi, \phi)) d\phi} B(K(\xi, \theta)) G(K(\xi, \theta)) d\theta.$$

This result can then be substituted back into Eq.(1.1) to eliminate all reference to “stress.” Of course, the result is an integro-differential equation, but it *does* explicitly show the dependence on past values of K :

$$\frac{\partial K}{\partial \tau} = \frac{\partial}{\partial \xi} \left[D(K) \frac{\partial K}{\partial \xi} + F(K) \frac{\partial}{\partial \xi} \int_0^\tau e^{-\int_\theta^\tau B(K(\xi, \phi)) d\phi} B(K(\xi, \theta)) G(K(\xi, \theta)) d\theta \right].$$

This is the straightforward nonlinear generalization of Eq.(27) of Aifantis [1], who considers various model equations for stress-assisted diffusion.

In Chapters 2–4, I will analyze a penetration problem based on Eqs.(1.1,1.2) where:

- $D(K)$, $F(K)$, $B(K)$, and $G(K)$ are smooth functions of K which will be required to satisfy two inequality constraints; and
- the dimensionless constant $\epsilon \equiv \frac{D(K_0)K_0}{F(K_0)G(K_0)}$ is small, where K_0 is a typical solvent concentration value.

Chapter 2 will present the basic initial-boundary value problem and scale it to a dimensionless form (thus bringing in ϵ). The assumption that $\epsilon \ll 1$ means that the stress controls the penetration of the solvent — thus the term “stress-driven diffusion.”

Chapter 3 will show that the solution to this problem has a steep front which progresses into the medium. A series method for calculating the position of this front and the solvent concentration behind the front will be developed in Section 3.2. The transition layer at the front is studied in Section 3.3. The role of the first inequality constraint on the coefficient functions will be illuminated there. What happens when this condition is violated is the subject of Section 3.4. In Section 3.5, the initial behavior of the solution (before the front develops) is remarked upon.

The asymptotic nature of the solution as $\tau \rightarrow \infty$ (after the front decays away) is the subject of Chapter 4. In Sections 4.1 and 4.2, $K(\xi, \tau)$ is shown to asymptote to a $\xi/\sqrt{\tau}$ type of similarity solution. Section 4.3 discusses what happens when the second inequality constraint on the coefficient functions is violated. Section 4.4 presents an interesting method of using the *long time* similarity solution to approximate the *short time* behavior, including the front.

In Chapter 5, I will modify Eq.(1.1) by adding a convective term $(-[A(K)K]_\xi)$ to the right hand side. This effect might arise if the penetrant can actually *flow* inside the medium — as it would, for example, if microscopic channels (crazes) open up

due to stress. Frisch, Wang, and Kwei [6] propose the use of such a convective term to explain Case II diffusion. This new term can lead to the existence of traveling wave solutions, which will stabilize the front for all times — the traveling wave replaces the similarity solution as the long time behavior. Section 5.1 shows the existence and uniqueness of the traveling wave under some assumptions on the coefficient functions (especially on $A(K)$). The modifications necessary to the analysis of Chapter 3 for the short time behavior are presented in Section 5.2. Finally, Section 5.3 discusses the interesting things that can happen to $K(\xi, \tau)$ when A is allowed to depend on Σ as well as on K .

The main tools used in this thesis are standard mathematical appliances. They include singular perturbation analysis with “inner” and “outer” regions, power series expansions, transformation to similarity variables, and numerical solutions of ordinary and partial differential equations. Throughout, various figures present the results of the computations. Since the numerical methods are fairly standard and do not in themselves constitute the main line of research, I have relegated their discussion to Appendix A.

Chapter 2

Setting Up the Problem

THE MODEL EQUATIONS under consideration in Chapters 2–4 are

$$K_\tau = [D(K)K_\xi + F(K)\Sigma_\xi]_\xi \quad (2.1)$$

$$\Sigma_\tau = B(K)[G(K) - \Sigma] . \quad (2.2)$$

In this chapter, these equations will be scaled to dimensionless form. The initial-boundary value problem that is the focus of this work will be presented, and several restrictions on the coefficient functions will be imposed.

The flux of solvent is denoted by J ; it is given by $J = -D(K)K_\xi - F(K)\Sigma_\xi$. Then Eq.(2.1) can also be written as $K_\tau = -J_\xi$. This is the usual law of conservation of solvent, saying that the solvent only piles up in places where the flux in and the flux out aren't balanced.

A number of restrictions are put on the coefficient functions $D(K)$, $F(K)$, $B(K)$, and $G(K)$. They are required to be smooth — at least twice continuously differentiable. $D(K)$ and $B(K)$ must be positive for all $K \geq 0$. For the most part I will assume that $F(0) = 0$. I will *always* assume that $G(0) = 0$. If Σ is interpreted as stress, then $F(0) = 0$ is like saying “you can't squeeze water from a dry sponge” — that is, no stress gradient Σ_ξ , however large, can cause a flux of solvent where there is no solvent. If $F(0) > 0$, then $K(\xi, \tau)$ might become negative at some point when a previously established stress gradient continues to force solvent out of a region even after all the solvent is gone (I have observed this in numerical solutions). The condition $G(0) = 0$ says that if there is no solvent present, the medium just relaxes

back to an unstressed state. If there never *was* any solvent at a particular location, then the stress there is zero.

Monotonicity Requirements

Two additional conditions are put on the coefficient functions. The first is

$$\frac{d}{dK} \left(\frac{F(K)G(K)B(K)}{K} \right) \geq 0; \quad (2.3)$$

in other words, $F(K)G(K)B(K)/K$ is non-decreasing. The role of this condition and what happens when it is violated will be discussed in detail in Sections 3.3 and 3.4. For now I will just mention that it is necessary for the solution to develop a steep front.

The second monotonicity condition is

$$D(K) + F(K)G'(K) > 0. \quad (2.4)$$

I call this a “monotonicity condition” because it will imply that the auxiliary function h (introduced in Eq.(4.4), far below) is increasing. This condition arises in the analysis of the long time behavior of the solution, as will be seen in Chapter 4. When this condition is violated, the analysis of the asymptotic nature of the solution is made much more complicated. The difficulties that arise are sketched out in Section 4.3.

Initial Conditions and Boundary Values

The initial-boundary value problem to be analyzed comprises Eqs.(2.1,2.2) and the conditions

$$K(\xi, 0) = \Sigma(\xi, 0) = 0 \quad \text{for } \xi > 0 \quad (2.5)$$

$$K(0, \tau) = K_0 \quad \text{for } \tau > 0. \quad (2.6)$$

Thus, at time $\tau = 0$ there is no solvent or stress in the material and the left edge of the material is suddenly exposed to an infinite reservoir of the solvent.

I will usually assume the material to be semi-infinite in extent. The case of a finite medium will be considered briefly in Section 4.3. In that case, a right edge boundary condition is needed:

$$K(L, \tau) = 0 \quad \text{for } \tau > 0,$$

where L is the thickness of the medium. This boundary condition says that the right edge of the medium is a perfect sink for the solvent.

A different plausible boundary condition at $\xi = L$ is $J(L, \tau) = 0$. This says that no solvent can pass through the right edge. It would be appropriate if the right edge is an impermeable membrane or if the true problem occurs in a domain of length $2L$ and is symmetric about the center. This alternative is not studied in this thesis.

Scaling

There are four quantities which can be scaled in Eqs.(2.1-2.6): K , Σ , ξ , and τ . There are five constants present in the equations: $D(K_0)$, $B(K_0)$, K_0 , $F(K_0)$, and $G(K_0)$. Thus, the non-dimensional form of the equations will contain one parameter — two if the thickness L is finite. For various reasons, I have chosen to put this parameter in the position occupied by “ $D(K)$ ” in Eq.(2.1).

$$\begin{aligned} \text{Let } K &= K_0 \cdot C && \text{(so that } C(0, t) \equiv 1), \\ \Sigma &= G(K_0) \cdot \sigma && \text{(so that } \sigma(0, t) \rightarrow 1 \text{ as } t \rightarrow \infty), \\ \xi &= \varphi \cdot x && \text{(\varphi a constant), and} \\ \tau &= t/B(K_0) && \text{(natural scaling of time);} \end{aligned}$$

here, C and σ are the dimensionless concentration and stress; x and t are the dimensionless space and time variables. Then Eqs.(2.1,2.2) become

$$\begin{aligned}\frac{\partial C}{\partial t} &= \frac{\partial}{\partial x} \left[\frac{D(K_0)}{B(K_0)\varphi^2} \cdot \frac{D(K_0C)}{D(K_0)} \cdot \frac{\partial C}{\partial x} + \frac{F(K_0)G(K_0)}{B(K_0)K_0\varphi^2} \cdot \frac{F(K_0C)}{F(K_0)} \cdot \frac{\partial \sigma}{\partial x} \right] \\ \frac{\partial \sigma}{\partial t} &= \frac{B(K_0C)}{B(K_0)} \cdot \left[\frac{G(K_0C)}{G(K_0)} - \sigma \right]\end{aligned}$$

Define the following constants and functions:

$$\begin{aligned}\varphi &= \left(\frac{F(K_0)G(K_0)}{B(K_0)K_0} \right)^{1/2} & \epsilon &= \frac{D(K_0)K_0}{F(K_0)G(K_0)} \\ d(C) &= \frac{D(K_0C)}{D(K_0)} & f(C) &= \frac{F(K_0C)}{F(K_0)} \\ g(C) &= \frac{G(K_0C)}{G(K_0)} & \beta(C) &= \frac{B(K_0C)}{B(K_0)}.\end{aligned}$$

Then the non-dimensional system corresponding to Eqs.(2.1–2.6) is:

$$C_t = [\epsilon d(C)C_x + f(C)\sigma_x]_x \quad (2.7)$$

$$\sigma_t = \beta(C)[g(C) - \sigma], \quad (2.8)$$

with the initial and boundary conditions

$$C(x, 0) = \sigma(x, 0) = 0 \quad \text{for } 0 < x < \ell \quad (2.9)$$

$$C(0, t) = 1 \text{ and } C(\ell, t) = 0 \quad \text{for } t > 0, \quad (2.10)$$

where $\ell = L/\varphi$; except in Section 4.3, $\ell = \infty$.

The coefficient functions have been scaled so that $d(1) = f(1) = \beta(1) = g(1) = 1$.

I am assuming that $d(C)$ and $\beta(C)$ are positive for all C . I will usually be assuming that $f(0) = 0$. The condition $g(0) = 0$ must always hold. The first monotonicity condition Eq.(2.3) now becomes

$$\frac{d}{dC} \left(\frac{f(C)g(C)\beta(C)}{C} \right) \geq 0; \quad (2.11)$$

in other words, $f(C)g(C)\beta(C)/C$ is non-decreasing. Because this function appears so frequently in the analysis below, I have given it a name of its own:

$$k(C) \equiv \frac{f(C)g(C)\beta(C)}{C}. \quad (2.12)$$

The second monotonicity condition Eq.(2.4) is scaled to become

$$\epsilon d(C) + f(C)g'(C) > 0. \quad (2.13)$$

If ϵ is taken to be small (see below), this condition effectively means that $g'(C) \geq 0$, or that $g(C)$ is non-decreasing in C . On the other hand, in the places where I apply Eq.(2.13), I usually don't need to have $\epsilon \ll 1$. In those cases, a large enough ϵ can compensate for $g'(C) < 0$.

These two monotonicity conditions are independent of each other in the sense that it is perfectly possible to have coefficient functions that satisfy just one condition, both conditions, or neither condition.

Size of ϵ

Since I chose to name the parameter in Eq.(2.7) " ϵ ," it is clear that I intend to consider it small. The reason for this is that large ϵ makes the system Eqs.(2.7–2.10) be a weakly perturbed diffusion equation and nothing interesting happens. For small ϵ , steep fronts develop in C and propagate with (initially) near-constant speed. This is the type of behavior which I call "interesting" and seek to explain below.

Most of the results in Chapter 4 do not depend on ϵ being small. They actually only require that Eq.(2.13) hold.

Chapter 3

Short Time Behavior

IN THIS RATHER LENGTHY CHAPTER, I will discuss the short time behavior of the nonlinear system given by Eqs.(2.7–2.10). By “short time,” I mean for times $t \leq O(1)$. On such a time scale, the solution $C(x, t)$ has a steep front which progresses into the medium. A power series method for approximating the solution behind the front will be developed and compared with numerical solutions. Stretching and matching will be used to derive the equations which govern the structure of the front. The crucial role of Eq.(2.11) in the formation of the front will be seen in these equations. (Eq.(2.13) does not come into this chapter at all.) For some special cases of the coefficient functions, the layer equations can be solved in closed form, but even for general coefficients satisfying Eq.(2.11), the structure of the front can be analyzed.

3.1 Numerical Solutions

Most of the numerical solutions presented herein have been run with $d(C) \equiv \beta(C) \equiv 1$, and with $g(C) = C$. Only $f(C)$ has been varied. The software used to generate the plots (described in Appendix A) *does* allow for general coefficients. As will become apparent in the analysis, the crucial function is $k(C) \equiv f(C)g(C)\beta(C)/C$. With the restrictions given earlier, $k(C) \equiv f(C)$, and so only varying $f(C)$ will not terribly restrict the range of solutions that can be obtained.

Figure 3.1 shows a numerical solution of Eqs.(2.7–2.10) with $f(C) = C$. Successive curves represent C and σ at progressively later times. The most prominent feature

is the propagation of a shock-like front at near-constant speed. Note also that σ goes to zero just at the front location. This indicates that behind the front, solvent transport is “stress-driven” (the flux is dominated by $-f(C)\sigma_x$ rather than by $-\epsilon d(C)C_x$) and in the front is a layer where diffusive and stress effects balance.

Other choices for the coefficient functions $f(C)$, $g(C)$, and $\beta(C)$ that satisfy the strict inequality in Eq.(2.11) give very similar results. When Eq.(2.11) is an *equality*, then $f(C)g(C)\beta(C) \equiv C$ or $k(C) \equiv 1$; the linear problem with $f(C) \equiv 1$ is an example. Figure 3.2 shows a numerical solution of this linear problem. The major difference from Fig. 3.1 is that the front “slumps down” much more. Part of the the explanation for this is that when $k(C) \equiv 1$, the front thickness is $O(\epsilon^{1/2})$; otherwise, it is $O(\epsilon)$. When Eq.(2.11) fails to hold altogether, then no front develops at all. These conclusions will be drawn later in Section 3.3, where the equations which determine the structure of the front are derived and analyzed.

3.2 Solution Away from the Front

The numerical results suggest that the zero-th order in ϵ “outer” solution (not considering the details inside the front) of the system Eqs.(2.7–2.10) has the form

$$\begin{aligned} C_{\text{Outer}} &= \begin{cases} C_O(x,t) & 0 < x < \mathcal{X}(t) \\ 0 & x > \mathcal{X}(t) \end{cases} \\ \sigma_{\text{Outer}} &= \begin{cases} \sigma_O(x,t) & 0 < x < \mathcal{X}(t) \\ 0 & x > \mathcal{X}(t) \end{cases}, \end{aligned}$$

where $\mathcal{X}(t)$ is the location of the front. The *ansatz* of this section is that C_O is discontinuous at $x = \mathcal{X}(t)$, σ_O is continuous there, and $\partial\sigma_O/\partial x$ is discontinuous

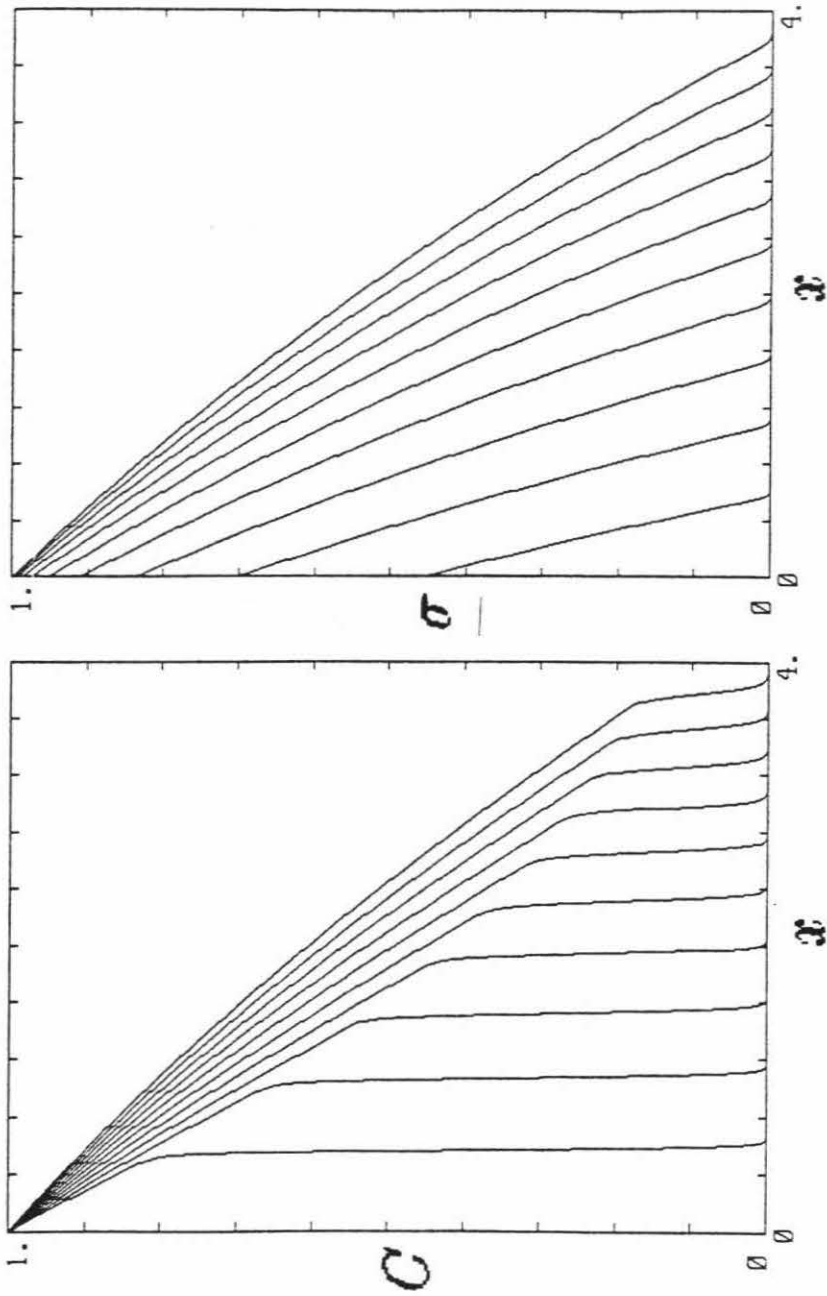


Figure 3.1: C and σ vs. x for $f(C) = C$.

$$g(C) = C, \quad d(C) \equiv \beta(C) \equiv 1, \quad \epsilon = 0.01.$$

Curves plotted at time intervals $\Delta t = 0.6$.

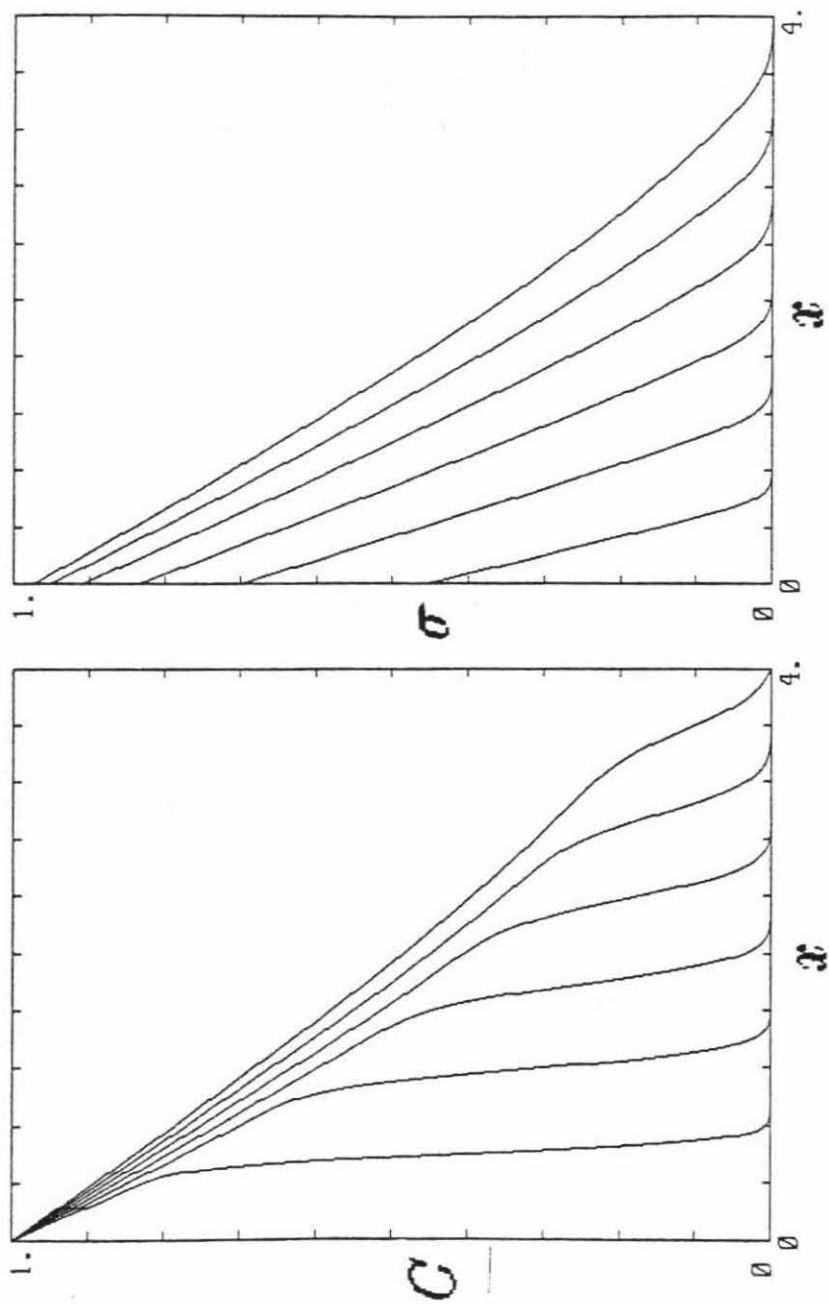


Figure 3.2: C and σ vs. x for $f(C) \equiv 1$.

$$g(C) = C, \quad d(C) \equiv \beta(C) \equiv 1, \quad \epsilon = 0.01.$$

Curves plotted at time intervals $\Delta t = 0.6$.

at the front. These conditions were arrived at by considering Fig. 3.1.

To zero order in ϵ , the “outer” equations are thus

$$\frac{\partial C_o}{\partial t} = \frac{\partial}{\partial x} \left[f(C_o) \frac{\partial \sigma_o}{\partial x} \right] \quad (3.1)$$

$$\frac{\partial \sigma_o}{\partial t} = \beta(C_o)[g(C_o) - \sigma_o], \quad (3.2)$$

with the initial and boundary conditions

$$C_o(x, 0) = \sigma_o(x, 0) = 0 \quad \text{for } x > 0 \quad (3.3)$$

$$C_o(0, t) = 1 \quad \text{for } t > 0 \quad (3.4)$$

$$\sigma_o(\mathcal{X}(t), t) = 0 \quad \text{for } t > 0 \quad (3.5)$$

$$\mathcal{X}(0) = 0. \quad (3.6)$$

Equation for Evolution of \mathcal{X}

An equation is also needed for the evolution of $\mathcal{X}(t)$. This can be provided in two equivalent ways. The more intuitive is by flux balance: whatever the flux J is at $x = \mathcal{X}(t) - 0$, as the solvent “pours over the edge,” the front will extend in proportion to J . That is, in a small time step dt , the amount of solvent that “pours over the edge” is $J(\mathcal{X}, t) dt$; this must be balanced by the new solvent that appears by motion of the front, $C_o(\mathcal{X}, t) \dot{\mathcal{X}} dt$. Thus conservation of solvent gives, recalling the definition of J ,

$$C_o(\mathcal{X}(t), t) \dot{\mathcal{X}}(t) = -f(C_o(\mathcal{X}(t), t)) \frac{\partial \sigma_o}{\partial x}(\mathcal{X}(t), t). \quad (3.7)$$

Note that there is no consumption of the solvent in order to advance the front — if C were temperature, I would say that there is no latent heat. This need not always be the case; for an example where advancing the front consumes solvent, see Cohen and Goodhart [4].

The more mathematical way to derive Eq.(3.7) is to integrate Eq.(3.1) with respect to x from $\mathcal{X}(t_0) - \delta$ to $\mathcal{X}(t_0) + \delta$, where t_0 is some fixed time and δ is small:

$$\frac{\partial}{\partial t} \int_{\mathcal{X}(t_0)-\delta}^{\mathcal{X}(t_0)+\delta} C_O(x, t) dx = \left[f(C_O) \frac{\partial \sigma_O}{\partial x} \right]_{\mathcal{X}(t_0)-\delta}^{\mathcal{X}(t_0)+\delta}.$$

Evaluating this for small δ and recalling that C_O and σ_O are identically zero ahead of the front gives Eq.(3.7) again.

Equation (3.7) is the necessary equation for the evolution of $\mathcal{X}(t)$, but it is more useful when cast into a different form. Differentiate Eq.(3.5) with respect to t :

$$\begin{aligned} 0 &= \frac{d}{dt} [\sigma_O(\mathcal{X}(t), t)] \\ &= \dot{\mathcal{X}} \frac{\partial \sigma_O}{\partial x}(\mathcal{X}, t) + \frac{\partial \sigma_O}{\partial t}(\mathcal{X}, t) \\ &= \dot{\mathcal{X}} \frac{\partial \sigma_O}{\partial x}(\mathcal{X}, t) + \beta(C_O(\mathcal{X}, t)) [g(C_O(\mathcal{X}, t) - \sigma_O(\mathcal{X}, t))]. \end{aligned}$$

Recalling again that $\sigma_O(\mathcal{X}, t) = 0$ gives

$$\frac{\partial \sigma_O}{\partial x}(\mathcal{X}, t) = -\frac{g(C_O(\mathcal{X}, t))\beta(C_O(\mathcal{X}, t))}{\dot{\mathcal{X}}(t)}. \quad (3.8)$$

Plugging this into Eq.(3.7) gives the key result:

$$\frac{d\mathcal{X}}{dt} = \left[\frac{f(C_O(\mathcal{X}, t))g(C_O(\mathcal{X}, t))\beta(C_O(\mathcal{X}, t))}{C_O(\mathcal{X}, t)} \right]^{1/2} = \sqrt{k(C_O(\mathcal{X}, t))}. \quad (3.9)$$

Here is the first indication of the role that the function $k(C)$ plays in this problem. The condition in Eq.(2.11) says that as $C(\mathcal{X}, t)$ drops down, so does the speed of the front. Apparently, by reversing Eq.(2.11), the front could be made to accelerate instead. This does not happen; instead, the effect of reversing the inequality in Eq.(2.11) is to destroy the existence of the front. This subject is discussed in Section 3.4.

Equations (3.1–3.6,3.9) are the outer equations to be solved. Of particular interest is the location of the front, $\mathcal{X}(t)$. Observe that $k(C) \equiv 1$ seems to be a special

case, as promised earlier, since then $\mathcal{X}(t) = t$. More interesting facts about this special case will come up later.

How Long Is “Short Time?”

A closed form solution of the outer equations seems unlikely even for simple cases such as $f(C) = g(C) = C$, $d(C) \equiv \beta(C) \equiv 1$. (For the linear case $f(C) \equiv 1$, $g(C) = C$, $d(C) \equiv \beta(C) \equiv 1$, the closed form outer solution will be given in Section 3.3.) Nevertheless, qualitative information about the outer solution can be derived. In particular, its short time behavior will be given below. The outer solution can only be valid for a finite time, since when $C_o(\mathcal{X}, t)$ shrinks to zero, Eq.(3.9) predicts that $\dot{\mathcal{X}} = 0$ (at least for $k(C) = o(C)$ as $C \rightarrow 0$). This would indicate that a steady-state situation develops, but in fact that is not what happens. The diffusive term $(\epsilon d(C)C_x)_x$ prevents this when $\ell = \infty$ — this will be shown in Chapter 4. Numerical solutions of the full system Eqs.(2.7–2.10) indicate that when $C_o(\mathcal{X}, t) \rightarrow 0$, the character of the solution changes but no steady state is reached unless $\ell < \infty$. The long time behavior of Eqs.(2.7–2.10) will be discussed in Chapter 4.

Initial Speed and Acceleration

Evaluation of Eq.(3.9) at $t = 0$ and at the left edge, with $C_o(0^+, 0^+) = 1$, implies $\dot{\mathcal{X}}(0) = 1$; that is, the front starts off with speed 1. The initial acceleration (or deceleration) can also be calculated:

$$\ddot{\mathcal{X}}(t) = \frac{k'(C_o(\mathcal{X}, t))}{2k(C_o(\mathcal{X}, t))^{1/2}} \left[\dot{\mathcal{X}}(t) \frac{\partial C_o}{\partial x}(\mathcal{X}, t) + \frac{\partial C_o}{\partial t}(\mathcal{X}, t) \right]. \quad (3.10)$$

At $t = 0$, $\mathcal{X} = 0$, so $C_o = 1$, and thus

$$\ddot{\mathcal{X}}(0) = \frac{1}{2}k'(1) \frac{\partial C_o}{\partial x}(0, 0) = \frac{1}{2} [f'(1) + g'(1) + \beta'(1) - 1] \frac{\partial C_o}{\partial x}(0, 0). \quad (3.11)$$

This is fine, except that $\frac{\partial C_O}{\partial x}(0,0)$ is as unknown as $\ddot{\mathcal{X}}(0)$. All is not lost, however: I shall derive two *new* equations that include this new unknown, another new unknown, and then solve for all three unknowns at once.

To get Eq.(3.9), I differentiated Eq.(3.5) with respect to t . Differentiate it *twice* this time:

$$\begin{aligned}
 0 &= \frac{d^2}{dt^2}[\sigma_O(\mathcal{X}, t)] \\
 &= \frac{d}{dt} \left[\dot{\mathcal{X}} \frac{\partial \sigma_O}{\partial x}(\mathcal{X}, t) + \beta(C_O(\mathcal{X}, t))g(C_O(\mathcal{X}, t)) - \beta(C_O(\mathcal{X}, t))\sigma_O(\mathcal{X}, t) \right] \\
 &= \ddot{\mathcal{X}} \frac{\partial \sigma_O}{\partial x}(\mathcal{X}, t) + \dot{\mathcal{X}}^2 \frac{\partial^2 \sigma_O}{\partial x^2}(\mathcal{X}, t) + \dot{\mathcal{X}} \frac{\partial^2 \sigma_O}{\partial x \partial t}(\mathcal{X}, t) \\
 &\quad + \left[\beta(C_O(\mathcal{X}, t))g'(C_O(\mathcal{X}, t)) + \beta'(C_O(\mathcal{X}, t))g(C_O(\mathcal{X}, t)) \right] \\
 &\quad \times \left[\dot{\mathcal{X}} \frac{\partial C_O}{\partial x}(\mathcal{X}, t) + \frac{\partial C_O}{\partial t}(\mathcal{X}, t) \right]
 \end{aligned} \tag{3.12}$$

To evaluate this at the origin, several simple calculations need to be made:

$$\text{Eq.(3.8) at } t = 0 \implies \frac{\partial \sigma_O}{\partial x}(0,0) = -1$$

$$\text{Eq.(3.2) at } x = t = 0 \implies \frac{\partial \sigma_O}{\partial t}(0,0) = 1$$

$$\frac{\partial}{\partial x} \text{ of Eq.(3.2) at } x = t = 0 \implies \frac{\partial^2 \sigma_O}{\partial x \partial t}(0,0) = [\beta'(1) + g'(1)] \frac{\partial C_O}{\partial x}(0,0) + 1$$

$$C(0, t) \equiv 1 \implies \frac{\partial C_O}{\partial t}(0,0) = 0.$$

Evaluation of Eq.(3.12) at $t = 0$ now gives

$$0 = -\ddot{\mathcal{X}}(0) + \frac{\partial^2 \sigma_O}{\partial x^2}(0,0) + 2[\beta'(1) + g'(1)] \frac{\partial C_O}{\partial x}(0,0) + 1. \tag{3.13}$$

This equation has introduced *another* unknown, viz., $\frac{\partial^2 \sigma_O}{\partial x^2}(0,0)$. The third equation necessary to close the system comes from evaluating Eq.(3.1) at the origin:

$$0 = f'(C_O) \frac{\partial C_O}{\partial x}(0,0) \frac{\partial \sigma_O}{\partial x}(0,0) + f(C_O) \frac{\partial^2 \sigma_O}{\partial x^2}(0,0)$$

$$= \frac{\partial^2 \sigma_O}{\partial x^2}(0,0) - f'(1) \frac{\partial C_O}{\partial x}(0,0). \quad (3.14)$$

Putting Eqs.(3.11,3.13,3.14) into matrix-vector form gives

$$\begin{pmatrix} 1 & 0 & -\frac{1}{2}[f'(1) + g'(1) + \beta'(1) - 1] \\ -1 & 1 & 2[g'(1) + \beta'(1)] \\ 0 & 1 & -f'(1) \end{pmatrix} \begin{pmatrix} \ddot{\chi}(0) \\ \frac{\partial^2 \sigma_O}{\partial x^2}(0,0) \\ \frac{\partial C_O}{\partial x}(0,0) \end{pmatrix} = \begin{pmatrix} 0 \\ -1 \\ 0 \end{pmatrix}. \quad (3.15)$$

Solving this system gives

$$\ddot{\chi}(0) = -\frac{f'(1) + g'(1) + \beta'(1) - 1}{1 + f'(1) + 3g'(1) + 3\beta'(1)} \quad (3.16)$$

$$\frac{\partial^2 \sigma_O}{\partial x^2}(0,0) = -\frac{2f'(1)}{1 + f'(1) + 3g'(1) + 3\beta'(1)} \quad (3.17)$$

$$\frac{\partial C_O}{\partial x}(0,0) = -\frac{2}{1 + f'(1) + 3g'(1) + 3\beta'(1)}. \quad (3.18)$$

The condition in Eq.(2.11) ensures that $f'(1) + g'(1) + \beta'(1) - 1 = k'(1)$ is non-negative, so $\ddot{\chi}(0)$ is non-positive if the denominator $1 + f'(1) + 3g'(1) + 3\beta'(1)$ is positive. I will *assume* that this is so — it does not follow from any previous assumptions. This new condition is equivalent to assuming that $g'(1) + \beta'(1) > -1$.

Thus the front slows down as it moves into the medium if $k'(1) > 0$. Below, I will show that if any derivative of $k(C)$ is non-zero at $C = 1$ and if $k(C)$ is non-decreasing (as assumed), then the front slows down even if $k'(1) = 0$.

Series Expansion

It is clearly possible to continue in this vein, but the algebra becomes quite tedious and confusing. A better way is to look for a power series solution:

$$C_O(x,t) = 1 + \sum_{p=1}^{\infty} \sum_{n=1}^p A_{pn} x^n t^{p-n}$$

$$\begin{aligned}\sigma_O(x, t) &= \sum_{p=1}^{\infty} \sum_{n=0}^p B_{pn} x^n t^{p-n} \\ \mathcal{X}(t) &= \sum_{p=1}^{\infty} E_p t^p.\end{aligned}$$

Observe that $A_{p0} = 0$ for all $p > 0$. This is because $C_O(0, t) = 1 \forall t$, so putting $x = 0$ into the series for C_O must give a series in t only that is just $\equiv 1$; thus, all the $x^0 t^p$ terms must be zero for $p > 0$. Note also that $\sigma(0, t) = 1 - e^{-t}$. The same reasoning now implies that $B_{p0} = (-1)^{p-1}/p!$.

In terms of what has already been done, the following identifications can be made:

$$\begin{aligned}A_{11} &= \frac{\partial C_O}{\partial x}(0, 0) &= -\frac{2}{1 + f'(1) + 3g'(1) + 3\beta'(1)} \\ B_{10} &= \frac{\partial \sigma_O}{\partial t}(0, 0) &= +1 \\ B_{11} &= \frac{\partial \sigma_O}{\partial x}(0, 0) &= -1 \\ B_{20} &= \frac{1}{2} \frac{\partial^2 \sigma_O}{\partial t^2}(0, 0) &= -\frac{1}{2} \\ B_{21} &= \frac{\partial^2 \sigma_O}{\partial x \partial t}(0, 0) &= \frac{1 + f'(1) + g'(1) + \beta'(1)}{1 + f'(1) + 3g'(1) + 3\beta'(1)} \\ B_{22} &= \frac{1}{2} \frac{\partial^2 \sigma_O}{\partial x^2}(0, 0) &= -\frac{f'(1)}{1 + f'(1) + 3g'(1) + 3\beta'(1)} \\ E_1 &= \dot{\mathcal{X}}(0) &= +1 \\ E_2 &= \frac{1}{2} \ddot{\mathcal{X}}(0) &= \frac{1}{2} \frac{f'(1) + g'(1) + \beta'(1) - 1}{1 + f'(1) + 3g'(1) + 3\beta'(1)}.\end{aligned}$$

Plugging the series expansions into Eqs.(3.1,3.2,3.5,3.9) yields a set of equations for the coefficients $\{A_{pn}, B_{pn}, E_p\}$ which can be solved in succession. This set of equations is nonlinear since the underlying problem is nonlinear. However, correctly ordering them enables their solution to be accomplished by solving a sequence of

linear equations. This is exactly analogous to the fact that solving for $\ddot{\mathcal{X}}(0)$ only involved solving the linear system Eq.(3.15). For each $P = 2, 3, \dots$, the next set of coefficients $\{A_{Pn}, B_{P+1,n}, E_{P+1}\}$ is determined once $\{A_{p-1,n}, B_{pn}, E_p\}$ is known for $p = 1, 2, \dots, P$.

Even with the power series formalism, the algebra involved in calculating the next set of coefficients $\{A_{21}, A_{22}, B_{31}, B_{32}, B_{33}, E_3\}$ is lengthy, although completely unambiguous. I have carried out this process with the use of *muMath*, a symbolic computation program [13]. The general answer for the next six coefficients, expressed in terms of $f'(1)$, $g'(1)$, $\beta'(1)$, $f''(1)$, $g''(1)$, and $\beta''(1)$, is a very complicated expression which is quite uninformative. A more useful way to present the result is to give the linear system which results. For any given set of coefficient functions, the solution can easily be evaluated numerically. This is the next order analog to Eq.(3.15):

$$\begin{pmatrix} -1 & -2f'(1) & 0 & 0 & 6 & 0 \\ -f'(1) & 0 & 0 & 2 & 0 & 0 \\ 0 & -\lambda'(1) & 0 & 1 & 0 & 0 \\ -\lambda'(1) & 0 & 2 & 0 & 0 & 0 \\ 0 & 0 & 1 & 1 & 1 & -1 \\ -k'(1) & -k'(1) & 0 & 0 & 0 & 6 \end{pmatrix} \begin{pmatrix} A_{21} \\ A_{22} \\ B_{31} \\ B_{32} \\ B_{33} \\ E_3 \end{pmatrix} = \begin{pmatrix} -4A_{11}B_{22}f'(1) + A_{11}^2f''(1) \\ -A_{11}B_{21}f'(1) \\ -B_{22} + A_{11}\beta'(1) + \frac{1}{2}A_{11}^2\lambda''(1) \\ -B_{21} - A_{11}\beta'(1) \\ -[B_{21} + 2B_{22}]E_2 - \frac{1}{6} \\ \frac{1}{2}A_{11}^2k''(1) \end{pmatrix}$$

where I have temporarily defined $\lambda(C) \equiv \beta(C)g(C)$ (to save space!). The first two equations above come from enforcing Eq.(3.1) to $O(x)$ and $O(t)$. The next two are derived by enforcing Eq.(3.2) to $O(x^2)$ and $O(xt)$. The fifth equation is the result of enforcing Eq.(3.5) to $O(t^3)$ and the sixth equation comes from enforcing Eq.(3.9) to $O(t^2)$. The value obtained for E_3 by solving this system agrees with the numerical value of the $O(t^2)$ term in Eq.(3.19) below.

When $f'(1) + g'(1) + \beta'(1) = 1$ (or $k'(1) = 0$), then $\ddot{\mathcal{X}}(0) = 2E_2 = 0$. In this special case, the general formula for E_3 simplifies to

$$\ddot{\mathcal{X}}(0) = 6E_3 = \frac{1}{2}A_{11}^2 k''(1).$$

This is just the last row of the above 6×6 system when $k'(1) = 0$. An alternative derivation is obtained by considering $\dot{\mathcal{X}}^2 = k(C_O(\mathcal{X}, t))$. Expanding both sides in a Taylor series to $O(t^2)$ gives the result above — which also agrees with the numerical value for the $O(t^2)$ term in Eq.(3.20) below.

If $k'(1) = 0$, then the monotonicity of $k(C)$ requires $k''(1) \leq 0$. If $k''(1) < 0$, then $\ddot{\mathcal{X}}(0) < 0$, and so the front slows down as it moves into the medium. If $k''(1) = 0$, then a similar argument with higher derivatives leads to the same conclusion: the front always slows down if $k(C) \neq 1$ and $k'(C) \geq 0$.

Specific Examples and Comparison with Numerical Results

It turns out to be straightforward to carry out the power series expansion for any *given* $f(C)$, $g(C)$, and $\beta(C)$. The reason is that at each step, numerical values are obtained for the coefficients. Proceeding to the next stage (higher order coefficients) merely involves manipulating numbers rather than increasingly unwieldy formulas.

I have carried out the calculation of the power series for the case of Fig. 3.1, where $f(C) = g(C) = C$, and $d(C) \equiv \beta(C) \equiv 1$. The result for the frontal speed is

$$\begin{aligned} \dot{\mathcal{X}}(t) = & 1 - \frac{1}{5}t + \frac{19}{650}t^2 - \frac{121}{33150}t^3 + \frac{337811}{767091000}t^4 \\ & - \frac{17241361}{343715775000}t^5 + \frac{8950276343963}{180711662148225000}t^6 + \dots \end{aligned} \quad (3.19)$$

The reason that I calculated so many terms was to make Eq.(3.19) a good approximation for as long a time as possible. The calculations for the t^3 and higher terms

were carried out with the use of *muMath* (I certainly couldn't have done them by hand!).

Figure 3.3 shows a plot of $\dot{\mathcal{X}}(t)$ vs. t from the numerical calculations which lead to Fig. 3.1, as well as showing plots of the 2nd through 6th order Taylor series from Eq.(3.19). This figure displays the general agreement of the series expansions from with the numerical $\dot{\mathcal{X}}(t)$. Notice that the range of time in Fig. 3.3 corresponds to that in Fig. 3.1, so that the approximation for $\dot{\mathcal{X}}(t)$ is holding almost up the the point where the whole idea of a front breaks down. (See Appendix A for a description of how $\mathcal{X}(t)$ is calculated from the finite-difference solution.)

If $f'(1) + g'(1) + \beta'(1) = 1$, Eq.(3.16) implies that $\ddot{\mathcal{X}}(0) = 0$. In this case, the front should not slow down as quickly. To test this, I ran the numerical simulation for $f(C) = C(2-C)$, $g(C) = C$, and $d(C) \equiv \beta(C) \equiv 1$, and also carried out the series expansion calculations (with *muMath*, as before). The results of the latter are:

$$\begin{aligned} \dot{\mathcal{X}}(t) = & 1 - \frac{1}{8}t^2 + \frac{3}{32}t^3 - \frac{91}{1536}t^4 + \frac{69}{2048}t^5 - \frac{2153}{147456}t^6 \\ & + \frac{39}{65536}t^7 + \frac{5823701}{660602880}t^8 - \frac{7379077}{528482304}t^9 + \dots \end{aligned} \quad (3.20)$$

Observe that the coefficients here are simpler than their analogs in Eq.(3.19). The reason for this is that in carrying out the process for calculating the series coefficients, the fact that $f'(1) = 0$ causes many terms to vanish, making both the algebra and the results simpler.

Figure 3.4 shows the numerical $\dot{\mathcal{X}}(t)$ vs. t , along with the 5th and 6th order Taylor series and three Padé approximants. These approximants are derived by fitting rational functions to $(\dot{\mathcal{X}}(t) - 1)/t^2$ in such a way that as many derivatives match

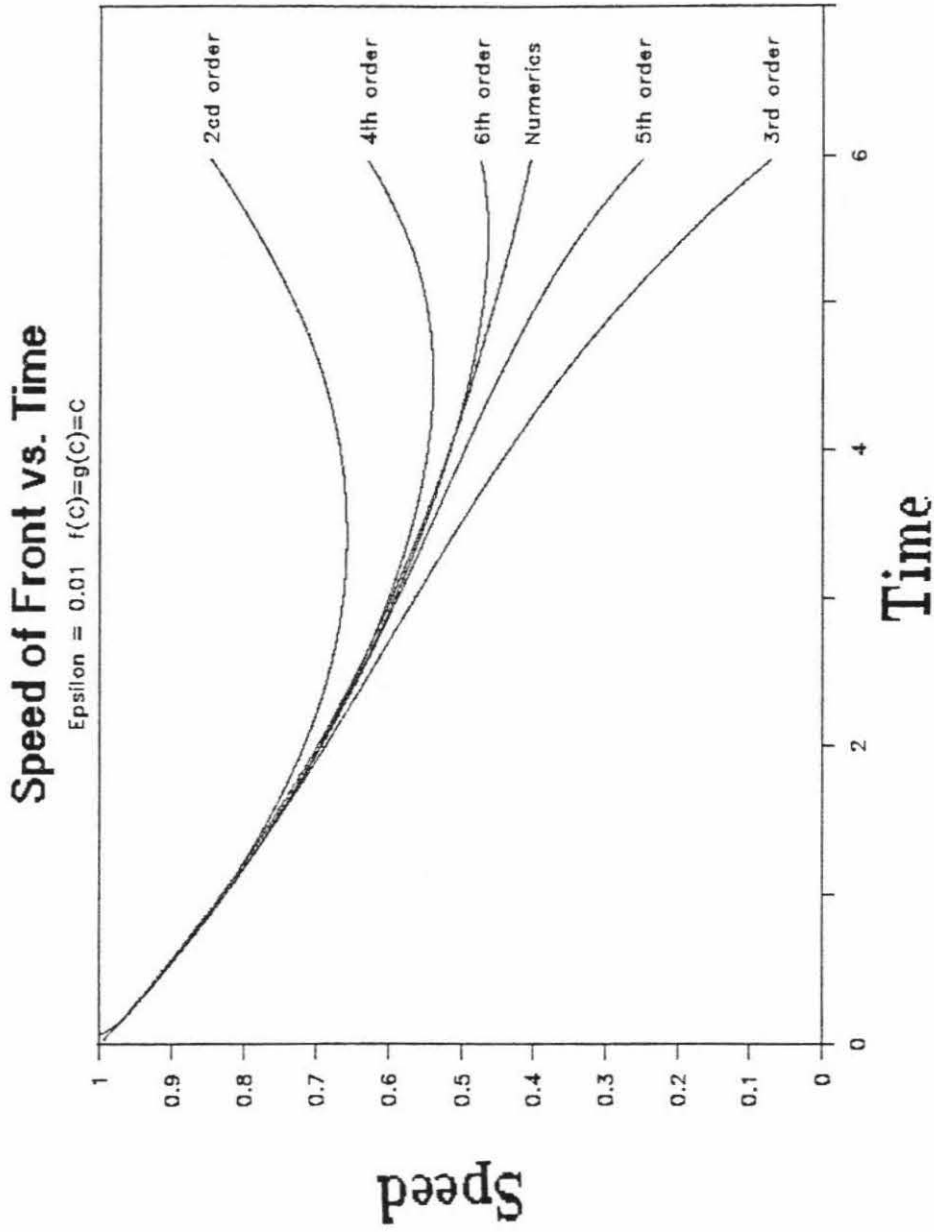


Figure 3.3: $\dot{\lambda}$ vs. t for $f(C) = C$.

$$g(C) = C, \quad d(C) \equiv \beta(C) \equiv 1, \quad \epsilon = 0.01.$$

at the origin as possible. For example, the (2,1) Padé approximation is

$$\dot{\chi}(t) \approx 1 - \frac{1 + \frac{15}{68}t}{8 + \frac{132}{17}t + \frac{829}{408}t^2} \cdot t^2.$$

Because there are four coefficients to be determined in this (2,1) Padé fraction, this approximation contains the same information as the 5th order Taylor series from Eq.(3.20). See [2, Chapter 8] for more information on Padé approximants, including an algorithm for calculating their coefficients from the Taylor series.

In this case, it appears that the Taylor series diverges around $t = 1$. The higher order series (up to ninth order) do not improve matters for larger t , although they do help for small t . Here is where the Padé approximants really shine. Apparently $\dot{\chi}(t)$ has a singularity near $t = -1$ and this ruins convergence of the Taylor series; however, the denominator of the Padé approximant can allow for this.

Figure 3.5 shows the two cases of $f(C)$ together. The case $f(C) = C(2 - C)$ *does* decelerate more slowly than $f(C) = C$. The effect is not as pronounced as one might expect from the fact that the former case has $\ddot{\chi}(0) = 0$ and the latter has $\ddot{\chi}(0) = -\frac{1}{5}$. The reason for this is that the higher order terms in Eq.(3.20) are more important than in Eq.(3.19) due to the fact that the former series has a smaller radius of convergence.

Besides the speed of the front, another interesting quantity is the rate at which solvent is taken up by the medium. This rate is defined as $R = \frac{d}{dt} \int_0^\infty C(x, t) dx$. Because solvent is conserved, this can also be expressed as $R = J(0, t) = [\text{flux in at left edge}]$. In the lowest order (in ϵ) approximation, $J(0, t) = -\sigma_x(0, t)$, so that the power series gives

$$R = - \sum_{p=1}^{\infty} B_{p1} t^{p-1}.$$

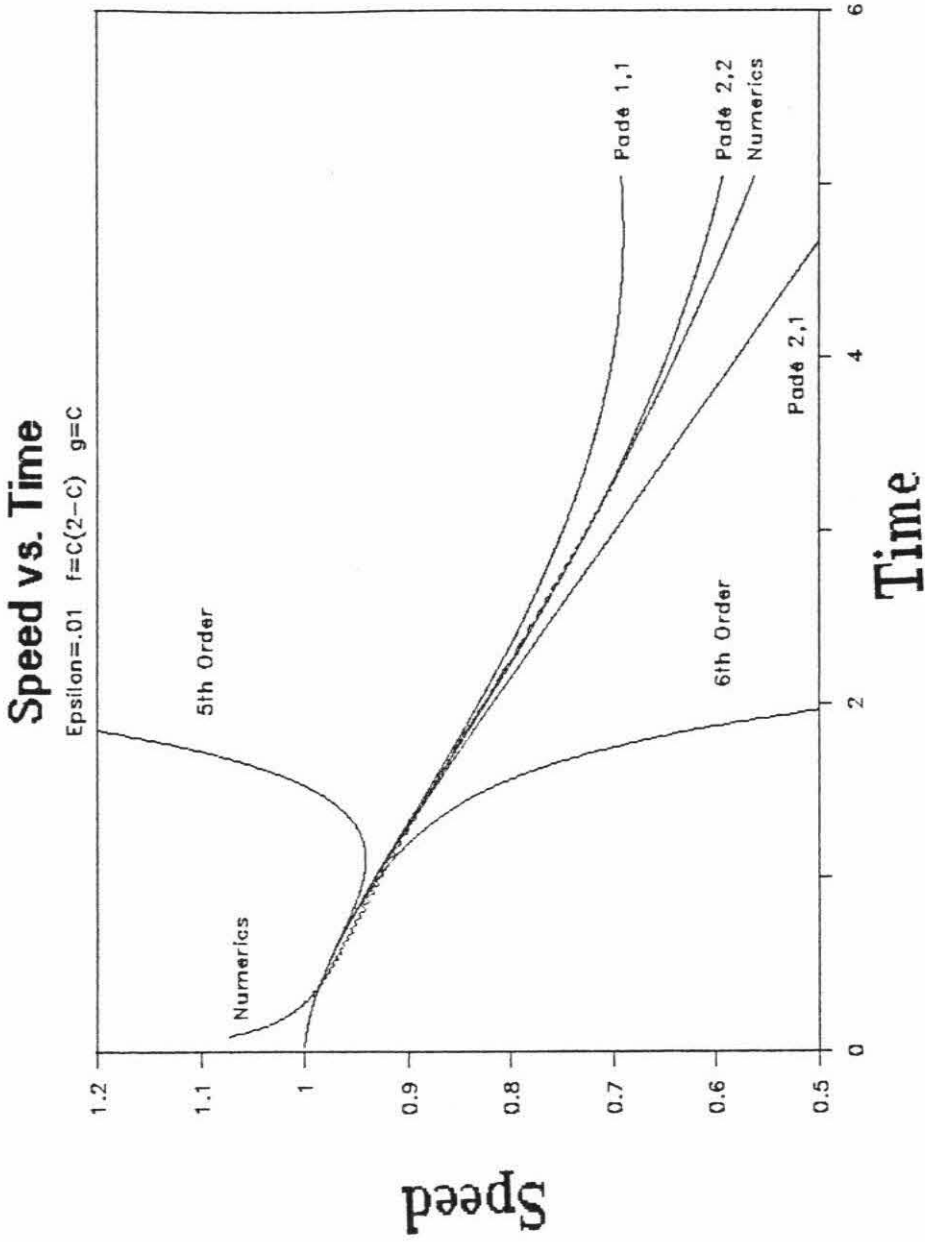


Figure 3.4: $\dot{\lambda}$ vs. t for $f(C) = C(2 - C)$.

$$g(C) = C, \quad d(C) \equiv \beta(C) \equiv 1, \quad \epsilon = 0.01.$$

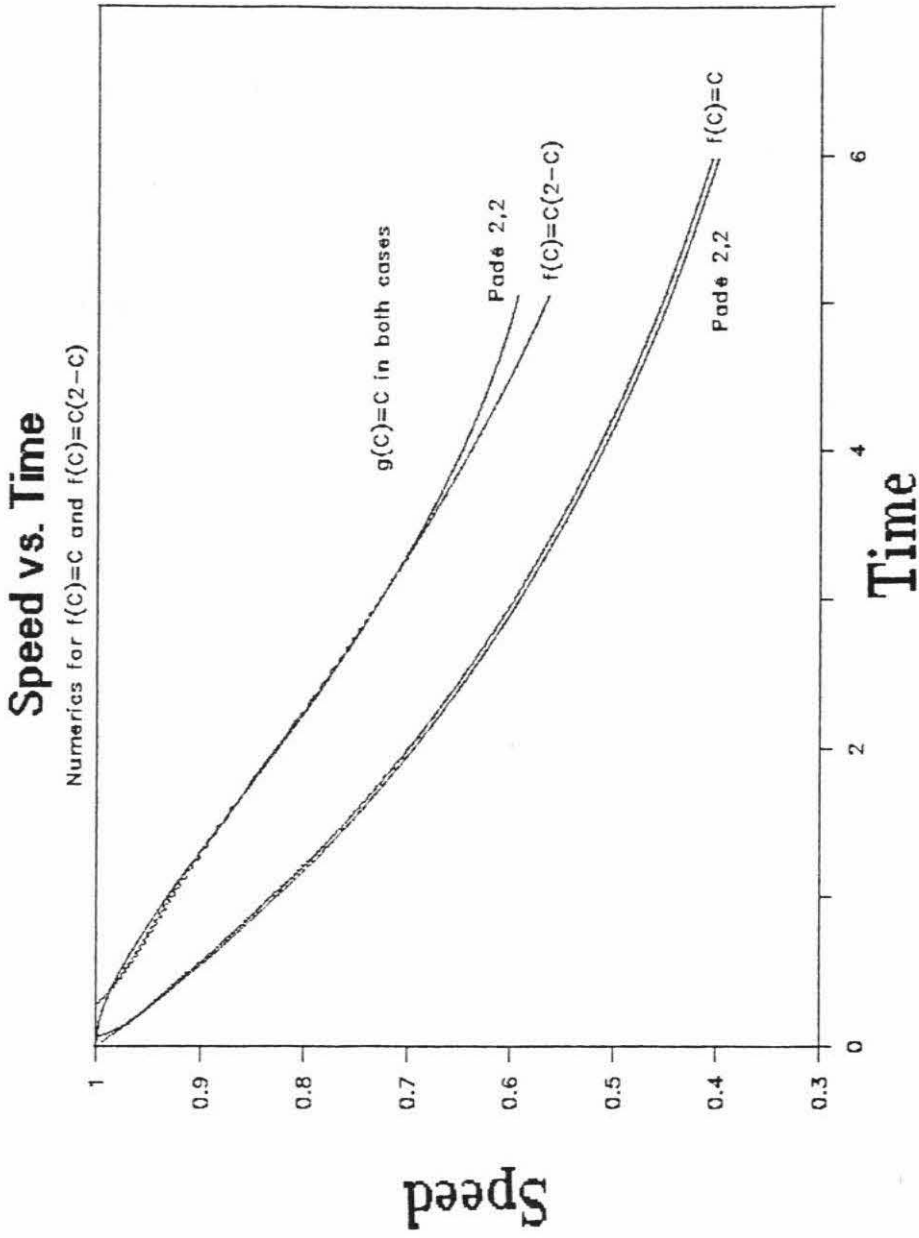


Figure 3.5: $\dot{\lambda}$ vs. t for $f(C) = C$ and $f(C) = C(2 - C)$

$$g(C) = C, \quad d(C) \equiv \beta(C) \equiv 1, \quad \epsilon = 0.01.$$

Figure 3.6 shows the plots of R vs. t for the two cases of Fig. 3.5. The numerically calculated values of R are displayed, along with the 5th order Taylor series expansions and the (2,2) Padé approximants. The Padé approximants show excellent agreement with the values from the numerical solutions to the partial differential equations.

In Section 4.4, I will develop another scheme for approximating the outer solution $C_0(x, t)$ for short times. The method there uses numerical solutions of ordinary differential equations, and so is less analytically oriented than the series method developed here. Further comparisons of these two approximation methods will be deferred to that section.

3.3 Solution Near the Front

A shock or transition layer is clearly needed near $x = \mathcal{X}(t)$ in the full system Eqs.(2.7–2.10). The correct scaling of this is a little tricky, so I will build up to it in steps.

The Linear System

The first step is to tackle the linear system with $f(C) \equiv d(C) \equiv \beta(C) \equiv 1$ and $g(C) = C$. This can be done in two ways: (a) eliminate σ to get a higher order system for C alone, or (b) use the system Eqs.(2.7,2.8) directly. Method (a) will not apply to the nonlinear system, but will help in using method (b) correctly.

The linear partial differential equations are

$$C_t = \epsilon C_{xx} + \sigma_{xx} \tag{3.21}$$

$$\sigma_t = C - \sigma. \tag{3.22}$$

Solvent Uptake Rate vs. Time

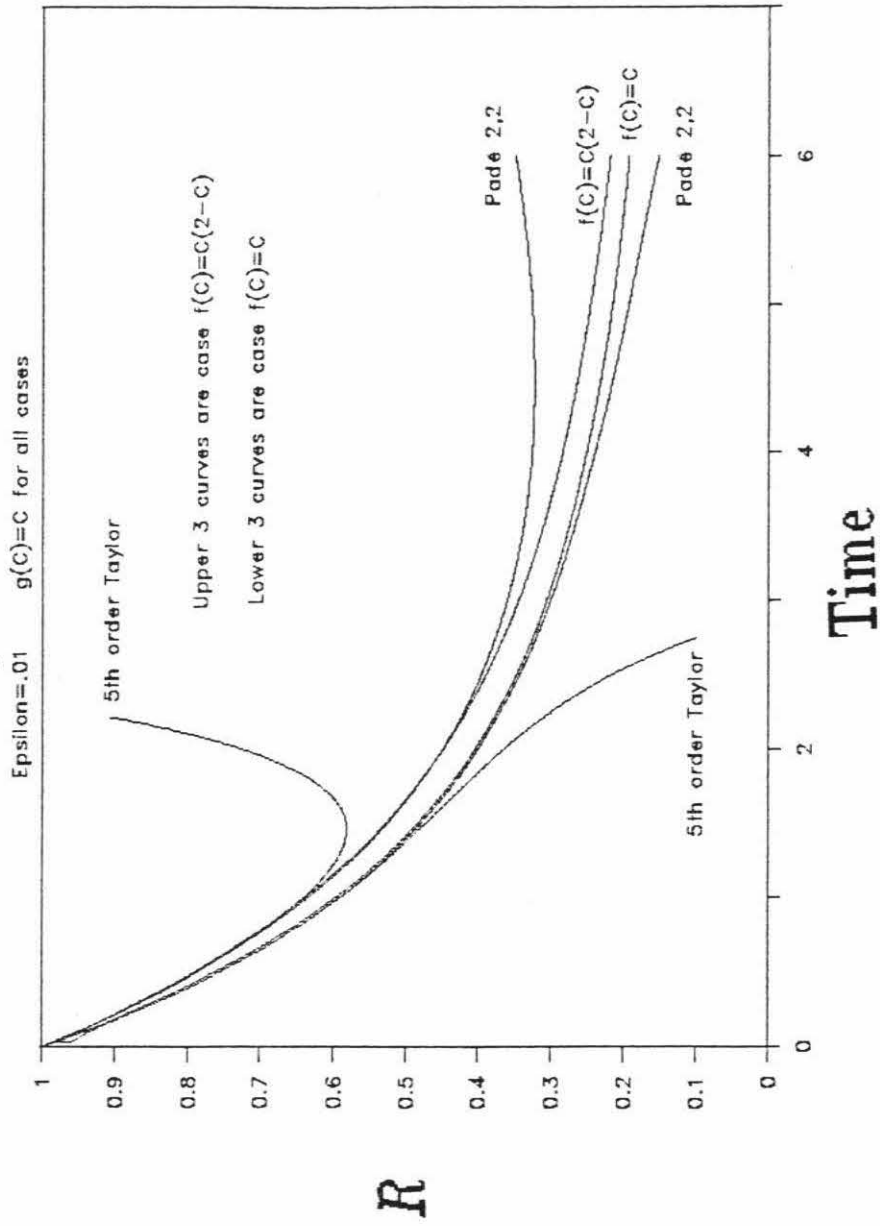


Figure 3.6: R vs. t for $f(C) = C$ and $f(C) = C(2 - C)$

$$g(C) = C, d(C) \equiv \beta(C) \equiv 1, \epsilon = 0.01.$$

Differentiate Eq.(3.21) with respect to t and Eq.(3.22) twice with respect to x , and eliminate σ_{xxt} and σ_{xx} between them. The result is

$$C_{tt} = (1 + \epsilon)C_{xx} - C_t + \epsilon C_{xxt}. \quad (3.23)$$

The outer ($\epsilon = 0$) solution for this equation satisfies

$$\frac{\partial^2 C_O}{\partial t^2} + \frac{\partial C_O}{\partial t} = \frac{\partial^2 C_O}{\partial x^2}. \quad (3.24)$$

Solving Eqs.(3.24,2.9,2.10) using the Laplace transform yields

$$C_O = \begin{cases} e^{-x/2} + x \int_x^t \frac{I_1(\sqrt{\tau^2 - x^2}/2)}{\sqrt{\tau^2 - x^2}/2} d\tau & 0 < x < t \\ 0 & x > t \end{cases} \quad (3.25)$$

Thus, $\mathcal{X}(t) \equiv t$. This is not surprising in light of Eq.(3.9), which predicts just that, or Eq.(3.24), which is a wave equation with speed $\equiv 1$.

Linear System Layer via Method (a)

Stretching and matching, as in Kevorkian and Cole [9], are used to find the transition layer near $x = t$. Introduce the new coordinates

$$\zeta = \frac{x - t}{\epsilon^p} \quad \eta = t \quad \implies \quad \frac{\partial}{\partial x} = \epsilon^{-p} \frac{\partial}{\partial \zeta} \quad \frac{\partial}{\partial t} = \frac{\partial}{\partial \eta} - \epsilon^{-p} \frac{\partial}{\partial \zeta},$$

where the correct scaling power p is to be found. These relationships imply that Eq.(3.23) transforms to

$$C_{\eta\eta} - 2\epsilon^{-p} C_{\zeta\eta} + \epsilon^{-2p} C_{\zeta\zeta} = (1 + \epsilon)\epsilon^{-2p} C_{\zeta\zeta} - C_\eta + \epsilon^{-p} C_\zeta + \epsilon^{1-2p}(C_{\zeta\zeta\eta} - \epsilon^{-p} C_{\zeta\zeta\zeta}). \quad (3.26)$$

The $\epsilon^{-2p} C_{\zeta\zeta}$ terms cancel, leaving the only possible dominant balance as $-p = 1 - 3p$ or $p = \frac{1}{2}$. Thus the layer thickness is $O(\epsilon^{1/2})$. The leading order layer equation is (with C_L being the leading order Layer solution)

$$\frac{\partial^3 C_L}{\partial \zeta^3} - \frac{\partial C_L}{\partial \zeta} = 2 \frac{\partial^2 C_L}{\partial \zeta \partial \eta}.$$

Since $\lim_{\zeta \rightarrow +\infty} C_L(\zeta, \eta) = 0$ (in order to match the outer solution C_O), integrating this equation once from ζ to $+\infty$ yields

$$\frac{\partial^2 C_L}{\partial \zeta^2} - C_L = 2 \frac{\partial C_L}{\partial \eta}. \quad (3.27)$$

The initial condition for this equation comes from Eqs.(2.9,2.10). It is just the statement that C_L starts at time $\eta = 0$ as a step function:

$$\begin{aligned} C_L(\zeta, 0) &= 0 \text{ for } \zeta > 0 \\ C_L(\zeta, 0) &= 1 \text{ for } \zeta < 0. \end{aligned} \quad (3.28)$$

The solution to Eqs.(3.27,3.28) is

$$C_L(\zeta, \eta) = \frac{1}{2} e^{-\eta/2} \operatorname{erfc} \left(\frac{\zeta}{\sqrt{2\eta}} \right); \quad (3.29)$$

in (x, t) coordinates, the layer solution is

$$C_L(x, t) = \frac{1}{2} e^{-t/2} \operatorname{erfc} \left(\frac{x-t}{\sqrt{2\epsilon t}} \right). \quad (3.30)$$

Equation (3.30) has no free parameters, so it is fortunate that it matches the outer solution to the left ($\zeta \rightarrow -\infty$). The combination of Eqs.(3.25,3.30) give the solution to the linear system to leading order. Notice that the boundary layer width is actually $O(\sqrt{\epsilon t})$, indicating that the front will slump down as time progresses. Figure 3.2 shows this quite clearly.

Linear System Layer via Method (b)

The next step is to use method (b) and try to get the same results as above. The same outer solution, Eq.(3.25), applies, with σ_O calculated by

$$\sigma_O(x, t) = \int_0^t e^{-(t-\tau)} C_O(x, \tau) d\tau.$$

Clearly, $\sigma_O(x, t) \equiv 0$ for $x > t$ and σ_O is continuous at $x = t$. Since σ is thus small near the transition layer, it should be scaled as well. Define ζ and η as before, and let $\sigma = \epsilon^q \rho$, where ρ is $O(1)$ and q is to be found. Then Eqs.(3.21,3.22) transform to

$$C_\eta - \epsilon^{-p} C_\zeta = \epsilon^{1-2p} C_{\zeta\zeta} + \epsilon^{q-2p} \rho_{\zeta\zeta} \quad (3.31)$$

$$\epsilon^q \rho_\eta - \epsilon^{q-p} \rho_\zeta = C - \epsilon^q \rho. \quad (3.32)$$

Equation (3.32) clearly requires $q = p$ for a balance to work. The dominant balance in Eq.(3.31) is then apparently $-p = 1 - 2p$ or $p = 1$. The layer equations become, to leading order in ϵ ,

$$\begin{aligned} \frac{\partial^2 C_L}{\partial \zeta^2} + \frac{\partial C_L}{\partial \zeta} + \frac{\partial^2 \rho_L}{\partial \zeta^2} &= 0 \\ C_L + \frac{\partial \rho_L}{\partial \zeta} &= 0. \end{aligned}$$

Differentiate the latter with respect to ζ and subtract from the former to get

$$\frac{\partial^2 C_L}{\partial \zeta^2} = 0.$$

This equation has *no* solution which matches to $C_O = e^{-\eta/2}$ as $\zeta \rightarrow -\infty$ and to $C_O = 0$ as $\zeta \rightarrow +\infty$. And the layer width is wrong: $O(\epsilon)$ instead of $O(\epsilon^{1/2})$. What went wrong?

What happened was that some of terms used in defining the dominant balance from Eq.(3.31) canceled out. In method (a), recall that the $\epsilon^{-2p} C_{\zeta\zeta}$ terms canceled in Eq.(3.26). If those had been left in, the apparent dominant balance would have been $1 - 3p = -2p$, giving $p = 1$ erroneously again. In Eq.(3.26), it would have been absurd to keep terms which obviously cancel, but the cancellation isn't so obvious in Eqs.(3.31,3.32).

What needs to be done is to solve Eq.(3.32) for ρ_ζ and substitute that result into Eq.(3.31) without dropping any terms as being subdominant. This procedure gives

$$\rho_\zeta = \epsilon^p(\rho + \rho_\eta) - C,$$

($p = q$ is still valid), and then

$$C_\eta - \epsilon^{-p}C_\zeta = \epsilon^{1-2p}C_{\zeta\zeta} + \epsilon^{-p}[\epsilon^p(\rho + \rho_\eta) - C]_\zeta,$$

or

$$C_\eta = \epsilon^{1-2p}C_{\zeta\zeta} + \rho_\zeta + \rho_{\zeta\eta}. \quad (3.33)$$

Equation (3.33) has the balance $p = \frac{1}{2}$, which is correct. Furthermore, Eq.(3.32) says that to lowest order, $\rho_\zeta = -C$. Substituting that into Eq.(3.33) gives the lowest order layer equation as

$$\frac{\partial C_L}{\partial \eta} = \frac{\partial^2 C_L}{\partial \zeta^2} - C_L - \frac{\partial C_L}{\partial \eta}. \quad (3.34)$$

Equations (3.27) and (3.34) are identical. Being careful with method (b) leads to the same answer as method (a).

Method (b) Applied to the Nonlinear System

Define

$$\zeta = \frac{x - \mathcal{X}(t)}{\epsilon^p} \quad \eta = t \quad \implies \quad \frac{\partial}{\partial x} = \epsilon^{-p} \frac{\partial}{\partial \zeta} \quad \frac{\partial}{\partial t} = \frac{\partial}{\partial \eta} - \epsilon^{-p} \dot{\mathcal{X}} \frac{\partial}{\partial \zeta}$$

and let $\sigma = \epsilon^p \rho$ (note that $p = q$ still holds). Then the nonlinear partial differential equations Eqs.(2.7,2.8) transform to

$$\begin{aligned} C_\eta - \epsilon^{-p} \dot{\mathcal{X}} C_\zeta &= [\epsilon^{1-2p} d(C) C_\zeta + \epsilon^{-p} f(C) \rho_\zeta]_\zeta \\ \epsilon^p \rho_\eta - \dot{\mathcal{X}} \rho_\zeta &= \beta(C) [g(C) - \epsilon^p \rho]. \end{aligned} \quad (3.35)$$

As before, solve for ρ_ζ , not dropping any “lower order terms”:

$$\rho_\zeta = \frac{\epsilon^p(\rho + \rho_\eta) - \beta(C)g(C)}{\dot{\chi}(\eta)},$$

and substitute this into Eq.(3.35) to get

$$\begin{aligned} C_\eta - \epsilon^{-p}\dot{\chi}C_\zeta &= \left[\epsilon^{1-2p}d(C)C_\zeta + \frac{\epsilon^{-p}}{\dot{\chi}}f(C)(\epsilon^p(\rho + \rho_\eta) - \beta(C)g(C)) \right]_\zeta \\ &= \epsilon^{1-2p}[d(C)C_\zeta]_\zeta + \frac{1}{\dot{\chi}}[f(C)(\rho + \rho_\eta)]_\zeta - \frac{\epsilon^{-p}}{\dot{\chi}}[f(C)g(C)\beta(C)]_\zeta. \end{aligned}$$

Rearranging, the result is

$$C_\eta = \epsilon^{1-2p}[d(C)C_\zeta]_\zeta + \frac{1}{\dot{\chi}}[f(C)(\rho + \rho_\eta)]_\zeta + \epsilon^{-p} \left[\dot{\chi}C - \frac{f(C)g(C)\beta(C)}{\dot{\chi}} \right]_\zeta. \quad (3.36)$$

Now, if $f(C)g(C)\beta(C) \equiv C$ (that is, $k(C) \equiv 1$), then Eq.(3.9) implies that $\dot{\chi} \equiv 1$. Then the last term in Eq.(3.36) is zero and the only balance possible is $p = \frac{1}{2}$, as in Eq.(3.33). But if $f(C)g(C)\beta(C) \neq C$, then the dominant balance is $1 - 2p = -p$, or $p = 1$. Thus the frontal layer thickness is either $O(\epsilon^{1/2})$ or $O(\epsilon)$, as claimed much earlier.

Layer Solution When $k(C) \neq 1$

In this case, the leading order layer equation becomes

$$\frac{\partial}{\partial \zeta} \left[d(C_L) \frac{\partial C_L}{\partial \zeta} + \dot{\chi}C_L - \frac{f(C_L)g(C_L)\beta(C_L)}{\dot{\chi}} \right] = 0.$$

Recalling that $\dot{\chi}$ is a function of η only and that $C_L \rightarrow 0$ as $\zeta \rightarrow +\infty$ (to match to the outer solution), integrate this equation once (and rearrange it slightly) to get

$$\frac{\partial C_L}{\partial \zeta} + \frac{C_L}{\dot{\chi}d(C_L)} \underbrace{\left[\dot{\chi}^2 - \frac{f(C_L)g(C_L)\beta(C_L)}{C_L} \right]}_{\equiv \mathcal{K}(C_L, \dot{\chi})} = 0. \quad (3.37)$$

For example, if $d(C) \equiv 1$ and $f(C)g(C)\beta(C) = C^r$, with $r > 1$ to satisfy Eq.(2.11), the solution to Eq.(3.37) is

$$C_L(\zeta, \eta) = \left(\frac{\dot{\chi}(\eta)^2}{1 + e^{(r-1)\dot{\chi}(\eta)\zeta}} \right)^{1/(r-1)}. \quad (3.38)$$

Thus, $\lim_{\zeta \rightarrow -\infty} C_L(\zeta, \eta) = \dot{\chi}(\eta)^{2/(r-1)}$. This exactly matches the outer solution at the front, where Eq.(3.9) gives $C_O(\mathcal{X}, t) = \dot{\chi}(t)^{2/(r-1)}$. This is pleasant, since Eq.(3.38) has no parameters to adjust for matching.

Note that the width of the shock layer in this special case is actually $O\left(\frac{\epsilon}{\dot{\chi}(t)}\right)$, as can be seen by inspecting Eq.(3.38). This is a general feature of the solution to Eq.(3.37), as can be seen by changing variables from ζ to $\tilde{\zeta}$ defined by $\zeta = \dot{\chi}(\eta) \cdot \tilde{\zeta}$. Thus the shock layer becomes thicker as the front slows down, but does not tend to slump down as much as the linear case did, where the thickness was $O(\sqrt{\epsilon t})$.

In general, the solution of Eq.(3.37) should go to zero as $\zeta \rightarrow +\infty$ and to a value which satisfies Eq.(3.9) as $\zeta \rightarrow -\infty$. This latter condition is just equivalent to setting the factor \mathcal{K} in Eq.(3.37) to zero. Furthermore, \mathcal{K} will be positive for $\zeta > -\infty$ since $f(C)g(C)\beta(C)/C$ is increasing in C — this implies for $C < C_L(-\infty, \eta)$ that $f(C)g(C)\beta(C)/C < \dot{\chi}^2$. Thus the second term in Eq.(3.37) is positive, so $\partial C_L/\partial \zeta$ is negative. This means that C_L decreases monotonically (as it should on physical grounds) and it can only stop decreasing when the second term of Eq.(3.37) goes to zero. This will only occur when $C_L \rightarrow 0$ since \mathcal{K} is positive for $C_L < C_O(\mathcal{X}, t)$. Thus there will be a solution to Eq.(3.37) which connects the two regions of the outer solution in a distance $O\left(\frac{\epsilon}{\dot{\chi}(t)}\right)$.

The fact that Eq.(3.37) seems to give $\dot{\chi} = \sqrt{k(C_O(\mathcal{X}, t))}$ independently of the derivation of Eq.(3.9) is worthy of note. Actually, it effectively *is* the same deriva-

tion, since Eq.(3.37) is just the expression of flux balance in the layer. Eq.(3.9) was derived as a consequence of flux balance, so when looked at in the correct light, it is not surprising that the results should agree.

If $d(C)$ is positive for all $C \in [0, 1]$, then the layer connection will range over all $\zeta \in (-\infty, +\infty)$ since the endpoints are smooth critical points for Eq.(3.37). Simple linearization shows that $C_L(\zeta, \eta)$ undergoes exponential decay onto its limits as $|\zeta| \rightarrow \infty$.

If $d(C) = O(C^a)$ as $C \rightarrow 0$, for some $a > 0$, then $C_L(\zeta, \eta) \rightarrow 0$ for some $\zeta < +\infty$. This is because for small C_L , Eq.(3.37) becomes

$$\frac{\partial C_L}{\partial \zeta} + \alpha C_L^{1-a} = 0,$$

where α is some positive function of η only. The general solution of this equation is

$$C_L(\zeta, \eta) = a^{1/a} (s(\eta) - \zeta)^{1/a},$$

where $s(\eta)$ is an arbitrary function of η . This solution can only be valid for $\zeta < s(\eta)$. In this case, the front becomes infinitely sharp. Since changing $s(\eta)$ by $O(1)$ can only change the actual position of the front by $O(\epsilon)$, to the order of accuracy carried thus far it is valid to take $s(\eta) \equiv 0$. I have not carried the possibility of an actual sharp front any farther. It seems possible that the results of Kath [8] could be extended to this problem.

Section 3.4 discusses the problems which arise when $k(C)$ is *not* increasing in C . Peculiar things can happen to $C(x, t)$.

Layer Solution When $k(C) \equiv 1$

In this case, the leading order layer equation is more complicated than Eq.(3.37).

Recalling that $\mathcal{X}(\eta) \equiv 1$ in this special case, the *pair* of leading order layer equations is:

$$\frac{\partial C_L}{\partial \eta} = \frac{\partial}{\partial \zeta} \left[d(C_L) \frac{\partial C_L}{\partial \zeta} + f(C_L) \left(\rho_L + \frac{\partial \rho_L}{\partial \eta} \right) \right] \quad (3.39)$$

$$\frac{\partial \rho_L}{\partial \zeta} = -\beta(C_L)g(C_L). \quad (3.40)$$

These equations are considerably messier than Eq.(3.37), since they are coupled partial differential equations while Eq.(3.37) is a single ordinary differential equation with η only appearing as a parameter. Accordingly, less can be said about the solution to Eqs.(3.39,3.40).

Motivated by the linear layer solution Eq.(3.29), change variables to:

$$\mu = \frac{\zeta}{\sqrt{2\eta}} \quad \nu = \sqrt{2\eta} \quad \Longrightarrow \quad \frac{\partial}{\partial \zeta} = \frac{1}{\nu} \frac{\partial}{\partial \mu} \quad \frac{\partial}{\partial \eta} = \frac{1}{\nu} \frac{\partial}{\partial \nu} - \frac{\mu}{\nu^2} \frac{\partial}{\partial \mu}.$$

The crucial step is the definition of μ . This will allow the infinitely steep initial conditions at the left edge to be represented. Observe that μ is the similarity variable for a pure diffusion equation. The 2's in definitions of μ and ν are for algebraic convenience. Defining ν as proportional to $\sqrt{\eta}$ will also be convenient later.

Equations (3.39,3.40) transform to

$$\nu \frac{\partial C_L}{\partial \nu} - \mu \frac{\partial C_L}{\partial \mu} = \frac{\partial}{\partial \mu} \left[d(C_L) \frac{\partial C_L}{\partial \mu} + f(C_L) \left(\nu \rho_L + \frac{\partial \rho_L}{\partial \nu} - \frac{\mu}{\nu} \frac{\partial \rho_L}{\partial \mu} \right) \right] \quad (3.41)$$

$$\frac{\partial \rho_L}{\partial \mu} = -\nu \beta(C_L)g(C_L). \quad (3.42)$$

Some tedious manipulation of these equations leads to

$$\begin{aligned} & \frac{\partial}{\partial \mu} \left[d(C_L) \frac{\partial C_L}{\partial \mu} \right] + 2\mu \frac{\partial C_L}{\partial \mu} + f'(C_L) \frac{\partial C_L}{\partial \mu} \frac{\partial \rho_L}{\partial \nu} \\ & + \nu \left[\rho_L f'(C_L) \frac{\partial C_L}{\partial \mu} - \left(2 - C_L \frac{f'(C_L)}{f(C_L)} \right) \frac{\partial C_L}{\partial \nu} \right] - \nu^2 C_L = 0. \end{aligned} \quad (3.43)$$

When $d(C) \equiv f(C) \equiv \beta(C) \equiv 1$ and $g(C) = C$, it is easy to verify that the linear layer solution Eq.(3.29) solves Eq.(3.43).

To further analyze Eqs.(3.42,3.43), expand the solutions in a power series in ν :

$$C_L(\mu, \nu) = C_{L0}(\mu) + C_{L1}(\mu)\nu + C_{L2}(\mu)\nu^2 + \dots \quad (3.44)$$

$$\rho_L(\mu, \nu) = \rho_{L1}(\mu)\nu + \rho_{L2}(\mu)\nu^2 + \dots \quad (3.45)$$

(If the transformation had been $\nu = \eta$, the expansion would have been in powers of $\nu^{1/2}$.) The first term of the ρ_L series is zero because of Eq.(3.42) and because of the initial condition $\sigma(x, 0) = 0$.

The lowest order in ν , leading order in ϵ , layer equations are now

$$\frac{d}{d\mu} \left[d(C_{L0}) \frac{dC_{L0}}{d\mu} \right] + 2\mu \frac{dC_{L0}}{d\mu} + f'(C_{L0}) \frac{dC_{L0}}{d\mu} \rho_{L1} = 0 \quad (3.46)$$

$$\frac{d\rho_{L1}}{d\mu} + \beta(C_{L0})g(C_{L0}) = 0, \quad (3.47)$$

with the boundary conditions

$$C_{L0}(-\infty) = 1 \quad C_{L0}(+\infty) = 0 \quad \rho_{L1}(+\infty) = 0.$$

Equation (3.47) plus the fact that $\beta(1)g(1) = 1$ says that $\rho_{L1}(\mu) \sim -\mu$ as $\mu \rightarrow -\infty$. This translates to $\frac{\partial \sigma}{\partial x}[\mathcal{X} - O(\sqrt{\epsilon}), t] = -1$ for small t , which corresponds to the series results in Section 3.2.

These results indicate that for short times, the frontal thickness goes as $O(\sqrt{\epsilon t})$, as in the linear case. The higher order terms in the series expansions Eqs.(3.44,3.45) can modify this rule as t (or ν) grows, however. Numerical results for $f(C) = C^r$, $g(C) = C^{1-r}$, $d(C) \equiv \beta(C) \equiv 1$ for $r \in (0, 1)$ show that as $r \rightarrow 1$, the front slumps down progressively faster. This can be understood by noting that for $r = 1$,

Eq.(2.8) says that $\sigma(x, t) = 1 - e^{-t}$ and so there is no stress term at all in Eq.(2.7). Only the diffusive term survives and there is no front. Thus for $r \approx 1$ the front should disappear more quickly since $\sigma(x, t)$ will be more nearly “flat” in x . This is exactly what the numerical simulations show.

3.4 When $k(C)$ Is *NOT* Increasing

Suppose that the factor $\mathcal{K}(C_L, \dot{\mathcal{X}})$ in Eq.(3.37) is positive for values of C a little bit less than $C_O(\mathcal{X} - 0, t)$ but for some positive C^* that $\mathcal{K}(C^*, \dot{\mathcal{X}})$ goes to zero. Then Equation (3.37) will not have a solution which matches the left outer solution to zero at the right. Instead, the layer solution C_L will connect $C_O(\mathcal{X} - O(\epsilon), t)$ to C^* as ζ goes from $-\infty$ to $+\infty$. What then? How can $\lim_{x \rightarrow +\infty} C(x, t) = 0$ be enforced?

The only possible answer is that another non-zero outer solution is needed to take up the slack from $x = \mathcal{X} + O(\epsilon)$ to $x = +\infty$. There is no other scaling of the layer equations which will give a “better” equation than Eq.(3.37). What is more, it is perfectly possible for a new front to develop in *this* outer solution. Thus it is possible to have a multiple front solution, with each front moving at different speeds. (If this happens, only the last front has its speed given by Eq.(3.9), since that result was derived assuming that the outer solution was zero ahead of the front.)

Figure 3.7 shows the results of a numerical simulation with the coefficient functions $f(C) = g(C) = \sqrt{C^{5/2} + .27 C \sin(2\pi C)}$, $d(C) \equiv \beta(C) \equiv 1$. In this totally artificial example, $\mathcal{K}[C, \dot{\mathcal{X}}(t)]$ is initially positive definite, when $\dot{\mathcal{X}}(t) \approx 1$, so that initially there is only one front. But as $\dot{\mathcal{X}}(t)$ decreases, $\mathcal{K}[C, \dot{\mathcal{X}}(t)]$ is no longer positive definite and a second front splits off from the first, with the two fronts connected

by a smooth (outer) type of solution region. The inset in Fig. 3.7 shows the graphs of $f(C)$ and of $k(C)$. Observe that $f(C)$ is monotonic increasing; the peculiar behavior results from a nearly flat region in the graph of $f(C)$.

When $k(C)$ is *decreasing* over the whole domain $C \in [0, 1]$, then all solutions to Eq.(3.37) are *increasing* since the factor \mathcal{K} is negative definite. This means that there is no layer solution C_L and that no fronts develop. This is borne out by numerical computations. Thus the case $k(C) \equiv 1$ is sort of a dividing line between solutions $C(x, t)$ with steep fronts and solutions $C(x, t)$ that are smooth.

3.5 Very Short Times

In the case $k(C) \equiv 1$, the layer solution is valid all the way back to $t = 0$. The frontal thickness goes as $O(\sqrt{\epsilon t})$ for small t (for $t = O(1)$ in the linear case) and so as $t \rightarrow 0$, the front becomes infinitely sharp, as required by the initial conditions.

In contrast, when $k(C) \neq 1$, the layer solution is *not* valid back to $t = 0$. The reason for this is that the frontal thickness is $O(\epsilon/\dot{\mathcal{X}}(t))$, which doesn't become infinitely sharp as $t \rightarrow 0$. This indicates the need for a very short time expansion, during which interval the front will establish itself. The purpose of this section is to establish the duration of this initial period.

As in the analysis of the $k(C) \equiv 1$ layer system, Eqs.(3.39,3.40), the key step is transforming the space variable to a similarity variable for the pure diffusion equation. Define

$$\zeta = \frac{x}{\sqrt{2t}} \quad \eta = 2t \quad \Longrightarrow \quad \frac{\partial}{\partial x} = \frac{1}{\sqrt{\eta}} \frac{\partial}{\partial \zeta} \quad \frac{\partial}{\partial t} = 2 \frac{\partial}{\partial \eta} - \frac{\zeta}{\eta} \frac{\partial}{\partial \zeta}.$$

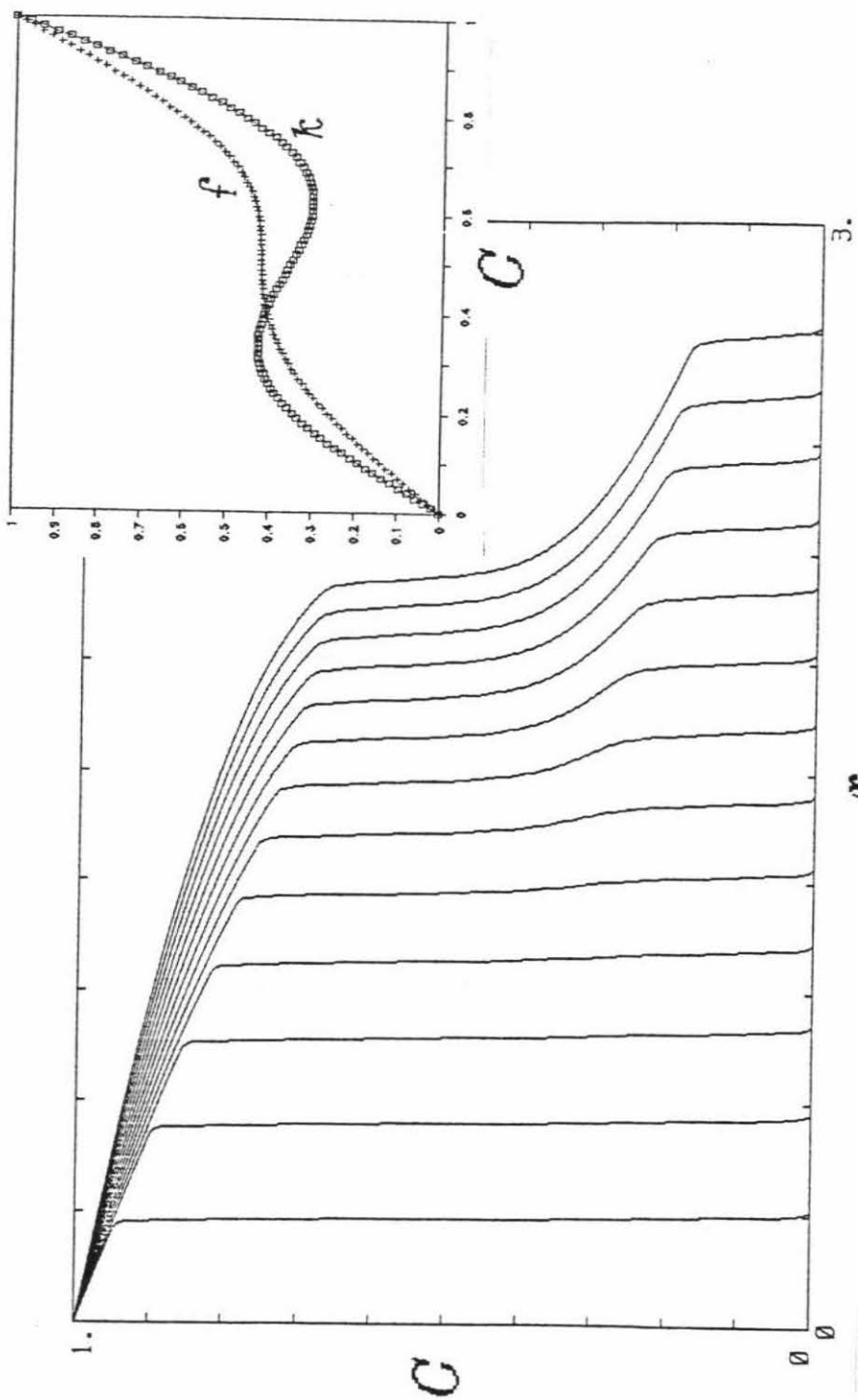


Figure 3.7: C vs. x for $f(C) = g(C) = \sqrt{C^{5/2} + .27 C \sin(2\pi C)}$.

$$d(C) = (3 + 7C)/10, \quad \beta(C) \equiv 1, \quad \epsilon = 0.01.$$

Curves plotted at time intervals $\Delta t = 0.3$.

Notice that, unlike the previous analysis, the time variable is not scaled by a square-root. The reason for this will be given a little later.

Equations (2.7,2.8) transform to

$$\begin{aligned}\epsilon [d(C)C_\zeta]_\zeta + \zeta C_\zeta + [f(C)\sigma_\zeta]_\zeta - 2\eta C_\eta &= 0 \\ 2\eta\sigma_\eta - \zeta\sigma_\zeta + \eta\beta(C)[\sigma - \eta g(C)] &= 0.\end{aligned}$$

The next step is to scale for very short times and distances. Let $\zeta = \epsilon^p \mu$ and $\eta = \epsilon^q \nu$, where p and q are to be found. Since $\sigma = O(t)$ for small t , also scale $\sigma = \epsilon^q \rho$. Then the equations are

$$\begin{aligned}\epsilon^{1-2p} [d(C)C_\mu]_\mu + \mu C_\mu + \epsilon^{q-2p} [f(C)\rho_\mu]_\mu - 2\nu C_\nu &= 0 \\ 2\epsilon^q \nu \rho_\nu - \epsilon^q \mu \rho_\mu + \epsilon^{2q} \nu \beta(C)\rho - \epsilon^q \nu \beta(C)g(C) &= 0.\end{aligned}$$

The dominant balance in the former equation is $1 - 2p = q - 2p = 0$ or $p = \frac{1}{2}$ and $q = 1$. Since $x = \epsilon^{p+q/2} \mu \sqrt{\nu}$ and $t = \epsilon^q \nu / 2$, the effective region being analyzed here is $O(\epsilon)$ in both space and time.

Define C_V and ρ_V as the leading order (in ϵ) very short time solutions. Then the equations for them are

$$\begin{aligned}\frac{\partial}{\partial \mu} \left[d(C_V) \frac{\partial C_V}{\partial \mu} + f(C_V) \frac{\partial \rho_V}{\partial \mu} \right] + \mu \frac{\partial C_V}{\partial \mu} - 2\nu \frac{\partial C_V}{\partial \nu} &= 0 \\ 2\nu \frac{\partial \rho_V}{\partial \nu} - \mu \frac{\partial \rho_V}{\partial \mu} - \nu \beta(C_V)g(C_V) &= 0.\end{aligned}$$

As before, expand the solutions in a power series in ν . Since $\sigma(x, 0) \equiv 0$, the ν^0 term is zero for the ρ expansion:

$$\begin{aligned}C_V(\mu, \nu) &= C_{V0}(\mu) + C_{V1}(\mu)\nu + C_{V2}(\mu)\nu^2 + \dots \\ \rho_V(\mu, \nu) &= \rho_{V1}(\mu)\nu + \rho_{V2}(\mu)\nu^2 + \dots\end{aligned}$$

At this point, I'll observe that in the analysis of Eqs.(3.39,3.40), the ν variable went as \sqrt{t} , but that here it goes as t . In the earlier problem, defining $\nu \propto t$ would have lead to a series in $\nu^{1/2}$, but in this problem, all of the $\nu^{1/2}$ terms cancel out. Thus $\nu \propto t$ is appropriate for this problem but not for the earlier one.

Getting back to the main track, the lowest order in ν , leading order in ϵ equation is simply

$$\frac{d}{d\mu} \left[d(C_{V0}) \frac{dC_{V0}}{d\mu} \right] + \mu \frac{dC_{V0}}{d\mu} = 0. \quad (3.48)$$

The boundary conditions are $C_{V0}(0) = 1$ and $C_{V0}(+\infty) = 0$.

Equation (3.48) is just what one gets if $f(C) \equiv 0$ in Eq.(2.7) and the transformation to similarity variables is made. Thus, for very short times, diffusion is all that counts. It takes until $\nu = O(1)$ or $t = O(\epsilon)$ for the stress effects to match the diffusive effects.

By defining the function $\lambda(C) \equiv \int_0^C d(C) dC$, Eq.(3.48) can be recast to the form $\lambda(C_{V0})_{\mu\mu} + \mu \frac{dC_{V0}}{d\mu} = 0$. This is exactly the problem that is analyzed in Section 4.2, except for the name of the dependent and independent variables. Given that $d(C) > 0$ for all $C \in [0, 1]$, it is proven there that $C_{V0}(\mu)$ exists and is unique.

Higher order (in ν) terms such as C_{V1} and ρ_{V1} could be calculated by solving linear ordinary differential equations. There is little reward for such effort, however, since the details of the $x = O(\epsilon)$, $t = O(\epsilon)$ region aren't of interest. The main result of this section is determining how long it takes the stress effects on C to catch up to diffusion — until $t \geq O(\epsilon)$.

Figure 3.8 shows the very short time stages of the same case as in Fig. 3.1. In these calculations, $f(C) = g(C) = C$, $d(C) \equiv \beta(C) \equiv 1$, and $\epsilon = 0.01$. Fifteen successive

$C(x, t)$ curves are plotted over the domain $x \in [0, 15\epsilon]$ at time interval $\frac{\epsilon}{2}$. The first 2 or 3 curves look more like the results of standard diffusion. By the time the last few curves are reached, the solution has clearly formed the front, which is moving off into the medium. This figure confirms that the front does not actually form until $t \geq O(\epsilon)$.

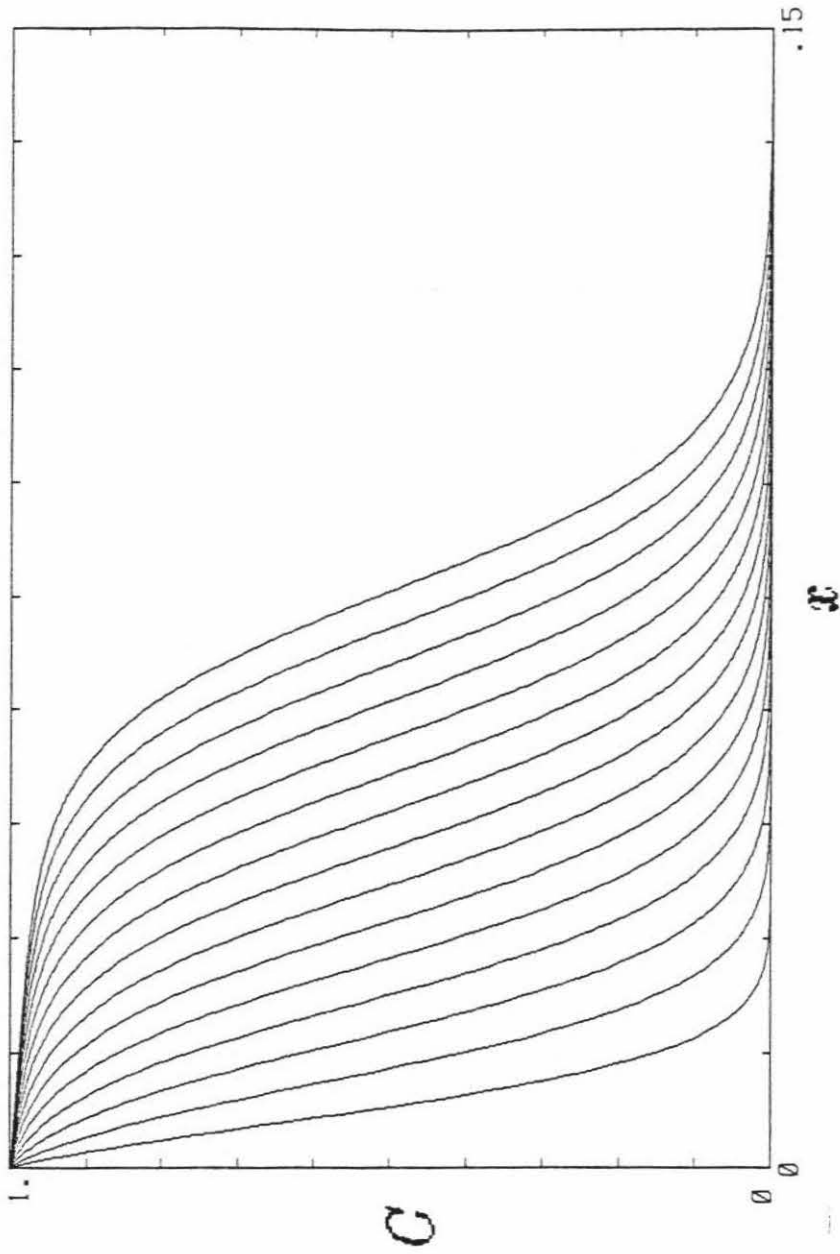


Figure 3.8: C vs. x at very short times, for $f(C) = C$

$$g(C) = C, \quad d(C) \equiv \beta(C) \equiv 1, \quad \epsilon = 0.01.$$

Curves plotted at time intervals $\Delta t = 0.005$.

Chapter 4

Long Time Behavior

WHEN THE FRONT DECAYS AWAY, numerical solutions indicate that the solvent profile $C(x, t)$ continues to propagate into the medium at an ever slower rate. Figure 4.1 shows the long time evolution of the same case as in Fig. 3.1, where $f(C) = C$. After the step in C at the front has disappeared, the whole graph of $C(x, t)$ continues to stretch out to the right. This suggests a similarity solution; this chapter will show that $C(x, t)$ is asymptotic to a $\frac{x}{\sqrt{t}}$ type of similarity solution as $t \rightarrow \infty$. The ordinary differential equation for the similarity solution will be derived and the existence of a unique solution will be demonstrated in the first two sections. The necessity for assuming Eq.(2.13) will become apparent in these sections; Section 4.3 will discuss the problems that arise when Eq.(2.13) does *not* hold true. In Section 4.4, the similarity solution will be used to approximate the short time behavior.

Note: The results of the first two sections of this chapter do *not* rely on ϵ being small. They only require that ϵ be positive. The asymptotic analysis in these sections is concerned with $t \rightarrow \infty$, *not* with $\epsilon \rightarrow 0^+$.

4.1 Asymptotic Similarity Solution

As has happened twice before, change the space variable x to a similarity variable for the pure diffusion equation by defining $\zeta = \frac{x}{\sqrt{2t}}$. Also define $\eta = \frac{1}{\sqrt{2t}}$ — this

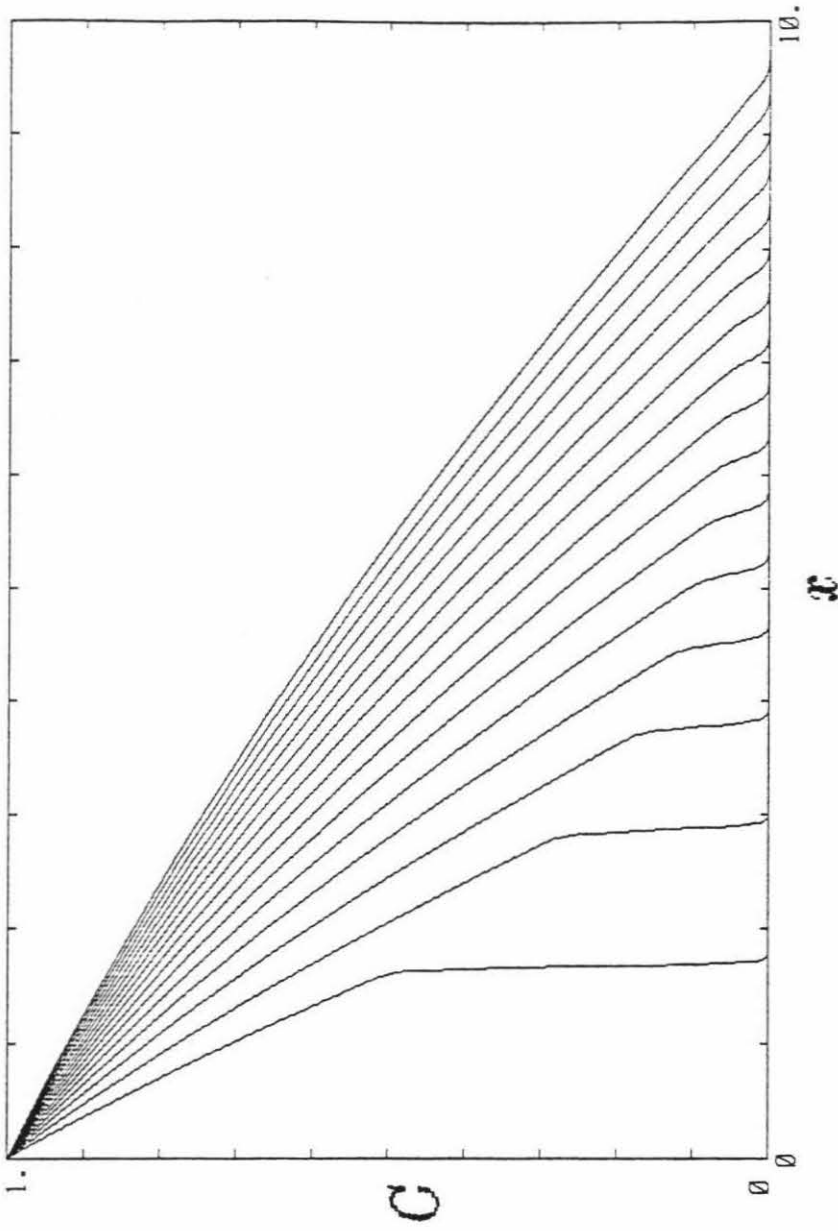


Figure 4.1: C vs. x for $f(C) = C$.

$$g(C) = C, \quad d(C) \equiv \beta(C) \equiv 1, \quad \epsilon = 0.01.$$

Curves plotted at time intervals $\Delta t = 2.0$.

will be appropriate for long times. Then partial derivatives transform by the rules

$$\frac{\partial}{\partial x} = \eta \frac{\partial}{\partial \zeta} \quad \text{and} \quad \frac{\partial}{\partial t} = -\eta^3 \frac{\partial}{\partial \eta} - \zeta \eta^2 \frac{\partial}{\partial \zeta}.$$

Then Eqs.(2.7,2.8) transform to

$$[\epsilon d(C)C_\zeta + f(C)\sigma_\zeta]_\zeta + \zeta C_\zeta + \eta C_\eta = 0 \quad (4.1)$$

$$\beta(C)[g(C) - \sigma] + \zeta \eta^2 \sigma_\zeta + \eta^3 \sigma_\eta = 0. \quad (4.2)$$

Long time $t \rightarrow \infty$ is the same as $\eta \rightarrow 0^+$. Therefore, expand the solutions to these equations as

$$\begin{aligned} C(\zeta, \eta) &= C_S(\zeta) + \eta C_1(\zeta) + \eta^2 C_2(\zeta) + \dots \\ \sigma(\zeta, \eta) &= \sigma_S(\zeta) + \eta \sigma_1(\zeta) + \eta^2 \sigma_2(\zeta) + \dots \end{aligned}$$

Then, on plugging these expansions into Eqs.(4.1,4.2), the $O(\eta^0)$ equation becomes

$$\frac{d}{d\zeta} \left[\epsilon d(C_S) \frac{dC_S}{d\zeta} + f(C_S) g'(C_S) \frac{dC_S}{d\zeta} \right] + \zeta \frac{dC_S}{d\zeta} = 0. \quad (4.3)$$

I have distinguished the lowest order terms C_S and σ_S with a subscript S to indicate that they are the surviving Similarity solution as $t \rightarrow \infty$.

Next, define $h(C)$ by

$$h(C) = \int_0^C \epsilon d(C) + f(C) g'(C) dC. \quad (4.4)$$

Then Eq.(4.3) takes the form

$$\frac{d^2}{d\zeta^2} h(C_S) + \zeta \frac{dC_S}{d\zeta} = 0. \quad (4.5)$$

The boundary conditions are from Eq.(2.10):

$$C_S(0) = 1 \quad \text{and} \quad C_S(\infty) = 0. \quad (4.6)$$

The solution to the boundary value problem Eqs.(4.5,4.6) provides the long time behavior of the solvent concentration. A numerical solution of this problem with $f(C) = g(C) = C$, $d(C) \equiv 1$ and $\epsilon = 0.01$, giving $h(C) = \epsilon C + \frac{1}{2}C^2$, compares very well with the later curves in Fig. 4.1.

It is not immediately obvious (at least to me) that a solution to the nonlinear boundary value problem Eqs.(4.5,4.6) exists or that it must be unique. The next section is devoted to the proof that $C_S(\zeta)$ *does* in fact exist and is unique.

4.2 Similarity Equation Has a Solution

At long last the requirement in Eq.(2.13) will be used! That equation simply states that $h'(C) > 0$ for all $C \in [0, 1]$. Thus there are bounds \mathcal{P} and \mathcal{Q} such that

$$0 < \mathcal{Q} \leq \frac{1}{h'(C)} \leq \mathcal{P} < \infty. \quad (4.7)$$

These bounds will be crucial in the analysis below.

Shooting for the Solution

Consider the initial value problem for C_I (where the I is a reminder for Initial) given by

$$\frac{d^2}{d\zeta^2} h(C_I) + \zeta \frac{dC_I}{d\zeta} = 0 \quad \text{with} \quad C_I(0; s) = 1 \quad \text{and} \quad \frac{dC_I}{d\zeta}(0; s) = s; \quad (4.8)$$

that is, C_I satisfies the same ordinary differential equation as C_S but instead of the boundary condition at $\zeta = \infty$, C_I has its first derivative equal to s at $\zeta = 0$. Here, s is any negative real number. I will show that there is a unique s such that $C_I(\infty; s) = 0$. This has some analogies with the “shooting” method used in the numerical solution of boundary value problems.

The solution to Eq.(4.8) may not be defined for all ζ . The coefficients $f(C)$, $g(C)$, and $d(C)$, are only defined for $C \in [0, 1]$, so $h(C)$ is only defined in that same domain. Thus, strictly speaking, if $C_I(\zeta^*; s) = 0$ then $C_I(\zeta; s)$ is undefined for $\zeta > \zeta^*$. But for any finite s , C_I will be defined over at least *some* interval. Of course, it is possible that C_I never goes to 0, even as $\zeta \rightarrow \infty$, in which case there is no problem with its definition for all $\zeta \geq 0$.

If $s < 0$, then C_I must be monotonically decreasing. To see this, assume that at some point ζ_0 , $\frac{dC_I}{d\zeta}(\zeta_0; s) = 0$. Then the function $C_I(\zeta; s) \equiv C_I(\zeta_0; s)$ is a perfectly good solution to the differential equation which matches the function and its derivative at ζ_0 . Since solutions to initial value problems are unique, this means that this is the *only* solution that passes through ζ_0 with slope 0 and the value of $C_I(\zeta_0; s)$. But this contradicts the statement that $s < 0$. Thus $dC_I/d\zeta < 0$ for $s < 0$. (When $s = 0$, then it is trivial that $C_I(\zeta; 0) \equiv 1$.)

Missing the Target — Shooting Too High

Next consider the derivative of C_I with respect to s (the *first variation* of C_I , as it is called). It satisfies the equation

$$\frac{d^2}{d\zeta^2} \left[h'(C_I) \frac{\partial C_I}{\partial s} \right] + \zeta \frac{d}{d\zeta} \left[\frac{\partial C_I}{\partial s} \right] = 0. \quad (4.9)$$

Since C_I is unknown for most values of s , solving this equation isn't particularly easy even though it is linear in $\frac{\partial C_I}{\partial s}$. But C_I is known for $s = 0$ and it is just a constant. Noting that the initial conditions on $\frac{\partial C_I}{\partial s}$ are

$$\frac{\partial C_I}{\partial s}(0; s) = 0 \quad \text{and} \quad \frac{d}{d\zeta} \frac{\partial C_I}{\partial s}(0; s) = 1, \quad (4.10)$$

the solution to Eqs(4.9,4.10) for $s = 0$ is easily calculated to be

$$\frac{\partial C_I}{\partial s}(\zeta; 0) = \sqrt{\frac{\pi h'(1)}{2}} \operatorname{erf} \left(\frac{\zeta}{\sqrt{2h'(1)}} \right).$$

The important thing to note is that $\frac{\partial C_I}{\partial s}(\zeta; 0)$ is bounded. This means that even as $\zeta \rightarrow \infty$, a small value of s will only produce a small change in $C_I(\zeta; s)$ from the identically 1 solution $C_I(\zeta; 0)$.

The desired solution has $C_S(\infty) = 0$. The above analysis shows that for small enough $|s|$ ($s < 0$), then $C_I(\infty; s) > 0$. The final step in the proof that $C_S(\zeta)$ exists is to show that when $|s|$ is large enough ($s < 0$) then $C_I(\zeta; s)$ must go to 0 for some $\zeta < \infty$. If this is true, then continuity of $C_I(\zeta; s)$ with respect to s ensures that some s^* exists such that $C_I(\zeta; s^*)$ is indeed just $C_S(\zeta)$, the solution to Eqs.(4.5,4.6).

Missing the Target — Shooting Too Low

Rewrite Eq.(4.8) as

$$h'(C_I) \frac{d^2 C_I}{d\zeta^2} + h''(C_I) \left(\frac{dC_I}{d\zeta} \right)^2 + \zeta \frac{dC_I}{d\zeta} = 0.$$

Divide by $h'(C_I) \frac{dC_I}{d\zeta}$ to get

$$\frac{d^2 C_I}{d\zeta^2} \bigg/ \frac{dC_I}{d\zeta} + \frac{h''(C_I)}{h'(C_I)} \cdot \frac{dC_I}{d\zeta} = -\frac{\zeta}{h'(C_I)}.$$

Recognizing that each term on the left is a logarithmic derivative, and recalling that $\frac{dC_I}{d\zeta} < 0$ and $h'(C_I) > 0$ gives

$$\frac{d}{d\zeta} \log \left| \frac{dC_I}{d\zeta} h'(C_I) \right| = -\frac{\zeta}{h'(C_I)}$$

Applying the bounds in Eq.(4.7) now yields the inequalities

$$-Q\zeta \geq \frac{d}{d\zeta} \log \left| \frac{dC_I}{d\zeta} h'(C_I) \right| \geq -P\zeta.$$

Integrate these inequalities from 0 to ζ to get

$$-\frac{Q\zeta^2}{2} \geq \log \left| \frac{dC_I}{d\zeta} h'(C_I) \right| - \log |sh'(1)| \geq -\frac{P\zeta^2}{2}.$$

Thus, upper and lower bounds on $\frac{dC_I}{d\zeta}$ are obtained:

$$\frac{|s|h'(1)}{h'(C_I)}e^{-Q\zeta^2/2} \geq \left| \frac{dC_I}{d\zeta} \right| \geq \frac{|s|h'(1)}{h'(C_I)}e^{-P\zeta^2/2}$$

Apply the bounds in Eq.(4.7) again, and change the signs to get

$$-P|s|h'(1)e^{-Q\zeta^2/2} \leq \frac{dC_I}{d\zeta} \leq -Q|s|h'(1)e^{-P\zeta^2/2}. \quad (4.11)$$

I have written $s = -|s|$ to emphasize that the above bounds are negative.

Now, integrate Eq.(4.11) from 0 to ζ . The results are upper and lower bounds for $C_I(\zeta)$:

$$1 - \sqrt{\frac{\pi}{2}} \frac{P}{Q^{1/2}} h'(1)|s| \operatorname{erf} \left(\zeta \sqrt{\frac{Q}{2}} \right) \leq C_I(\zeta; s) \leq 1 - \sqrt{\frac{\pi}{2}} \frac{Q}{P^{1/2}} h'(1)|s| \operatorname{erf} \left(\zeta \sqrt{\frac{P}{2}} \right). \quad (4.12)$$

Since $\operatorname{erf}(x) \rightarrow 1$ as $x \rightarrow +\infty$, two conclusions can be drawn from Eq.(4.12). When $|s| > \sqrt{\frac{2}{\pi}} \frac{P^{1/2}}{Q h'(1)}$, then the upper bound goes to zero for some $\zeta < +\infty$, and so $C_I(\zeta; s)$ must also go to zero somewhere. This completes the existence proof for $C_S(\zeta)$, the solution to Eqs.(4.5,4.6).

The other conclusion to be drawn from Eq.(4.12) comes from the lower bound. When $|s| < \sqrt{\frac{2}{\pi}} \frac{Q^{1/2}}{P h'(1)}$, then $C_I(\zeta; s) > 0$ for all $\zeta \in (0, +\infty)$. Thus the critical value of s^* that gives $C_I(+\infty; s^*) = 0$ can be bounded between two values. How useful these bounds on s^* are depends on how close Q is to P .

Uniqueness of C_S

Consider again the variational function $\frac{\partial C_I}{\partial s}$. Integrate Eq.(4.9) from 0 to ζ to find

$$\frac{d}{d\zeta} \left[h'(C_I) \frac{\partial C_I}{\partial s} \right] + \zeta \frac{\partial C_I}{\partial s} = \int_0^\zeta \frac{\partial C_I}{\partial s} d\zeta + h'(1). \quad (4.13)$$

Now, suppose that $\frac{\partial C_I}{\partial s}(\zeta^*; s) = 0$ for some $\zeta^* > 0$ and that ζ^* is the *first* such positive zero of $\frac{\partial C_I}{\partial s}$ — thus, $\frac{\partial C_I}{\partial s}(\zeta; s) > 0$ for $\zeta \in (0, \zeta^*)$. Evaluating Eq.(4.13) at ζ^* gives

$$h'(C_I(\zeta^*; s)) \frac{d}{d\zeta} \frac{\partial C_I}{\partial s}(\zeta^*; s) = \int_0^{\zeta^*} \frac{\partial C_I}{\partial s} d\zeta + h'(1). \quad (4.14)$$

The right hand side of Eq.(4.14) is positive but the left hand side is non-positive since ζ^* is the *first* zero of $\frac{\partial C_I}{\partial s}$. This is a contradiction, and so $\frac{\partial C_I}{\partial s}(\zeta; s) > 0$ for all $\zeta > 0$.

This result implies that $C_I(\zeta; s)$ is monotonic increasing in s , at least for finite ζ . Thus, if there are *two* values s_1 and s_2 that have $C_I(\infty; s_j) = 0$, then all values $s \in [s_1, s_2]$ also satisfy this boundary condition. Therefore, if C_S is *not* unique, then $\lim_{\zeta \rightarrow \infty} \frac{\partial C_I}{\partial s}(\zeta; s) = 0$ for all s such that $\lim_{\zeta \rightarrow \infty} C_I(\zeta; s) = 0$. For all such s , Eq.(4.9) is asymptotically

$$h'(0) \frac{d^2}{d\zeta^2} \frac{\partial C_I}{\partial s} + \zeta \frac{d}{d\zeta} \frac{\partial C_I}{\partial s} = 0$$

so that $\frac{\partial C_I}{\partial s}(\zeta; s) \sim A \operatorname{erfc} \left(\frac{\zeta}{\sqrt{2h'(0)}} \right) + B$ as $\zeta \rightarrow \infty$, for some constants A and B .

If $B = 0$, then $\frac{\partial C_I}{\partial s}(\zeta; s)$ goes to zero exponentially fast as $\zeta \rightarrow \infty$. But then evaluating Eq.(4.13) as $\zeta \rightarrow \infty$ gives zero on the left and a positive value on the right. Thus $\frac{\partial C_I}{\partial s}(\zeta; s)$ remains positive even as $\zeta \rightarrow \infty$ and uniqueness of $C_S(\zeta)$ is proven.

4.3 When $h(C)$ Is *NOT* Increasing

What happens when $h(C)$ is not monotonic increasing? The brief answer to this question is that the solution may become discontinuous! The problem becomes

difficult to analyze, and this section is made up mostly of conjectures and speculations, guided by a little analysis.

Finite Medium and Equilibrium

The first case I will consider is a finite medium. To what state does the system go as $t \rightarrow +\infty$? An equilibrium solution (C_E, σ_E) satisfies the equations

$$\begin{aligned} \frac{d}{dx} \left[\epsilon d(C_E) \frac{dC_E}{dx} + f(C_E) \frac{d\sigma_E}{dx} \right] &= 0 \\ g(C_E) - \sigma_E &= 0, \end{aligned}$$

together with the boundary conditions

$$C_E(0) = 1 \quad \text{and} \quad C_E(\ell) = 0. \quad (4.15)$$

The differential equation can be rewritten as

$$\frac{d}{dx} \left[\epsilon d(C_E) \frac{dC_E}{dx} + f(C_E) g'(C_E) \frac{dC_E}{dx} \right] = 0,$$

or more compactly as

$$\frac{d^2}{dx^2} h(C_E) = 0, \quad (4.16)$$

where $h(C)$ is the same function introduced in Eq.(4.4) in Section 4.1.

Assuming that $h(C)$ is monotonic, then Eqs.(4.16,4.15) are easily solved, at least implicitly. Clearly, $h(C_E(x)) = ax + b$ for some constants a and b . The right boundary condition and the fact that $h(0) = 0$ imply that the solution can in fact be written as $h(C_E(x)) = A(\ell - x)$, where A is a constant. The left boundary condition now says that $A = h(1)/\ell$. Under the assumptions on $h(C)$, there is no trouble about inverting the equation $h(C_E(x)) = A(\ell - x)$ to find a unique equilibrium solution $C_E(x)$.

Observe that if $\ell \rightarrow \infty$, then $A \rightarrow 0$ but that $A\ell$ remains finite (fixed, in fact). The equilibrium solution is given by $h(C_E(x)) = A\ell - Ax$, so that as $\ell \rightarrow \infty$, for any finite x , $h(C_E(x)) = A\ell$ or $C_E(x) = 1$. Thus there is no equilibrium solution for $\ell = \infty$, as claimed earlier in Section 3.2. The closest thing there is to an equilibrium state for a semi-infinite medium is the asymptotic similarity solution discussed earlier. This state of affairs is analogous to what occurs for the pure diffusion equation.

But what if $h(C)$ is *not* monotonic? Then the equilibrium solution $C_E(x)$ is apparently multi-valued! This is not very reasonable. The usual suspicion would be a discontinuous solution. This is exactly what the numerical solutions show — assuming that the numerical method has any validity when the solution is discontinuous.

Away from any discontinuity, the equilibrium solution must still satisfy $h(C_E(x)) = Ax + B$, but it is not so clear that A and B must be the same on either side of the jump. Since the flux must be a constant at equilibrium, in fact A must be equal across any jump, but this argument does not apply to B . Thus the equilibrium solution can be written in the form

$$h(C_E(x)) = \begin{cases} h(1) - Ax & \text{for } x < x_* \\ A(\ell - x) & \text{for } x > x_* \end{cases},$$

where x_* is the location of the jump. The problem is to find the two constants A and x_* . For a reasonable solution, the condition that $C_E(x_* - 0) > C_E(x_* + 0)$ can be imposed, but this is only a mild restriction on the variability of A and x_* .

The partial differential equations do not appear to give any guidance for selecting the solution. One idea is to linearize about the putative equilibrium state and see if

stability arguments can select the solution. This does not work: no discontinuous equilibrium solution is more stable than any other. Even imposing the *ad hoc* condition that B must be the same across the jump, implying that $A = \ell/h(1)$, still leaves a great deal of flexibility in choosing x_* .

The rest of this section is predicated on the assumption that the numerical results have some validity even when the solution becomes discontinuous. The basis for this assumption is the conservative nature of numerical difference scheme used (see Appendix A). Eq.(2.7) for $C(x, t)$ is also a conservation law, and so it is not *too* unreasonable to hope that a discrete conservation law and a continuous conservation law might have some features in common.

The position of the equilibrium discontinuity seems to depend on the previous history of $C(x, t)$. Figure 4.2 shows the final state of two numerical calculations. Both runs had the same coefficient functions: $f(C) = C$, $g(C) = C/\beta(C) = [2 - \tanh(8C - 4)] \cdot C$, and $\epsilon d(C) \equiv 0.03$. The medium length is $\ell = 1$. The choice of $g(C)$ was made to model a phase transition in the medium: when $C > \frac{1}{2}$, then the medium suddenly becomes less able to support stress. This is intended to model the transition from glassy to rubbery that occurs in some polymers. The relaxation time $1/\beta(C)$ undergoes a corresponding decline across the phase transition.

Curve **A** in Fig. 4.2 was calculated with $C(0, t) = 1$ for all $t > 0$; that is, C is raised to 1 at $x = 0$ instantly. Curve **B** had $C(0, t) = \frac{1}{2}$ for $0 < t \leq 2$ and then $C(0, t) = 1$ for $t > 2$; that is, C is raised up to 1 in two stages. The resulting equilibrium states are different. This indicates that deciding the location of the jump cannot be done by linearizing about the equilibrium state, since in such an analysis the early time behavior of the solution does not come in at all.

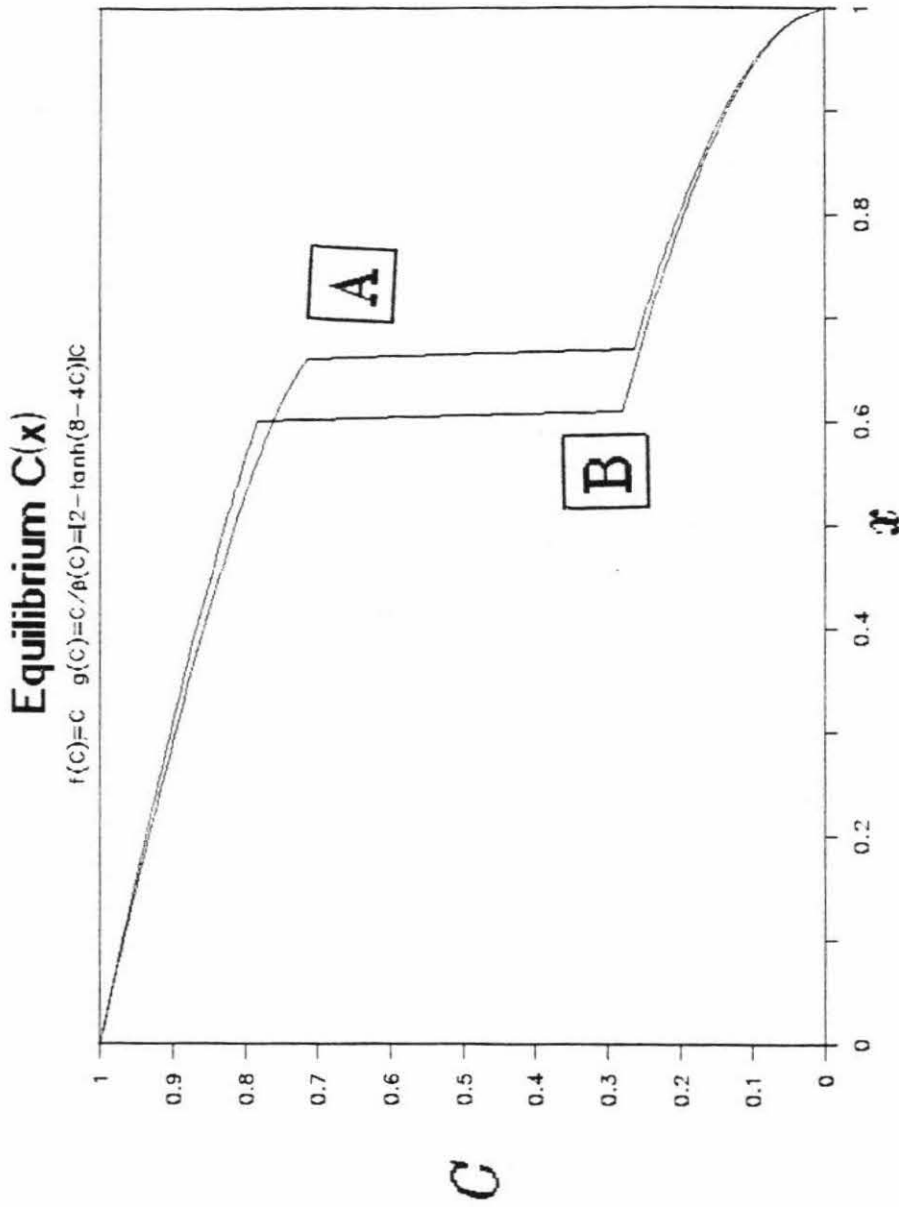


Figure 4.2: Equilibrium Discontinuous Solutions

$$f(C) = C, \quad g(C) = C/\beta(C) = [2 - \tanh(8C - 4)] \cdot C, \quad \epsilon d(C) \equiv 0.03.$$

$$\boxed{A}: C(0, t) = 1 \quad \forall t > 0$$

$$\boxed{B}: C(0, t) = \frac{1}{2} \quad \forall t \in (0, 2]; \quad C(0, t) = 1 \quad \forall t > 2$$

Non-Equilibrium Discontinuities

The solution need not get all the way to equilibrium for a discontinuity to develop. Figure 4.3 shows the results of a numerical solution with the same coefficients as in Fig. 4.2, but with a longer medium. The solution $C(x, t)$ still has a progressing front, but a discontinuity has developed behind the front.

It would be very interesting to be able to make the discontinuity in the solution actually propagate. I have never seen this happen in any numerical run. In every case, once $C(x, t)$ starts to steepen up towards the discontinuity, the location of the jump becomes frozen as if set in concrete. In fact, the initial motivation for introducing the convective term in Chapter 5 was to break the discontinuity free and make it move. This did not work, but it lead to other interesting results.

4.4 Similarity and Short Time Outer Solutions

Examining Fig. 4.1, I was struck by the fact that the solutions to the left of the fronts look quite a bit like pieces of the asymptotic similarity solution C_S . This motivated me to try to fit the short time outer solutions $C_O(x, t)$ with an appropriately stretched piece of $C_S(\zeta)$. The goal of this section is to find a function $\mathcal{S}(t)$ (short for *Scale*) such that

$$C_O(x, t) \approx C_S(\mathcal{S}(t)x) \quad \text{for } 0 < x < \mathcal{X}(t). \quad (4.17)$$

It was very easy to find such a $\mathcal{S}(t)$ numerically that gave a very good fit for the case $f(C) = C$ in Fig. 4.1. This suggests using Eq.(4.17) as the basis for a different kind of approximation to $C_O(x, t)$.

The only unknowns are three functions of one variable: $C_S(\zeta)$, $\mathcal{X}(t)$, and $\mathcal{S}(t)$. Furthermore, $C_S(\zeta)$ can be calculated from Eqs.(4.5,4.6) using a standard boundary

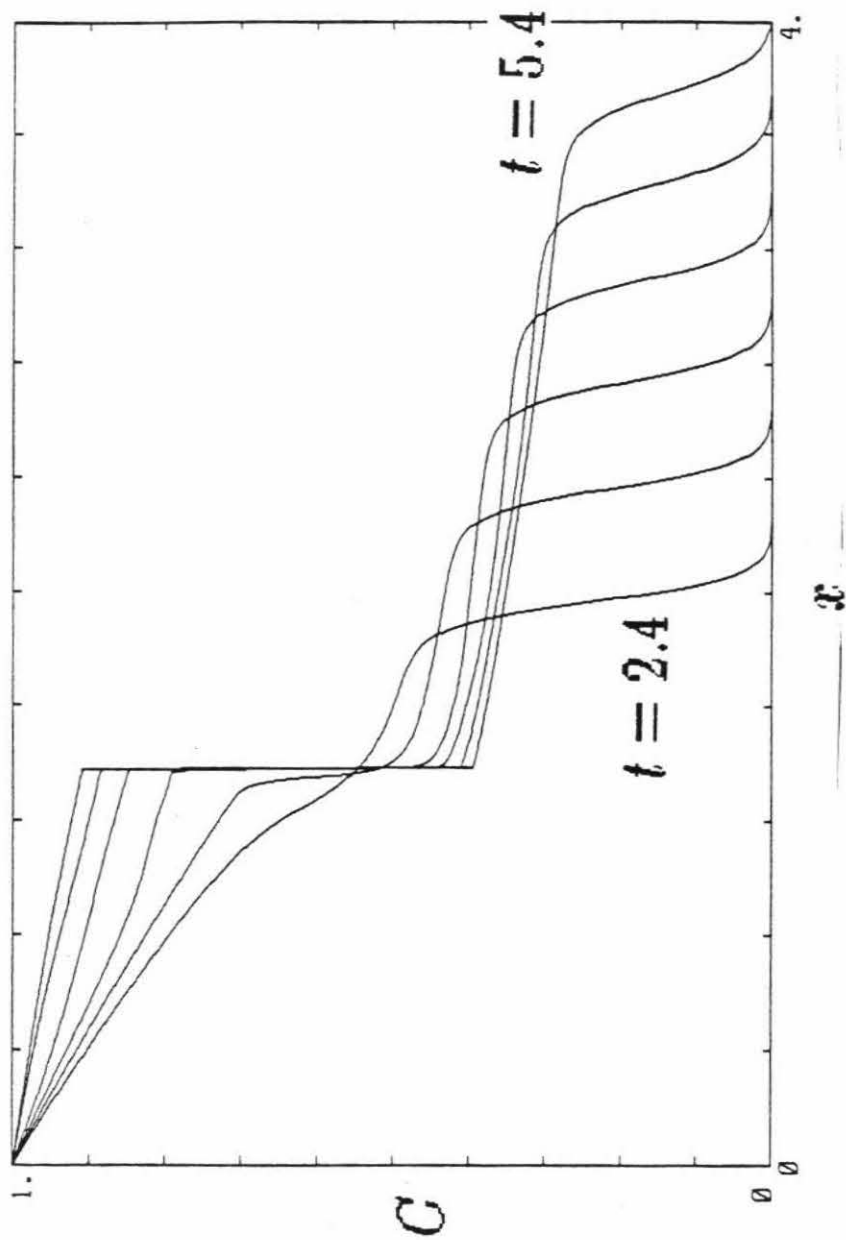


Figure 4.3: Discontinuous Solution with a Front
 $f(C) = C, g(C) = C/\beta(C) = [2 - \tanh(8C - 4)] \cdot C, \epsilon d(C) \equiv 0.03.$
Curves plotted at time interval $\Delta t = 0.6$, starting at $t = 2.4$.

value code such as *COLSYS*. Equation (3.9) gives an equation for the evolution of $\mathcal{X}(t)$:

$$\dot{\mathcal{X}} = \left(\frac{fg\beta}{C_S} \right)^{\frac{1}{2}}, \quad (4.18)$$

where the Argument of C_S is $\mathcal{A}(t) \equiv \mathcal{X}(t)\mathcal{S}(t)$, and the arguments of f , g , and β are $C_S(\mathcal{A})$. All that is needed to round out the system is some equation for the evolution of $\mathcal{S}(t)$.

The partial differential equation Eq.(3.1) cannot be expected to hold exactly when the approximation in Eq.(4.17) is made, but clearly Eq.(3.1) must be imposed in *some* sense. My first thought was to require the PDE to hold in the mean; that is, require

$$\int_0^{\mathcal{X}(t)} \left(\frac{\partial C_O}{\partial t} - \frac{\partial}{\partial x} \left[f(C_O) \frac{\partial C_O}{\partial x} \right] \right) dx = 0 \quad \text{for all } t > 0.$$

This, however, leads to a complicated integro-differential equation for $\mathcal{S}(t)$.

It would be nice to get just an ordinary differential equation for $\mathcal{S}(t)$. Requiring the PDE Eq.(3.1) to hold only at *one* point will give such a result. Pick this point to be $x = \mathcal{X}(t)$: at the front. This is the point where Eq.(4.18) applies.

The condition that will yield the equation for $\mathcal{S}(t)$ is thus

$$\left[\frac{\partial C_O}{\partial t} - f'(C_O) \frac{\partial C_O}{\partial x} \frac{\partial \sigma_O}{\partial x} - f(C_O) \frac{\partial^2 \sigma_O}{\partial x^2} \right]_{x=\mathcal{X}(t)} = 0. \quad (4.19)$$

Using Eq.(4.17) gives

$$\frac{\partial C_O}{\partial t} \Big|_{x=\mathcal{X}} = \mathcal{X} \dot{\mathcal{S}} C'_S \quad (4.20)$$

$$\frac{\partial C_O}{\partial x} \Big|_{x=\mathcal{X}} = \mathcal{S} C'_S. \quad (4.21)$$

Here and below, the arguments of C_S and C'_S are both $\mathcal{A} = \mathcal{X}\mathcal{S}$; the arguments of the functions f , g , and β are $C_S(\mathcal{A})$.

Equations (3.8,3.9) combine to give

$$\left. \frac{\partial \sigma_O}{\partial x} \right|_{x=\mathcal{X}} = - \left(\frac{C_S \beta g}{f} \right)^{\frac{1}{2}} \quad (4.22)$$

The only thing missing from Eq.(4.19) is $\frac{\partial^2 \sigma_O}{\partial x^2}(\mathcal{X}, t)$. This can be evaluated from Eq.(3.12):

$$\left. \frac{\partial^2 \sigma_O}{\partial x^2} \right|_{x=\mathcal{X}} = - \frac{1}{\dot{\mathcal{X}}^2} \left[(\beta g)' \left(\frac{\partial C_O}{\partial x} \dot{\mathcal{X}} + \frac{\partial C_O}{\partial t} \right) + \frac{\partial^2 \sigma_O}{\partial x \partial t} \dot{\mathcal{X}} + \frac{\partial \sigma_O}{\partial x} \ddot{\mathcal{X}} \right]_{x=\mathcal{X}} \quad (4.23)$$

The only pieces of *this* that are missing are $\ddot{\mathcal{X}}$ and $\frac{\partial^2 \sigma_O}{\partial x \partial t}(\mathcal{X}, t)$. The first is supplied by differentiating Eq.(4.18); this has already been done in Eq.(3.10). The second is supplied by differentiating Eq.(2.8) with respect to x :

$$\left. \frac{\partial^2 \sigma_O}{\partial x \partial t} \right|_{x=\mathcal{X}} = \left[(\beta g)' \frac{\partial C_O}{\partial x} - \beta \frac{\partial \sigma_O}{\partial x} \right]_{x=\mathcal{X}} \quad (4.24)$$

Equations (4.20–4.24) can now be plugged into Eq.(4.19). As can be imagined, the algebra is messy and so is the resulting ordinary differential equation for $\mathcal{S}(t)$. The equation is simplified somewhat by presenting it as an equation for $\mathcal{A}(t)$:

$$\dot{\mathcal{A}} = 2 \frac{\frac{\beta C_S}{|C'_S|} - \frac{k' C_S}{k^{1/2}} \frac{\mathcal{A}}{\mathcal{X}}}{3 + C_S \left(\frac{\beta'}{\beta} + \frac{g'}{g} - \frac{f'}{f} \right)}. \quad (4.25)$$

I have written $-C'_S = |C'_S|$ as a reminder that C_S is strictly decreasing. Also, recall that all functions are to be evaluated at the front: C_S and C'_S at \mathcal{A} ; f , g , β , f' , g' , and β' at $C_S(\mathcal{A})$ — and $k(C)$ is shorthand for $f(C)g(C)\beta(C)/C$.

Since C_S can be pre-computed without reference to \mathcal{X} or \mathcal{A} , Eqs.(4.18,4.25) are a pair of first order ordinary differential equations for the position of the front (\mathcal{X}) and the argument of the similarity solution at the front (\mathcal{A}).

The initial conditions are just $\mathcal{X}(0) = 0$ and $\mathcal{A}(0) = 0$. These, however, are not quite enough to specify the solution of the ODEs. This is because $\frac{\mathcal{A}}{\mathcal{X}}$ occurs in Eq.(4.25), and $\lim_{t \rightarrow 0} \frac{\mathcal{A}}{\mathcal{X}} = \mathcal{S}(0)$ has not yet been provided. This difficulty is easily overcome. Combining Eq.(3.18) and Eq.(4.21) gives the result

$$\lim_{t \rightarrow 0} \frac{\mathcal{A}}{\mathcal{X}} = \mathcal{S}(0) = \frac{2}{|C'_S(0)[1 + f'(1) + 3g'(1) + 3\beta'(1)]}. \quad (4.26)$$

This result can also be derived by using L'Hospital's rule on Eq.(4.25). With this result in hand, all the information necessary to use a standard initial value ODE routine is now available.

Results and Comparison with Padé Approximants

I was planning to show a figure with plots of $\dot{\mathcal{X}}(t)$ from the numerical solution of the PDEs and from this section's similarity approximation — this figure would have been a new version of Fig. 3.5. However, the similarity approximation to $\dot{\mathcal{X}}(t)$ in both cases ($f(C) = C$ and $f(C) = C(2 - C)$) is so good that it plots directly on top of the curve from the numerical solution of the PDEs. Thus, the proposed figure would be rather boring. The same remarks apply to plots of the solvent uptake rate $R(t)$ — an updated version of Fig. 3.6 would also be very dull, since the similarity approximation to $R(t)$ is very good in both cases.

Instead, Fig. 4.4 shows the relative errors in the front position \mathcal{X} and the total solvent uptake $\int C dx$. The case here is $f(C) = C(2 - C)$ (as usual, $g(C) = C$, $d(C) \equiv \beta(C) \equiv 1$). The similarity approximation is seen to give accurate results for $t > 0.5$ — better than 1%.

Why does this work so well? After all, the solution $C_S(\zeta)$ is supposed to be good for “long times” and the frontal behavior being modeled here is strictly a “short time” phenomenon.

Relative Errors in $X(t)$ and in $\int C dx$

Similarity Approximation - Numerics

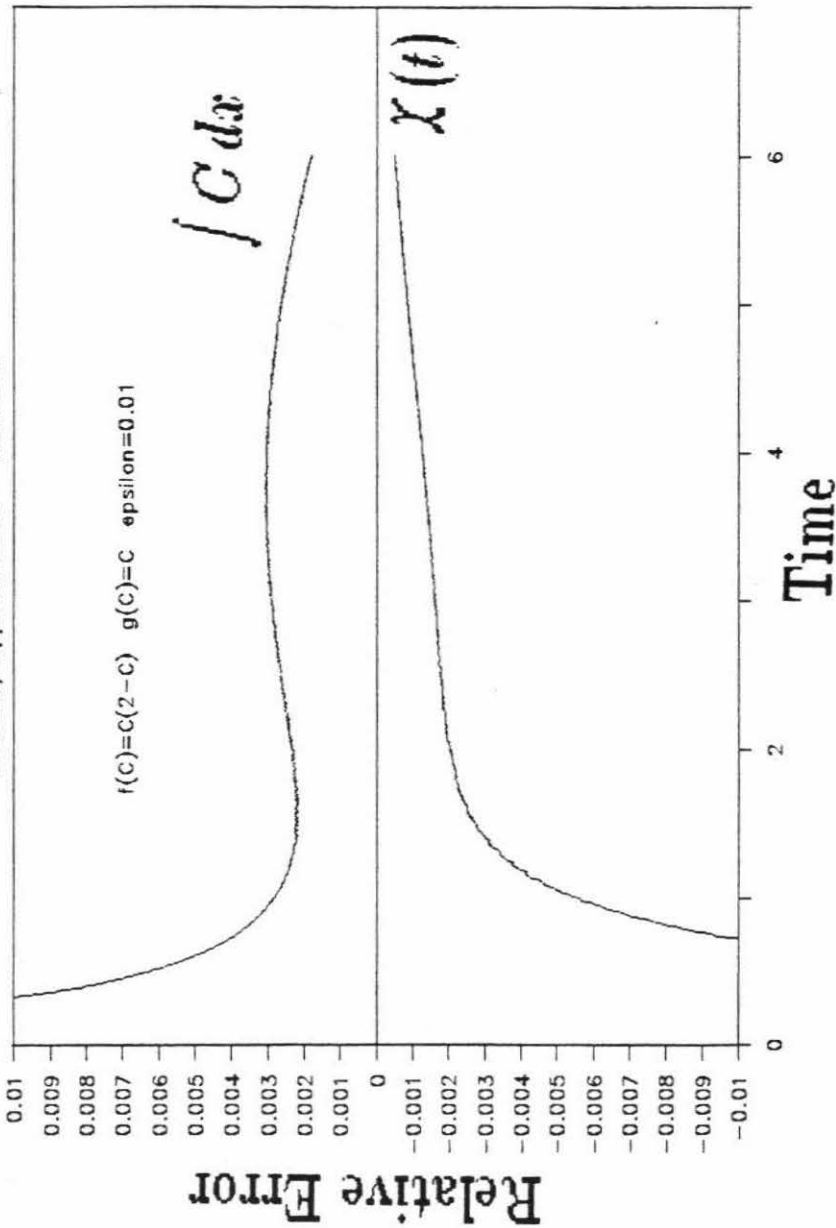


Figure 4.4: Errors in \mathcal{X} , $\int C dx$ from Similarity Approximation

“Error” means $\mathcal{X}_{\text{approx}}(t) - \mathcal{X}_{\text{true}}(t)$ and similarly for $\int C dx$.

$$f(C) = C(2 - C), \quad g(C) = C, \quad \beta(C) \equiv 1, \quad \epsilon d(C) \equiv 0.01$$

Here is my answer to this question. If the front has passed x some time ago, then it *has* been a long time at that location. Thus to expect the solution to look like C_S well behind the front is not unreasonable. As for the region near the front, applying Eq.(4.19) forces $C(x,t)$ to match up with C_S at $x = \mathcal{X}(t)$. Thus, the natural evolution onto C_S *behind* the front and the forced fit to C_S *at* the front together mean that $C_S(\mathcal{S}(t)x)$ has a good chance to approximate $C(x,t)$ well everywhere.

The Taylor series and Padé approximant method for locating $\mathcal{X}(t)$ and other quantities of interest involving $C_O(x,t)$ has the advantage that it is analytical in nature. Thus, the approximations can, in principle, be derived by hand. In practice, however, to get the higher terms in the series (necessary for the (2,2) Padé fractions which worked so well) requires so much algebra that a computer is needed.

The method presented in this section requires a computer from the start. The solutions $C_S(\zeta)$, $\mathcal{A}(t)$, and $\mathcal{X}(t)$ to the ordinary differential equations must be calculated numerically. One advantage that this method has over the Taylor series and Padé fractions is that with a series expansion, you never quite know when to stop. For the case $f(C) = g(C) = C$, $\beta(C) \equiv d(C) \equiv 1$, the (1,1) Padé approximation to $\dot{\mathcal{X}}(t)$ is very good, but for the case $f(C) = C(2 - C)$, $g(C) = C$, $\beta(C) \equiv d(C) \equiv 1$, it is necessary to go to the (2,2) Padé fraction to get good accuracy. With the method of this section, you have no choice! You solve three ODEs and you are done. Another advantage is that the series method only uses local information from f , g , and β near $C = 1$; that is, only the derivatives at $C = 1$ are used. In contrast, the similarity approximation via ODEs uses the actual values of $f(C)$, $g(C)$, and $\beta(C)$ (and their derivatives) over the whole range $C \in [0, 1]$.

In a problem of practical importance, the best procedure would be to calculate both approximations. With the correct software, the approximations could be calculated in a few minutes on a personal computer. The numerical solution of the PDEs (see Appendix A) is a much more time consuming task, requiring use of a faster computer or waiting on a PC for a few hours. Of course, the full numerical solution is more comforting.

Difficulties, Peculiarities, and Conjectures

One disadvantage of the similarity approximation method is that it can fail. There is nothing to prevent the denominator ($\equiv \mathcal{D}(\mathcal{A}) \equiv 3 + C_S \frac{\beta'}{\beta} + C_S \frac{g'}{g} - C_S \frac{f'}{f}$) on the right hand side of Eq.(4.25) from going to zero. Indeed, if $f(C) = C^a$ and $\beta(C)g(C) = C^b$, then $\mathcal{D}(\mathcal{A}) \equiv 3 + b - a$. If $a = 4$ and $b = 1$ (say), then this is *identically* zero! In such a case, the derivation of Eq.(4.25) breaks down. The similarity approximation becomes the statement that the numerator of the right hand side of Eq.(4.25) is zero. This could be interpreted as a nonlinear equation for \mathcal{A} given \mathcal{X} — the system of two ODEs would be reduced to one ODE and a nonlinear equation.

It would be an unusual problem that had $\mathcal{D}(\mathcal{A})$ vanish identically. A more likely difficulty is that \mathcal{D} will have an isolated zero. This can be pre-determined (before any computation with the ODEs for C_S , \mathcal{A} , and \mathcal{X}) simply by plotting \mathcal{D} as a function of C over the range $C \in [0, 1]$.

In several numerical trials, I have computed the similarity approximation with $f(C)$, $g(C)$ and $\beta(C)$ chosen to give a $\mathcal{D}(\mathcal{A})$ that has a simple zero for some $C \in (0, 1)$. In each case, the numerator in Eq.(4.25) seemed to vanish at the same time that the denominator did. I say “seemed to vanish” since the numerical

computations aren't exact and numerical integration of a differential equation with a singularity (or near-singularity) does have its difficulties. Despite this lead, I have been unable to prove that the numerator must vanish along with the denominator. It seems plausible, but that's all I can say.

Another difficulty arises when \mathcal{D} is negative definite. Near $t = 0$, Eq.(4.25) is approximately of the form $\dot{\mathcal{A}} = a \frac{\mathcal{A}}{t} - b$, where $a = -2k'(1)/\mathcal{D}(0)$ and $b = 2/[|C'_s(0)|\mathcal{D}(0)]$. The general solution to this linearized ordinary differential equation for \mathcal{A} is $\mathcal{A}(t) = bt/(a - 1) + \alpha t^a$, where α is an arbitrary constant. Now, if $\mathcal{D}(0) < 0$, then $a > 0$ and $b < 0$. It is easy to make $a > 1$. If this is the case, the solution to Eq.(4.25) has an arbitrary additive term that grows very quickly. This part will be excited by numerical errors and can easily swamp the linear growth part. Note that $\mathcal{D}(0) > 0$ implies that $a < 0$ and so any small excitation of the arbitrary part decays away in time. Basically, for $\mathcal{D}(0) < 0$, the ordinary differential equation Eq.(4.25) is ill posed near $t = 0$. In practice, the above problems make the similarity approximation developed here useful *only for \mathcal{D} positive-definite*.

An intriguing possibility from Eq.(4.25) is that $\dot{\mathcal{A}}(t)$ may actually go to zero and even become negative at some time. If this happened, then $C(\mathcal{X}(t), t)$ would start increasing, and thus $\dot{\mathcal{X}}(t)$ would also increase. The front would have "bounced" off of some support level.

Define $\mathcal{N}(\mathcal{A}, \mathcal{X})$ to be the numerator of the right hand side of Eq.(4.25):

$$\mathcal{N}(\mathcal{A}, \mathcal{X}) \equiv C_s \left(\frac{\beta}{|C'_s|} - \frac{\mathcal{A}}{\mathcal{X}} \frac{k'}{k^{1/2}} \right).$$

By hypothesis, $k'(C) \geq 0$; thus, the two terms in the brackets are both positive. It is easy to *imagine* that one term can dominate for a time, and then the other takes over and \mathcal{N} (and so $\dot{\mathcal{A}}$) changes sign.

Suppose that at time $t = t_0$, $\dot{\mathcal{A}}(t_0) = 0$ (and so $\mathcal{N}[\mathcal{A}(t_0), \mathcal{X}(t_0)] = 0$). Equation (4.25) can be written as $\dot{\mathcal{A}} = 2\frac{\mathcal{N}}{\mathcal{D}}$. Notice that \mathcal{D} depends only on \mathcal{A} , and so

$$\begin{aligned}\ddot{\mathcal{A}}(t_0) &= \left[\frac{2}{\mathcal{D}} \frac{\partial \mathcal{N}}{\partial \mathcal{X}} \dot{\mathcal{X}} \right]_{t=t_0} \\ &= \left[\frac{2}{\mathcal{D}} \frac{k' C_S \mathcal{A}}{\mathcal{X}^2} \right]_{t=t_0}\end{aligned}$$

The only thing that *may* not be positive in this last expression in \mathcal{D} . If in fact $\mathcal{D}[\mathcal{A}(t_0)] > 0$, then $\ddot{\mathcal{A}}(t_0) > 0$ and so even if $\dot{\mathcal{A}}$ does go to zero, it must immediately increase to positive values again.

Thus, the only possibility for $\dot{\mathcal{A}} < 0$ is to have $\mathcal{D} < 0$. In that case, if $\dot{\mathcal{A}}$ goes to zero at $t = t_0$, then $\ddot{\mathcal{A}}(t_0) < 0$, and so $\dot{\mathcal{A}}$ will cross into negative values. Unfortunately, the case $\mathcal{D} < 0$ is just the one that throws doubt on the whole similarity approximation scheme.

I have tried to find evidence of such a “bounce” via numerical solution of the PDEs with various coefficient functions. To create the conditions for such a situation, I chose coefficients that would keep \mathcal{D} negative. Also, I would try to make $k'(C_*)$ small for some $C_* < 1$ on the reasoning that $k'(C_*)$ small should make \mathcal{N} become positive for $C \approx C_*$. On the other hand, \mathcal{N} must start out negative at $t = 0$. With \mathcal{D} negative, if \mathcal{N} can be made positive, then $\dot{\mathcal{A}}$ will become negative as well.

The above paragraph has many “ifs” in it, with the biggest “if” being the validity of the similarity approximation when \mathcal{D} is negative. I never saw a “bounce” in any numerical trial. When $C(\mathcal{X}, t)$ approached the C_* level, the solution behind the front usually ceased to resemble a piece of $C_S(\zeta)$. Just behind the front, the solution would rise up and become “bumpy,” but the front itself would continue

on and leave this behavior behind to smooth itself out.

Based on these trials, I don't believe in the possibility of the "bouncing front." This remains a conjecture, however, since I have been unable to show that $C_O(\mathcal{X}(t), t)$ must always decrease as t increases.

Chapter 5

Convective Term and Traveling Waves

THE RESULTS of Chapter 4 show that the long time behavior of the solvent concentration is to become a similarity solution: $C(x, t) = C_S(x/\sqrt{t})$. In this chapter, I will show that adding a convective velocity term to the partial differential equation for C can result in the asymptotic nature of the solution being converted into a traveling wave: $C(x, t) = C_T(x - vt)$, where v is a constant speed.

The New Equations

With no further ado or fanfare:

$$\frac{\partial C}{\partial t} = \frac{\partial}{\partial x} \left[\epsilon d(C) \frac{\partial C}{\partial x} + f(C) \frac{\partial \sigma}{\partial x} - \underbrace{a(C)C}_{\text{new term}} \right] \quad (5.1)$$

$$\frac{\partial \sigma}{\partial t} = \beta(C)[g(C) - \sigma]. \quad (5.2)$$

Recall that things are scaled so that $d(1) = f(1) = \beta(1) = g(1) = 1$. Other conditions that I will enforce on these original four coefficient functions are:

- They are all as smooth as needed — at least twice continuously differentiable;
- $d(C)$ and $\beta(C)$ are bounded away from zero;
- $f(0) = g(0) = 0$; thus $f(C) = O(C)$ and $g(C) = O(C)$ as $C \rightarrow 0$;
- $g'(C) > 0$ for all $C \in [0, 1]$.

I will assume that the convective velocity $a(C)$ is positive and increasing in C ; in particular, $a'(1) > 0$. I will also assume $a(C)$ to be twice continuously differentiable. There is no scaling freedom left, so $a(1)$ is arbitrary.

A convective term such as the one introduced in Eq.(5.1) could be the result of an applied pressure in the reservoir of solvent in the region $x < 0$. An alternative source for such a term is “crazing,” in which microscopic faults form in the medium as it is deformed and stressed by the invading solvent. These faults then act as paths for more rapid infiltration of the solvent. By this reasoning, it might be reasonable to expect a to depend on σ as well. I will consider the more general case of $a(C, \sigma)$ briefly at the end of this chapter.

In Section 5.1 I will show that a traveling wave solution to Eqs.(5.1,5.2) exists on the doubly infinite interval $x \in (-\infty, +\infty)$. Following that, in Section 5.2 I will analyze the “short time” behavior of Eqs.(5.1,5.2) on the semi-infinite interval with the initial and boundary conditions as given before in Eqs.(2.9,2.10).

5.1 Traveling Wave Solution

The goal of this section is to demonstrate the existence of a unique solution of the form $C(x, t) = C_T(x - vt)$ and $\sigma(x, t) = \sigma_T(x - vt)$ with $C_T(-\infty) = 1$, and $C_T(+\infty) = 0$ (these then imply that $\sigma_T(-\infty) = 1$ and $\sigma_T(+\infty) = 0$, given the conditions on $g(C)$). This analysis in this section in no way depends on ϵ being small, just on its being positive. The speed v is to be found in the analysis (it won't be hard!).

A Phase Plane System

Let $\eta = x - vt$. Then the partial differential equations Eqs.(5.1,5.2) become the ordinary differential equations below (primes denote differentiation with respect to η):

$$\begin{aligned} [\epsilon d(C_T)C_T' + f(C_T)\sigma_T' + (v - a(C_T))C_T]' &= 0 \\ v\sigma_T' + \beta(C_T)[g(C_T) - \sigma_T] &= 0. \end{aligned}$$

Integrate the first equation from η to $+\infty$ and rearrange the results a little to get the (C_T, σ_T) phase plane system:

$$C_T' = \frac{f(C_T)\beta(C_T)}{\epsilon v d(C_T)} \left[\underbrace{\left(g(C_T) - \frac{v(v - a(C_T))C_T}{f(C_T)\beta(C_T)} \right)}_{\equiv r(C_T)} - \sigma_T \right] \quad (5.3)$$

$$\sigma_T' = -\frac{\beta(C_T)}{v} [g(C_T) - \sigma_T]. \quad (5.4)$$

Now, $(C_T, \sigma_T) = (0, 0)$ is a fixed point of this system since $g(0) = 0$. To have a traveling wave solution connect from $(C_T, \sigma_T) = (1, 1)$ to $(0, 0)$ over the range $\eta \in (-\infty, +\infty)$, then $(1, 1)$ must also be a fixed point of this system. Equation (5.3) then implies that $\boxed{v = a(1)}$. With this choice, the desired traveling wave is given by the (C_T, σ_T) phase plane connection between the two fixed points $(1, 1)$ and $(0, 0)$. To demonstrate the existence of this connection is my next task.

Since $a(C)$ has been assumed to be increasing, then $v - a(C)$ is positive for $C < 1$. Thus $r(C) < g(C)$ for $C < 1$. Furthermore, since $f(C) = O(C)$ as $C \rightarrow 0$, it is easy to see that $r(C)$ must go to zero for some C strictly between 0 and 1.

Figure 5.1 displays the situation. There are two curves, the graphs of $\sigma_T = g(C_T)$ and $\sigma_T = r(C_T)$, that separate the (C_T, σ_T) plane into four regions, quaintly labeled $\boxed{\text{I}}$, $\boxed{\text{II}}$, $\boxed{\text{III}}$, and $\boxed{\text{IV}}$. Clearly, the only possibility for the desired connection must be entirely confined to region $\boxed{\text{IV}}$, since an orbit that enters any other region can never approach the origin or reenter region $\boxed{\text{IV}}$. The key to finding the desired connecting orbit will be the analysis of the fixed points $(0, 0)$ and $(1, 1)$.

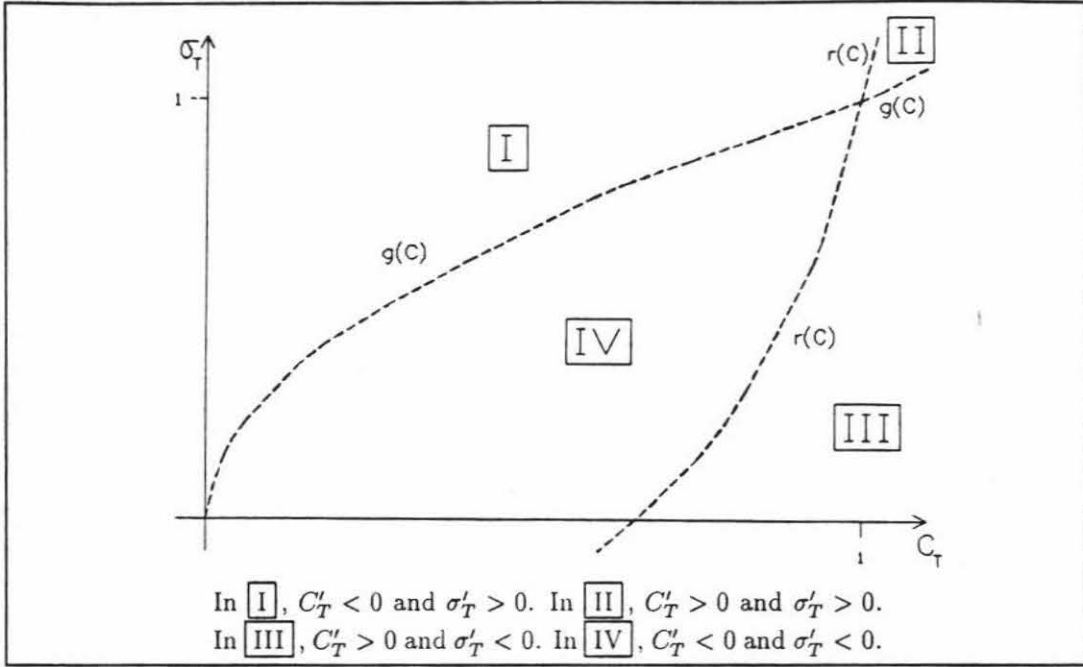


Figure 5.1: Layout of (C_T, σ_T) Phase Plane

Analysis of $(0,0)$

The linearization of Eqs.(5.3,5.4) about $(C_T, \sigma_T) = (0,0)$ is the system

$$\begin{pmatrix} C_T' \\ \sigma_T' \end{pmatrix} = \begin{pmatrix} -\frac{a(1) - a(0)}{\epsilon d(0)} & 0 \\ -\frac{\beta(0)g'(0)}{a(1)} & \frac{\beta(0)}{a(1)} \end{pmatrix} \begin{pmatrix} C_T \\ \sigma_T \end{pmatrix},$$

which clearly has one eigenvalue of each sign. Thus, $(0,0)$ is a saddle point. Only one orbit can enter this point as $\eta \rightarrow +\infty$: the orbit corresponding to the negative (stable) eigenvalue. The unstable direction is just $\begin{pmatrix} 0 \\ 1 \end{pmatrix}$ and the stable direction is

$$\begin{pmatrix} 1 \\ \frac{g'(0)}{1 + a(1)\frac{a(1) - a(0)}{\epsilon d(0)\beta(0)}} \end{pmatrix}.$$

The slope (the second element) is positive and less than $g'(0)$, so the stable orbit entering the origin comes from region IV. This is a hopeful sign, since that is

where the connection orbit must come from.

Analysis of (1, 1)

Linearize Eqs.(5.3,5.4) about (1, 1) by letting $C_T = 1 + c$ and $\sigma_T = 1 + \rho$. The linearized system is then

$$\begin{pmatrix} c' \\ \rho' \end{pmatrix} = \frac{1}{a(1)} \begin{pmatrix} \frac{r'(1)}{\epsilon} & -\frac{1}{\epsilon} \\ -g'(1) & 1 \end{pmatrix} \begin{pmatrix} c \\ \rho \end{pmatrix}.$$

Note that $r'(1) > g'(1)$ since $a'(1) > 0$ (by hypothesis). It is easy to show that the eigenvalues of this linearization are

$$\lambda_{\pm} = \frac{1}{2a(1)} \left[(r'(1)/\epsilon + 1) \pm \sqrt{(r'(1)/\epsilon - 1)^2 + 4g'(1)/\epsilon} \right].$$

What is more, a little algebra shows that $\lambda_+ > \lambda_- > 0$. Thus, the point $(C_T, \sigma_T) = (1, 1)$ is an unstable node with unequal eigenvalues. Search for the eigenvectors in the form $\begin{pmatrix} 1 \\ y_{\pm} \end{pmatrix}$; then the slopes y_{\pm} are given by

$$y_{\pm} = \frac{\epsilon}{2} \left[(r'(1)/\epsilon - 1) \mp \sqrt{(r'(1)/\epsilon - 1)^2 + 4g'(1)/\epsilon} \right].$$

From this, it is clear that $y_+ < 0$. It is also true that $g'(1) < y_- < r'(1)$ — this is not quite so obvious, but a little algebra will establish this. This means that the less unstable direction lies between the curves $\sigma_T = g(C_T)$ and $\sigma_T = r(C_T)$.

Connecting Things Up

With these facts about the singular points in hand, Figure 5.2 can be adduced. In this drawing, the local behaviors of the nonlinear system Eqs.(5.3,5.4) have been sketched in.

These are the factors that went into Fig. 5.2: Consider the family of curves emanating from (1, 1) into region IV. The less unstable direction points into this region

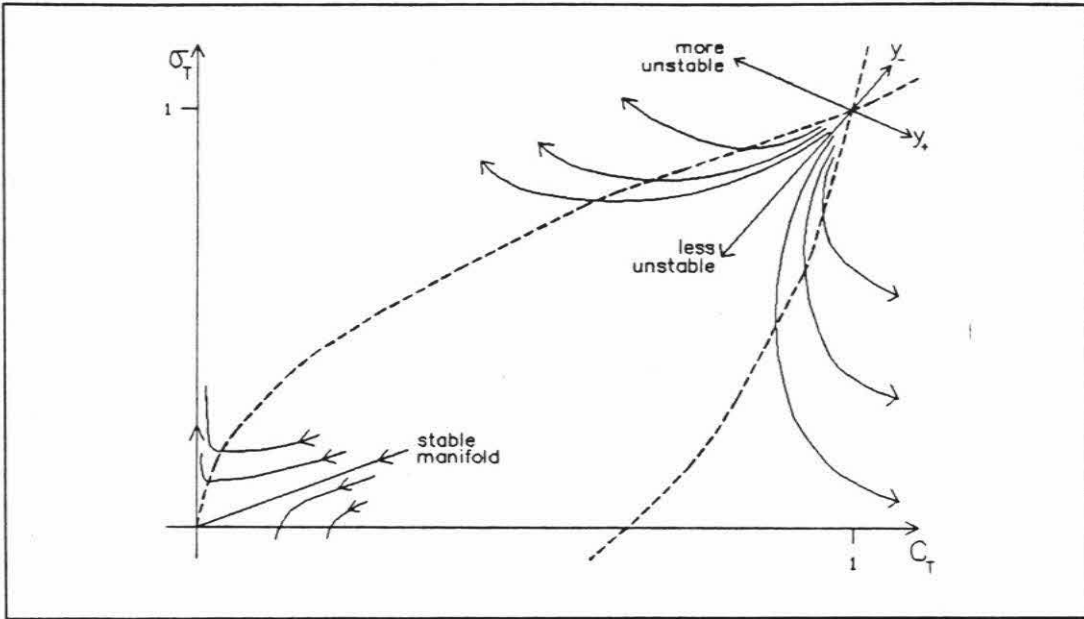


Figure 5.2: Local Behavior in (C_T, σ_T) Phase Plane

and the more unstable direction points into regions **I** and **III** (recall $y_+ < 0$, while $r'(1) > g'(1) > 0$). Locally, the flow must look as in Fig. 5.2, with orbits “peeling off” from the less unstable direction to either side in order to be attracted to the more unstable direction. Since the more unstable direction lies in regions **I** and **III**, these orbits that start near the less unstable direction must cross the dividing curves $\sigma_T = g(C_T)$ and $\sigma_T = r(C_T)$.

An orbit that crosses from region **IV** into region **I** crosses the curve $\sigma_T = g(C_T)$, along which $\sigma_T' = 0$. Since $C_T' < 0$ in these regions, the orbit must be concave upwards with a local minimum along $\sigma_T = g(C_T)$. Similarly, an orbit that crosses from region **IV** into region **III** must be concave rightwards and be locally vertical along $\sigma_T = r(C_T)$.

Now consider any orbit that has a segment in region **IV**. Imagine tracking that orbit backward as η decreases to $-\infty$. As long as the orbit stays in region **IV**,

it has $C'_T < 0$ and $\sigma'_T < 0$, so that as η decreases, the orbit must move up and to the right.

How could such an orbit *leave* region IV as η decreases (or enter it as η increases, if you like)? It cannot pass through the bounding curve $\sigma_T = r(C_T)$ because to do so it must be vertical ($C'_T = 0$) at that point. That is geometrically impossible since the orbit is *above* the curve. Similarly, it cannot pass through the bounding curve $\sigma_T = g(C_T)$ because to do so it must be horizontal ($\sigma'_T = 0$) at that point. That is geometrically impossible since the orbit is to the *right* of the curve (recall that $g'(C) > 0$ by assumption, so it is not possible for any point in region IV to be directly to the left of any portion of the $\sigma_T = g(C_T)$ bounding curve).

Thus, any orbit in region IV must remain there as $\eta \rightarrow -\infty$. There is only one place that such an orbit can go to as $\eta \rightarrow -\infty$, and that is the singular point at $(1, 1)$. Fortunately, this singular point is attracting as $\eta \rightarrow -\infty$.

In particular, the stable orbit that falls into $(0, 0)$ as $\eta \rightarrow +\infty$ must connect back to $(1, 1)$ as $\eta \rightarrow -\infty$. *This is the desired connection and provides the traveling wave solution.* It is clearly unique since there is only one orbit that falls into the origin as $\eta \rightarrow +\infty$.

In fact, it is easy to see that the orbits that leave region IV through the bounding curve $\sigma_T = g(C_T)$ form a continuous family. They range from the ones that leave near $(1, 1)$, as seen in the upper right of Fig. 5.2 to the ones that leave near $(0, 0)$, as seen in the lower left of that figure. The ultimate member of that family is the one that connects to the origin. A similar argument can be made about the orbits that leave region IV through the bounding curve $\sigma_T = r(C_T)$ or through the portion of the C_T axis to the left of the zero of $r(C_T)$.

With this argument, it is apparent that assuming $a(C)$ to be increasing over the whole interval $C \in [0, 1]$ is not required. What is required is that $a'(1) > 0$ and that $a(C) < a(1)$ for all $C < 1$. With these restrictions, the above analyses still hold: $a'(1) > 0$ implies that $r'(1) > g'(1)$, which was needed, and $a(C) < a(1)$ for $C < 1$ implies that $r(C) < g(C)$ for $C < 1$, which was also needed.

Note that it is not necessary that the orbit that leaves $(1, 1)$ directly along the less unstable direction be the one that connects to $(0, 0)$. Since all orbits in region IV go to $(1, 1)$ as $\eta \rightarrow -\infty$, none of the arguments above pick *this* orbit out as special. This should be contrasted to the case at $(0, 0)$, where only one orbit enters the singular point and so it *must* be the desiderated trajectory.

Finally, the conditions used here are *sufficient* for the existence of the traveling wave solution, but they are not *necessary*. For example, it is possible to have a traveling wave solution even if $g'(C)$ is not always positive. However, if $g'(C) < 0$ anywhere, the problems discussed in Section 4.3 can arise: the solution $C(x, t)$ may become discontinuous.

Even if $a(C) > a(1)$ for some $C \in (0, 1)$, a traveling wave solution can still exist — it's just that the demonstration above does not work.

5.2 Early Times

The traveling wave solution is valid for the doubly infinite interval $x \in (-\infty, +\infty)$. After sufficient time has passed, the left boundary $x = 0$ is effectively at $\eta = -\infty$ and so it is plausible that the traveling wave solution provides the long time behavior for Eqs.(5.1,5.2). But what about before “sufficient time” has passed?

How do the results of Chapter 3 (with $a(C) \equiv 0$) go over to the new equations in this chapter? My goal now is to sketch out the answer to this question.

Adopting the same paradigm as in Chapter 3, the first step is to derive an equation for the evolution of $\mathcal{X}(t)$. This is done exactly as in Section 3.2: conservation of solvent at the front gives

$$\begin{aligned} C_O(\mathcal{X}, t)\dot{\mathcal{X}} &= J(\mathcal{X}, t) \\ &= -f(C_O(\mathcal{X}, t))\frac{\partial\sigma_O}{\partial x}(\mathcal{X}, t) + a(C_O(\mathcal{X}, t))C_O(\mathcal{X}, t). \end{aligned} \quad (5.5)$$

Equation (3.8) still holds good $\left[\frac{\partial\sigma_O}{\partial x}(\mathcal{X}, t) = -\beta g/\dot{\mathcal{X}}\right]$. Plugging this into Eq.(5.5) results in the quadratic equation $\dot{\mathcal{X}}^2 - a\dot{\mathcal{X}} - k = 0$. Taking the positive root gives the new version of Eq.(3.9):

$$\frac{d\mathcal{X}}{dt} = \frac{1}{2}a(C_O(\mathcal{X}, t)) + \sqrt{\frac{1}{4}a(C_O(\mathcal{X}, t))^2 + k(C_O(\mathcal{X}, t))}. \quad (5.6)$$

In particular, $\dot{\mathcal{X}}(0) = \frac{1}{2}a(1) + \sqrt{\frac{1}{4}a(1)^2 + 1}$, which is greater than 1 *and* greater than $a(1)$ (the traveling wave speed). Since both $k(C)$ and $a(C)$ are presumed to be increasing, then $\dot{\mathcal{X}}$ is an increasing function of $C_O(\mathcal{X}, t)$. Under the assumptions in this chapter, $k(0) = 0$, so that if $C_O(\mathcal{X}, t)$ drops to 0, then $\dot{\mathcal{X}} = a(0) < a(1)$. This means that there must be some intermediate value $C_{\text{trav}} \in (0, 1)$ such that $\dot{\mathcal{X}} = a(1)$ when $C_O(\mathcal{X}, t) = C_{\text{trav}}$.

Thus, I conjecture that the front will decay in magnitude only to the value C_{trav} . As it approaches this height, the solvent profile should approach the traveling wave $C_T(x - a(1)t - x_o)$, where x_o is some constant shift chosen to align the traveling wave.

The layer equation for C_L can be derived as in Section 3.3. Parallel machinations

lead to the updated version of Eq.(3.37) (recall that $\zeta = (x - \mathcal{X})/\epsilon$):

$$\frac{\partial C_L}{\partial \zeta} + \frac{C_L}{\dot{\mathcal{X}} d(C_L)} [\dot{\mathcal{X}}^2 - a(C_L)\dot{\mathcal{X}} - k(C_L)] = 0. \quad (5.7)$$

The same reasoning as before shows that this equation has a solution that matches to $C_O(\mathcal{X}, t)$ as $\zeta \rightarrow -\infty$ and to 0 as $\zeta \rightarrow +\infty$.

Figure 5.3 shows an example of this behavior. In this case, $f(C) \equiv g(C) = a(C) = C$, $d(C) \equiv \beta(C) \equiv 1$, and $\epsilon = 0.02$. To calculate the final height of the front, set $a(1) = \frac{1}{2}a(C_{\text{trav}}) + \sqrt{\frac{1}{4}a(C_{\text{trav}})^2 + k(C_{\text{trav}})}$, or $1 = \frac{1}{2}C_{\text{trav}} + \sqrt{\frac{1}{4}C_{\text{trav}}^2 + C_{\text{trav}}}$, or $C_{\text{trav}} = \frac{1}{2}$. The initial speed should be $(1 + \sqrt{5})/2 \approx 1.618$. Figure 5.3 clearly shows the decay onto $C_{\text{trav}} = \frac{1}{2}$ and the inset clearly shows the front slowing down from its initial burst of enthusiasm to the more leisurely speed of the traveling wave.

An interesting result from Eq.(5.7) is that $k(C)$ no longer needs to be an increasing function of C for the layer solution to exist. What is required is that $\dot{\mathcal{X}}^2 - a(C_L)\dot{\mathcal{X}} - k(C_L)$ be positive for all $C_L < C_O(\mathcal{X}, t)$. This forces $\frac{\partial C_L}{\partial \zeta}$ to be negative and so C_L must decrease to 0 as $\zeta \rightarrow +\infty$. Define $C_o \equiv C_O(\mathcal{X}, t)$. Using Eq.(5.6), this positivity constraint can be expressed as

$$[a(C_o) - a(C_L)] \left[\frac{1}{2}a(C_o) + \sqrt{\frac{1}{4}a(C_o)^2 + k(C_o)} \right] + [k(C_o) - k(C_L)] > 0 \quad \forall C_L < C_o. \quad (5.8)$$

This inequality can be used to show that $\dot{\mathcal{X}}$ must be an increasing function of C_o , even if $k(C_o)$ is not. Let $C_L \rightarrow C_o$ in Eq.(5.8). Then it becomes

$$a'(C_o)\dot{\mathcal{X}} + k'(C_o) \geq 0. \quad (5.9)$$

Now, $\dot{\mathcal{X}}^2 - a(C_o)\dot{\mathcal{X}} - k(C_o) = 0$ for all C_o . Differentiating with respect to C_o gives

$$2\dot{\mathcal{X}} \frac{d\dot{\mathcal{X}}}{dC_o} - a'(C_o)\dot{\mathcal{X}} - a(C_o) \frac{d\dot{\mathcal{X}}}{dC_o} - k'(C_o) = 0.$$

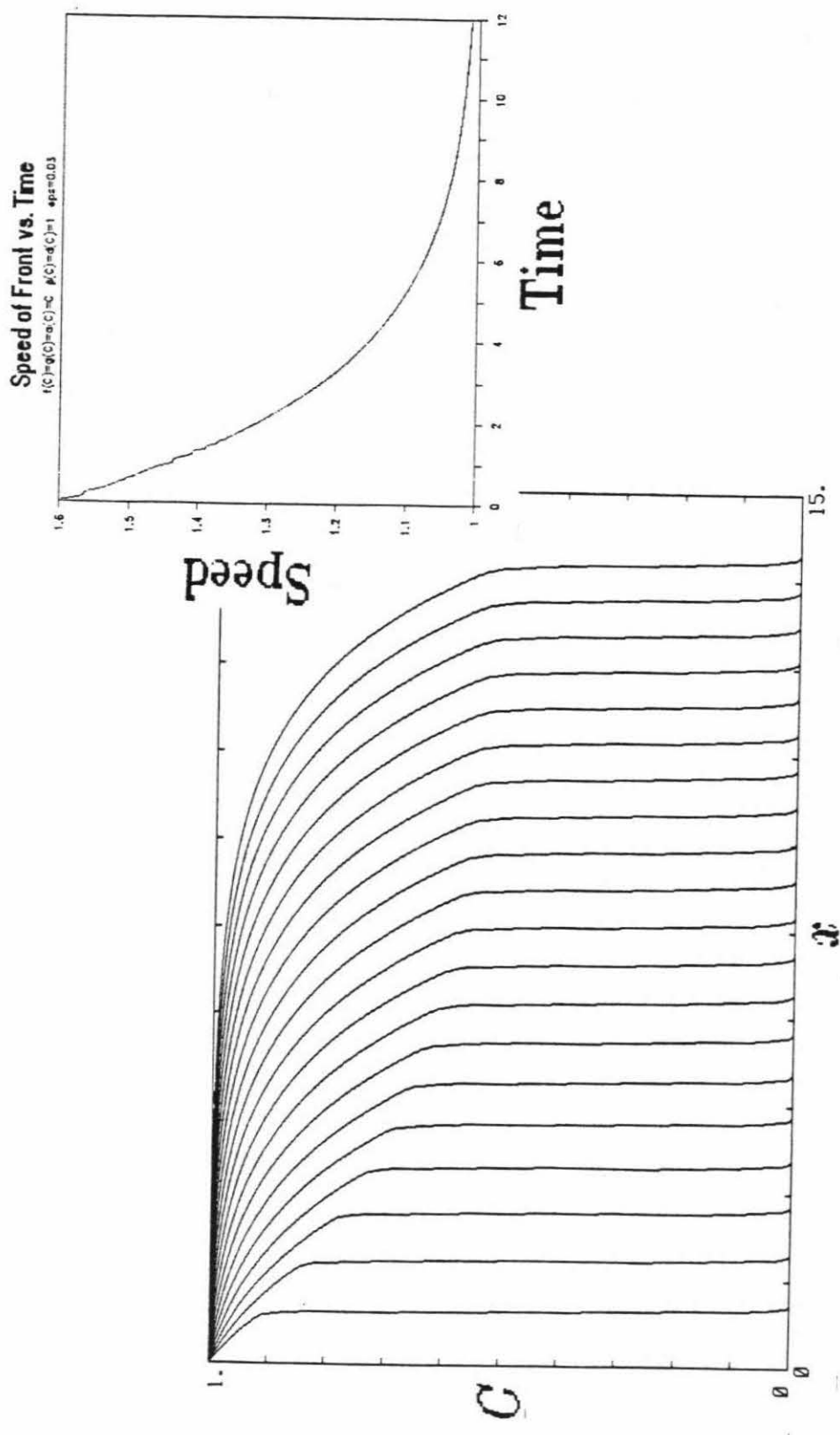


Figure 5.3: C vs. x for $f(C) = a(C) = C$.
 $g(C) = C$, $d(C) \equiv \beta(C) \equiv 1$, $\epsilon = 0.03$.
 Curves plotted at time intervals $\Delta t = 0.6$.

Rearranging this result yields

$$\frac{d\dot{\mathcal{X}}}{dC_o} = \frac{a'(C_o)\dot{\mathcal{X}} + k'(C_o)}{2\dot{\mathcal{X}} - a(C_o)}.$$

Equation (5.6) shows that the denominator is positive and Eq.(5.9) shows that the numerator is non-negative. Thus $\frac{d\dot{\mathcal{X}}}{dC_o} \geq 0$, and so $\dot{\mathcal{X}}$ must be an increasing function of $C_o(\mathcal{X}, t)$ if the layer equation is to be able to connect to 0 as $\zeta \rightarrow +\infty$ — that is, if there is to be only one layer, not two as in Fig. 3.7.

5.3 When a Depends on σ

Replacing $a(C)$ in Eq.(5.1) by $a(C, \sigma)$ is an easy generalization to make. The speed of the traveling wave must then become $v = a(1, 1)$. The proof of the existence of the traveling wave orbit needs only a few modifications if $a(C, \sigma)$ is assumed to be an increasing function of both C and σ : $a(C_1, \sigma_1) > a(C_2, \sigma_2)$ when both $C_1 > C_2$ and $\sigma_1 > \sigma_2$ hold. The curve $\sigma_T = r(C_T)$ is replaced with the locus of $C'_T = 0$, and as long as this lies below the curve $\sigma_T = g(C_T)$, the proof can proceed virtually unfettered.

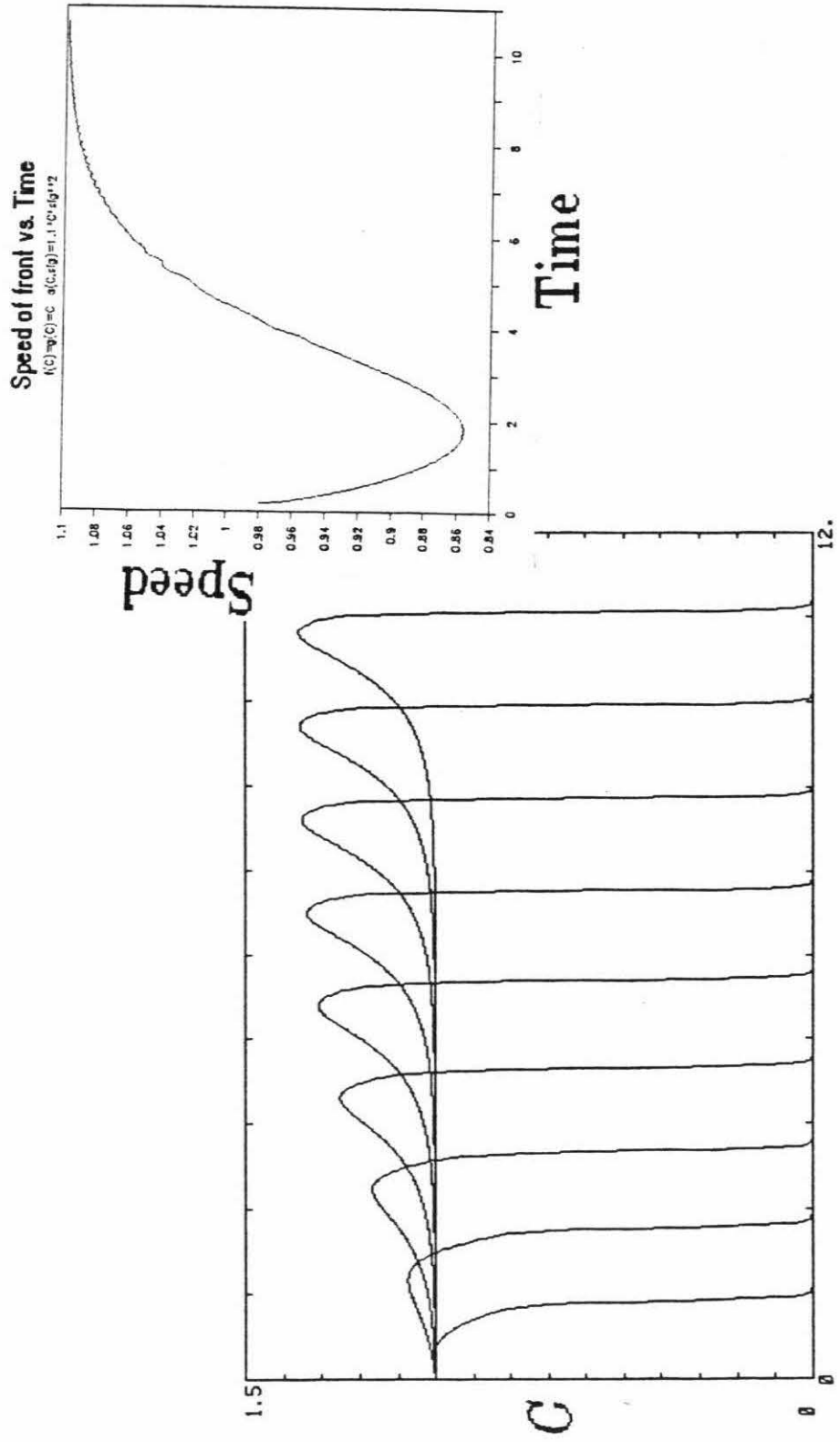
The argument that leads to Eq.(5.6) is easily modified to give the generalized result

$$\frac{d\mathcal{X}}{dt} = \frac{1}{2}a(C_o(\mathcal{X}, t), 0) + \sqrt{\frac{1}{4}a(C_o(\mathcal{X}, t), 0)^2 + k(C_o(\mathcal{X}, t))}. \quad (5.10)$$

The convective velocity $a(C, \sigma)$ in this formula has $\sigma \leftarrow 0$ because it must be evaluated at the front, and at the front, $\sigma = 0$ (to lowest order in ϵ).

Figure 5.4 shows an amusing result suggested by all of the above. In this figure, $f(C) = g(C) = C$, $d(C) \equiv \beta(C) \equiv 1$, and $a(C, \sigma) = 1.1C\sigma^2$. Since $a(C, 0) = 0$, the result above gives $\dot{\mathcal{X}} = \sqrt{k(C_o(\mathcal{X}, t))} = \sqrt{C_o(\mathcal{X}, t)}$, as in Eq.(3.9). But the

solution should evolve to a traveling wave with speed $v = 1.1$, and so the front must *accelerate* at some point. Also, since the power on σ is greater than 1, it turns out that all of the analysis that leads to Eq.(3.16) still holds true. Thus for this case, $\ddot{\mathcal{X}}(0) = -\frac{1}{5}$. Therefore the front must first weaken in magnitude and slow down, and then, as the effect of the convective term kicks in, the front must strengthen and accelerate. In addition, the final $C_O(\mathcal{X}, t)$ must be 1.21 to support the speed $v = 1.1$. The main body of Fig. 5.4 shows the behavior of $C(x, t)$ and the inset shows $\dot{\mathcal{X}}(t)$. The above predictions are borne out by the numerical computations.



x

Figure 5.4: C vs. x for $f(C) = C$, $a(C, \sigma) = 1.1C\sigma^2$.

$$g(C) = C, \quad d(C) \equiv \beta(C) \equiv 1, \quad \epsilon = 0.02.$$

Curves plotted at time intervals $\Delta t = 1.2$.

Appendix A

Number Crunching

THE NUMERICAL SCHEME USED TO SOLVE the partial differential equations is relatively simple. A nonlinear Crank-Nicholson type of finite differencing is used and the resulting nonlinear equations are iterated twice to advance to the next time step. The discussion in this section will focus on the system with the convective term, Eqs.(5.1,5.2). By omitting all terms with $a(C)$, the numerical method and code described below can easily be specialized to the system of Chapters 2-4.

Put a uniform mesh down on the interval $[0, \ell]$. (Thus, no attempt is made to refine the mesh around the moving front.) Replacing spatial derivatives in Eq.(5.1) with centered differences gives (for interior mesh points)

$$\begin{aligned} \frac{\partial C_n}{\partial t} \approx & \frac{1}{\Delta x^2} \left[\begin{array}{l} \epsilon d_{n+\frac{1}{2}} \cdot (C_{n+1} - C_n) - \epsilon d_{n-\frac{1}{2}} \cdot (C_n - C_{n-1}) \\ + f_{n+\frac{1}{2}} \cdot (\sigma_{n+1} - \sigma_n) - f_{n-\frac{1}{2}} \cdot (\sigma_n - \sigma_{n-1}) \end{array} \right] \quad (\text{A.1}) \\ & + \frac{1}{2\Delta x} \left[\begin{array}{l} a_{n+1} \cdot C_{n+1} \quad \quad \quad - a_{n-1} \cdot C_{n-1} \end{array} \right] \\ \equiv & \mathcal{R}_n(t), \end{aligned}$$

where

Δx = (uniform) mesh spacing in x ,
(must resolve the front of width $\sim \epsilon$);

C_n, σ_n = $C(n\Delta x, t), \sigma(n\Delta x, t)$ (mesh values of C, σ);

function _{n} = function(C_n);

function _{$n+\frac{1}{2}$} = function $[\frac{1}{2}(C_{n+1} + C_n)]$

$[\frac{1}{2}$ function(C_{n+1}) + $\frac{1}{2}$ function(C_n) is also OK]; and

“function” = d, f, β, g , or a .

Note that $n = 0$ corresponds to the left boundary. The right boundary ($x = \ell$) will be at $n = N$; that is, $\Delta x = \ell/N$. Thus, Eq.(A.1) is a set of $N - 1$ ordinary differential equations for the set $\{C_n(t) : n = 1, 2, \dots, N - 1\}$. All of these equations have the initial condition $C_n(0) = 0$. There are no differential equations for $C_0(t)$ and $C_N(t)$ since those values are given by the boundary conditions on $C(x, t)$: $C_0(t) \equiv 1$ and $C_N(t) \equiv 0$ for all $t > 0$.

Equation (A.1) is discretized in time in an implicit way. Let k be the time index (as n is the space index), Δt be the time spacing, and define $C_{n,k} = C(n\Delta x, k\Delta t)$ (similarly define $\sigma_{n,k}$). Then central differences are applied at to Eq.(A.1) about the time $t = (k + \frac{1}{2})\Delta t$:

$$\frac{C_{n,k+1} - C_{n,k}}{\Delta t} = \frac{1}{2}\mathcal{R}_{n,k} + \frac{1}{2}\mathcal{R}_{n,k+1}. \quad (\text{A.2})$$

I have adapted the notation from Eq.(A.1) so that $\mathcal{R}_{n,k}$ here is the same as $\mathcal{R}_n(k\Delta t)$ there. The fact that centered differences are used throughout (including the average on the right hand side of Eq.(A.2)) means that this method has a truncation error of $O(\Delta x^2 + \Delta t^2)$.

Since $\mathcal{R}_{n,k+1}$ appears on the right hand side, Eq.(A.2) is a ferociously nonlinear system for the set $\{C_{n,k+1} : n = 1, 2, \dots, N - 1\}$, even assuming that $\{\sigma_{n,k+1} : n = 0, 2, \dots, N\}$ was known. My program (listing below) tackles this system by an iterative scheme. The diffusive part $[(\epsilon d(C)C_x)_x]$ and the convective part $[(a(C)C)_x]$ are treated implicitly, as in the Crank-Nicholson method, but the stress part $[(f(C)\sigma_x)_x]$ is lumped entirely to the right hand side. Iterating in this fashion avoids the use of Newton's method, which would require supplying the derivatives of all the nonlinear coefficient functions. I wanted to develop a code that could have routines for the coefficient functions just "plugged in" without the user (me) having

any need to worry about their derivatives. The routine below fits this prescription.

The effect of these decisions is to expand Eq.(A.2) as follows:

$$\begin{aligned}
 \frac{C_{n,k+1} - C_{n,k}}{\Delta t} = & \\
 & \frac{1}{2\Delta x^2} \left[\begin{array}{ll} \epsilon d_{n+\frac{1}{2},k} \cdot (C_{n+1,k} - C_{n,k}) & - \epsilon d_{n-\frac{1}{2},k} \cdot (C_{n,k} - C_{n-1,k}) \\ + f_{n+\frac{1}{2},k} \cdot (\sigma_{n+1,k} - \sigma_{n,k}) & - f_{n-\frac{1}{2},k} \cdot (\sigma_{n,k} - \sigma_{n-1,k}) \end{array} \right] \\
 & + \frac{1}{4\Delta x} \left[\begin{array}{ll} a_{n+1,k} \cdot C_{n+1,k} & - a_{n-1,k} \cdot C_{n-1,k} \end{array} \right] \\
 & + \frac{1}{2\Delta x^2} \left[\begin{array}{ll} \epsilon \hat{d}_{n+\frac{1}{2},k+1} \cdot (C_{n+1,k+1} - C_{n,k+1}) & - \epsilon \hat{d}_{n-\frac{1}{2},k+1} \cdot (C_{n,k+1} - C_{n-1,k+1}) \\ + \hat{f}_{n+\frac{1}{2},k+1} \cdot (\hat{\sigma}_{n+1,k+1} - \hat{\sigma}_{n,k+1}) & - \hat{f}_{n-\frac{1}{2},k+1} \cdot (\hat{\sigma}_{n,k+1} - \hat{\sigma}_{n-1,k+1}) \end{array} \right] \\
 & + \frac{1}{4\Delta x} \left[\begin{array}{ll} \hat{a}_{n+1,k+1} \cdot C_{n+1,k+1} & - \hat{a}_{n-1,k+1} \cdot C_{n-1,k+1} \end{array} \right].
 \end{aligned} \tag{A.3}$$

In Eq.(A.3), the unknowns are the $C_{n,k+1}$ values. A variable or function with a "hat" accent (as in $\hat{\sigma}$ or \hat{f}) is nominally at the $k + 1$ time level, but is evaluated with an à priori estimate of the values at $t = (k + 1)\Delta t$. On the first iteration to go from level k to level $k + 1$, these à priori values $\hat{C}_{n,k+1}$ and $\hat{\sigma}_{n,k+1}$ are given just by copying the values at time level k . On subsequent iterations, they are the product of the last iteration.

Putting all the unknown $C_{n,k+1}$ values on the left side and all the known values (including the values of $\hat{\sigma}_{n,k+1}$) on the right side leads to a tridiagonal linear system for the unknowns. This is easily solved by Gaussian elimination without pivoting, which is stable because the tridiagonal matrix is diagonally dominant if $\frac{\Delta t}{2\Delta x} \max |a| < 1$.

The second step in the iteration scheme is to solve for the new values in the set $\{\sigma_{n,k+1} : n = 0, 1, \dots, N\}$. Since Eq.(5.2) is just an ordinary differential equation at each grid point, this is easily done with a single step method.

The iteration scheme now loops back. Eq.(A.3) can be solved again for new values of $C_{n,k+1}$, using the previous iteration's output. Then $\sigma_{n,k+1}$ can be re-computed, etc. In practice, two iterations are quite sufficient. This can be viewed as a predictor-corrector scheme.

The Code

The following FORTRAN routine marches $C(x,t)$ and $\sigma(x,t)$ one time step into the future — from t to $t + \Delta t$. The functions C and σ are stored in the arrays C and S in the COMMON block /CN/, along with various controlling parameters. The coefficient functions $ed(C)$, $f(C)$, $\beta(C)$, $g(C)$, and $a(C)$ must be supplied by the user in FUNCTION subprograms named DD, FF, BETA, GG, and AA, respectively. Comments are in a small sans serif type face.

```

SUBROUTINE CNITER
  IMPLICIT REAL*8 (A-H,O-Z)      do everything in double precision
C
  PARAMETER ( NPTMAX = 1021 )    maximum number of points in grid
C
  COMMON / CN / DX,DT,TOTTIM,       $\Delta x, \Delta t, t$ 
  X          CLEFT,CRIGHT,          $C(0,t + \Delta t), C(\ell,t + \Delta t)$ 
  X          C(NPTMAX),S(NPTMAX),   $C(x,t), \sigma(x,t)$ 
  X          NPTS,MAXITE           mesh size, no. of iterations
C                                  Note  $\ell = (NPTS - 1) * DX$ .
C  The following are local and temporary arrays
C
  REAL*8 C1(NPTMAX),S1(NPTMAX),C1NEW(NPTMAX),      new C,  $\sigma$ 
  X      SUBD(NPTMAX),DIAG(NPTMAX),SUPD(NPTMAX),  matrix entries
  X      RHS(NPTMAX)                             linear system RHS
C
  DO 100 N=1,NPTS      initial iteration has future values set to current values
    C1(N) = C(N)
    S1(N) = S(N)
100  CONTINUE
  C1(1) = CLEFT      set boundary conditions at  $t + \Delta t$ 
  C1(NPTS) = CRIGHT

```

```

C
C Pre-compute some parts of the RHS of the equations
C
      XLAM = 0.5D0 * DT / DX**2
      XMU  = 0.25D0 * DT / DX
C
      EPHALF = FF( 0.5D0*(C(1)+C(2)) )     $f_{\frac{1}{2}}$ 
      DPHALF = DD( 0.5D0*(C(1)+C(2)) )     $\epsilon d_{\frac{1}{2}}$ 
      AMID   = AA( C(1) )                   $a_0$ 
      APL    = AA( C(2) )                   $a_1$ 
C
      DO 200 N=2,NPTS-1      FORTRAN N is math  $n + 1$  due to indexing
      EMHALF = EPHALF         $f_{n-\frac{1}{2}}$ 
      DMHALF = DPHALF         $\epsilon d_{n-\frac{1}{2}}$ 
      AMIN   = AMID           $a_{n-1}$ 
      AMID   = APL            $a_n$ 
C
      EPHALF = FF( 0.5D0*(C(N)+C(N+1)) )     $f_{n+\frac{1}{2}}$ 
      DPHALF = DD( 0.5D0*(C(N)+C(N+1)) )     $\epsilon d_{n+\frac{1}{2}}$ 
      APL    = AA( C(N+1) )                   $a_{n+1}$ 
C
      RHS(N) = C(N)
X          + XLAM * ( DPHALF * ( C(N+1)-C(N) )
X                    - DMHALF * ( C(N)-C(N-1) )
X                    + EPHALF * ( S(N+1)-S(N) )
X                    - EMHALF * ( S(N)-S(N-1) ) )
X
X          - XMU * ( APL*C(N+1) - AMIN*C(N-1) )
200 CONTINUE
C
C Loop back point for iteration:
C (a) using C1, S1 (best guesses at new time values), calculate
C coefficients for the equations to update C1
C (b) solve for C1, then update S1
C (c) loop MAXITE times
C
      NITER = 0      number of times through the loop
500 CONTINUE
      EPHALF = FF( 0.5D0*(C1(1)+C1(2)) )    initialize coefficients
      DPHALF = DD( 0.5D0*(C1(1)+C1(2)) )
      AMID   = AA( C1(1) )
      APL    = AA( C1(2) )
C
      DO 600 N=2,NPTS-1
      EMHALF = EPHALF      as in loop above, "age" the coefficients
      DMHALF = DPHALF

```

```
      AMIN = AMID
      AMID = APL
C
      EPHALF = FF( 0.5D0*(C1(N)+C1(N+1)) )
      DPHALF = DD( 0.5D0*(C1(N)+C1(N+1)) )
      APL = AA( C1(N+1) )
C
      SUBD(N) = -XLAM * DMHALF - XMU * AMIN           matrix elements:
      SUPD(N) = -XLAM * DPHALF + XMU * APL           subdiagonal
      DIAG(N) = 1.D0 + XLAM * ( DMHALF + DPHALF )   superdiagonal
      C1NEW(N) = RHS(N)                             diagonal
      X      + XLAM * ( EPHALF * (S1(N+1)-S1(N))     right hand side
      X      - EMHALF * (S1(N)-S1(N-1)) )
600  CONTINUE
C
C  Adjust RHS of equations to force boundary conditions
C
      C1NEW(2) = C1NEW(2) - SUBD(2) *CLEFT
      C1NEW(NPTS-1) = C1NEW(NPTS-1) - SUPD(NPTS-1)*CRIGHT
C
C  Solve tridiagonal system for C1NEW(2) ... C1NEW(NPTS-1)
C
      CALL TDSOLV( NPTS-2 , SUBD(2) , DIAG(2) , SUPD(2) , C1NEW(2) )
C
      C1NEW(1) = CLEFT      slip in the boundary conditions
      C1NEW(NPTS) = CRIGHT
C
C  Advance all S1's, since there is no BC for  $\sigma$ 
C
      DO 700 N=1,NPTS
      C1(N) = C1NEW(N)      recycle C1NEW back into C1
      CMEAN = 0.5D0*(C(N)+C1(N))
      BMEAN = BETA( CMEAN )
      BFAC = EXP( -DT*BMEAN )
      S1(N) = BFAC * S(N) + (1.D0-BFAC)*GG( CMEAN )
700  CONTINUE
C
      NITER = NITER + 1
      IF( NITER .GE. MAXITE )GOTO 8000      loop back if needed
      GOTO 500
C


---


8000 CONTINUE
      DO 8100 N=1,NPTS      assign values at  $t + \Delta t$  to output
      C(N) = C1(N)
      S(N) = S1(N)
8100 CONTINUE
      RETURN
```

```

END

SUBROUTINE TDSOLV( N , SUBD,D,SUPD , X )
C
C Solve the tridiagonal system
C SUBDi Xi-1 + Di Xi + SUPDi Xi+1 = rhsi
C where rhsi is stored in X(i) on entry. The method used is LU
C decomposition without pivoting. D is altered (and X, of course).
C
REAL*8 SUBD(N) , D(N) , SUPD(N) , X(N) , DL
C
DO 100 I=2,N LU decompose and forward substitute loop
  DL = SUBD(I) / D(I-1)
  D(I) = D(I) - DL*SUPD(I-1)
  X(I) = X(I) - DL*X(I-1)
100 CONTINUE
C
X(N) = X(N) / D(N)
DO 200 I=N-1,1,-1 back substitute loop
  X(I) = ( X(I) - SUPD(I)*X(I+1) ) / D(I)
200 CONTINUE
RETURN
END

```

Computation of \mathcal{X}

Another minor point to be covered is the numerical determination of the location of the front, $\mathcal{X}(t)$. Given a set of mesh values $\{C_{n,k}, n = 0, 1, \dots, N, k \text{ fixed}\}$, the routine that finds \mathcal{X} looks for the value n_* that maximizes $|C_{n_*+1,k} - C_{n_*,k}|$. Then a cubic polynomial in n (or x) is fit to the four points $C_{n_*-1,k}$, $C_{n_*,k}$, $C_{n_*+1,k}$, and $C_{n_*+2,k}$. The steepest point on this polynomial is the location \mathcal{X} .

When calculating an approximate $\dot{\mathcal{X}}$ by $\dot{\mathcal{X}}_k \approx (\mathcal{X}_{k+1} - \mathcal{X}_{k-1})/(2\Delta t)$, the result is a somewhat jagged function of t . This is what gives the figures showing numerical $\mathcal{X}(t)$ results their "fuzzy" look. The problem comes from the fact that only 2 or 3 mesh points are in the layer at the front and so the actual position of the front is not resolved very finely. When the resulting values of \mathcal{X} are differenced, they end up with a lot of numerical noise.

Bibliography

- [1] AIFANTIS, E.C., *On the Problem of Diffusion in Solids*, Acta Mech., **37** (1980), pp.265-296.
- [2] BENDER, CARL M. AND ORSZAG, STEVEN A., *Advanced Mathematical Methods for Scientists and Engineers*, McGraw-Hill, New York, 1978.
- [3] CHRISTENSEN, R.M., *Theory of Viscoelasticity*, Academic Press, New York, 1971.
- [4] COHEN, DONALD S. AND GOODHART, CHARLES, *Sorption of a Finite Amount of Swelling Solvent in a Glassy Polymer*, J. Polym. Sci. Polym. Phys. Ed., **25** (1987), pp.611-617.
- [5] DURNING, C.J., *Differential Sorption in Viscoelastic Fluids*, J. Polym. Sci. Polym. Phys. Ed., **23** (1985), pp.1831-1855.
- [6] FRISCH, H.L., WANG, T.T., AND KWEI, T.K., *Diffusion in Glassy Polymers, II*, J. Polym. Sci. A-2, **7** (1969), pp.879-887.
- [7] JOST, W., *Diffusion in Solids, Liquids, Gases*, Academic Press, New York, 1960.
- [8] KATH, WILLIAM LAWRENCE, *Propagating and Waiting Fronts in Nonlinear Diffusion*, Ph.D. thesis, Dept. Appl. Math., California Institute of Technology, Pasadena, CA, 1981.
- [9] KEVORKIAN, J. AND COLE, J.D., *Perturbation Methods in Applied Mathematics*, Springer-Verlag, New York, 1981.
- [10] STANLEY, ELIZABETH ANN, *Diffusion in Glassy Polymers*, Ph.D. thesis, Dept. Appl. Math., California Institute of Technology, Pasadena, CA, 1984.
- [11] THOMAS, NOREEN AND WINDLE, A.H., *Transport of methanol in poly-(methyl-methacrylate)*, Polymer, **19** (1978), pp.255-265.
- [12] THOMAS, N.L. AND WINDLE, A.H., *A Theory of Case II Diffusion*, Polymer, **23** (1982), pp.529-542.
- [13] *Microsoft muMath Symbolics Mathematics Package*, The Soft Warehouse, Honolulu, 1983.